Planetary boundary layer and atmospheric turbulence.

Szymon P. Malinowski
Marta Wacławczyk

Institute of Geophysics UW

2017/18

Lecture 11

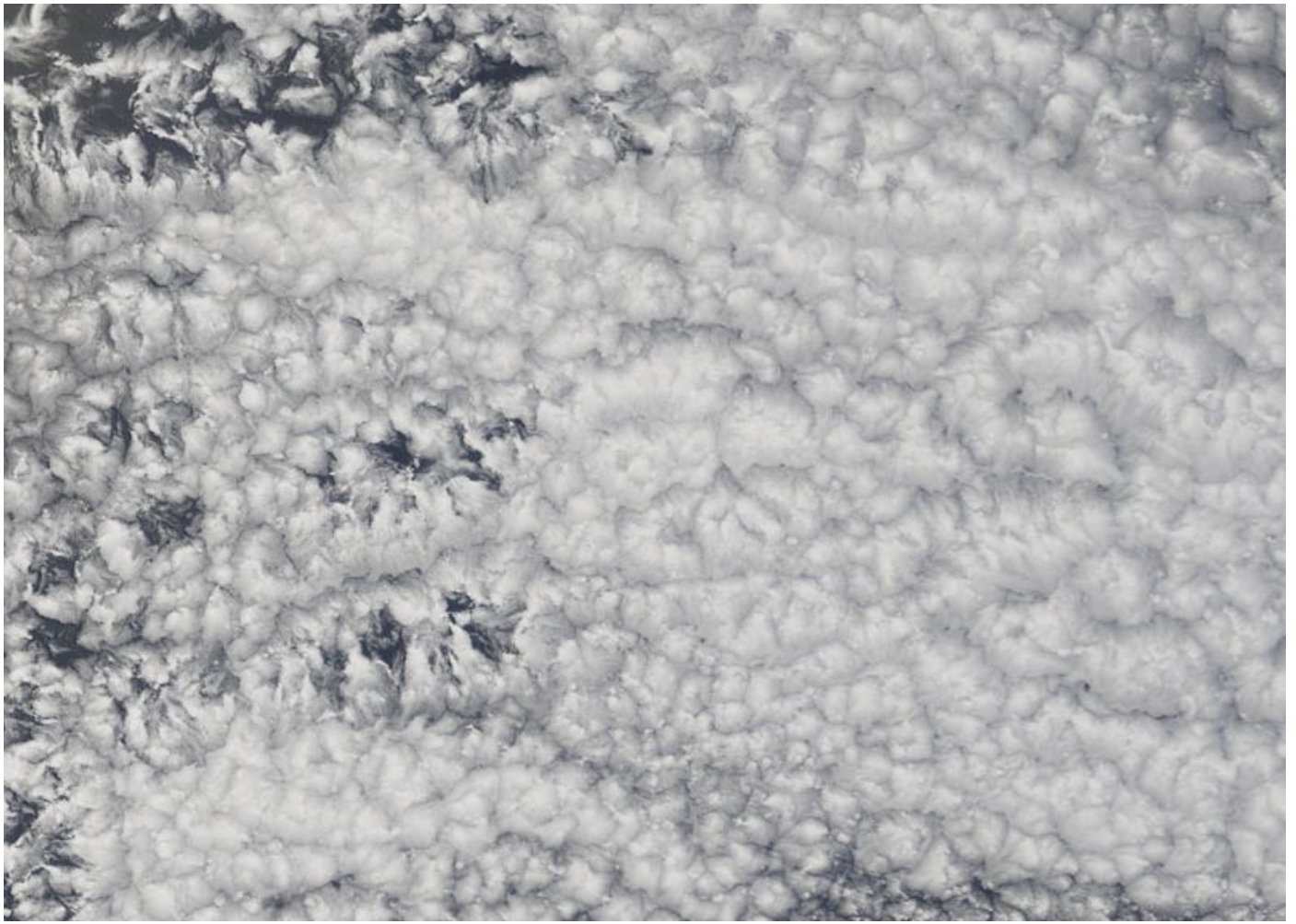

Why Stratocumulus Clouds:
- essential element in Earth's radiation budget, covering ~ 20% of the globe;
- simple geometry (plain parallel cloud in below capping inversion),
- despite this, mixing processes at Sc top not well understood.

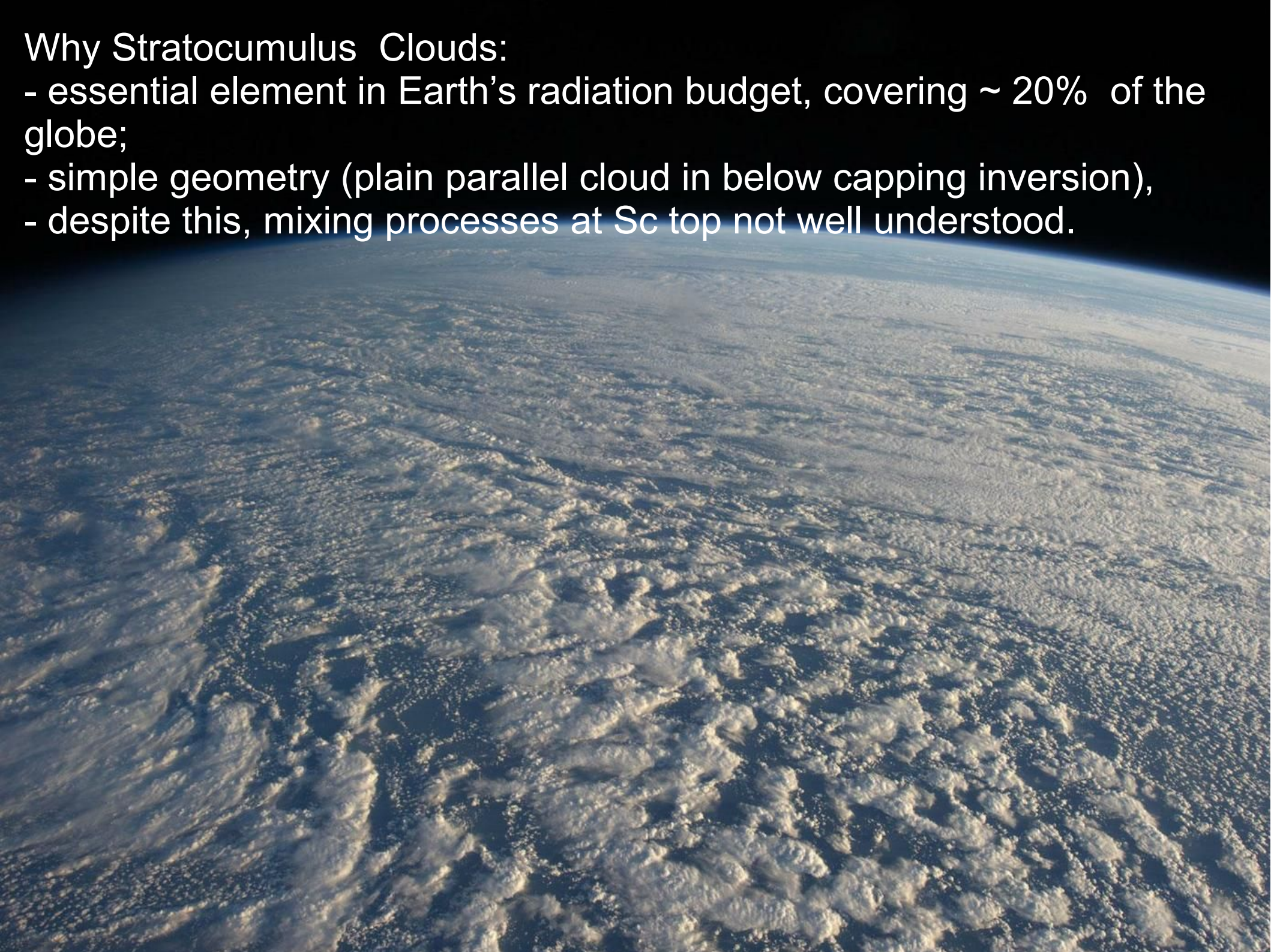

Shallow convection regimes over ocean.

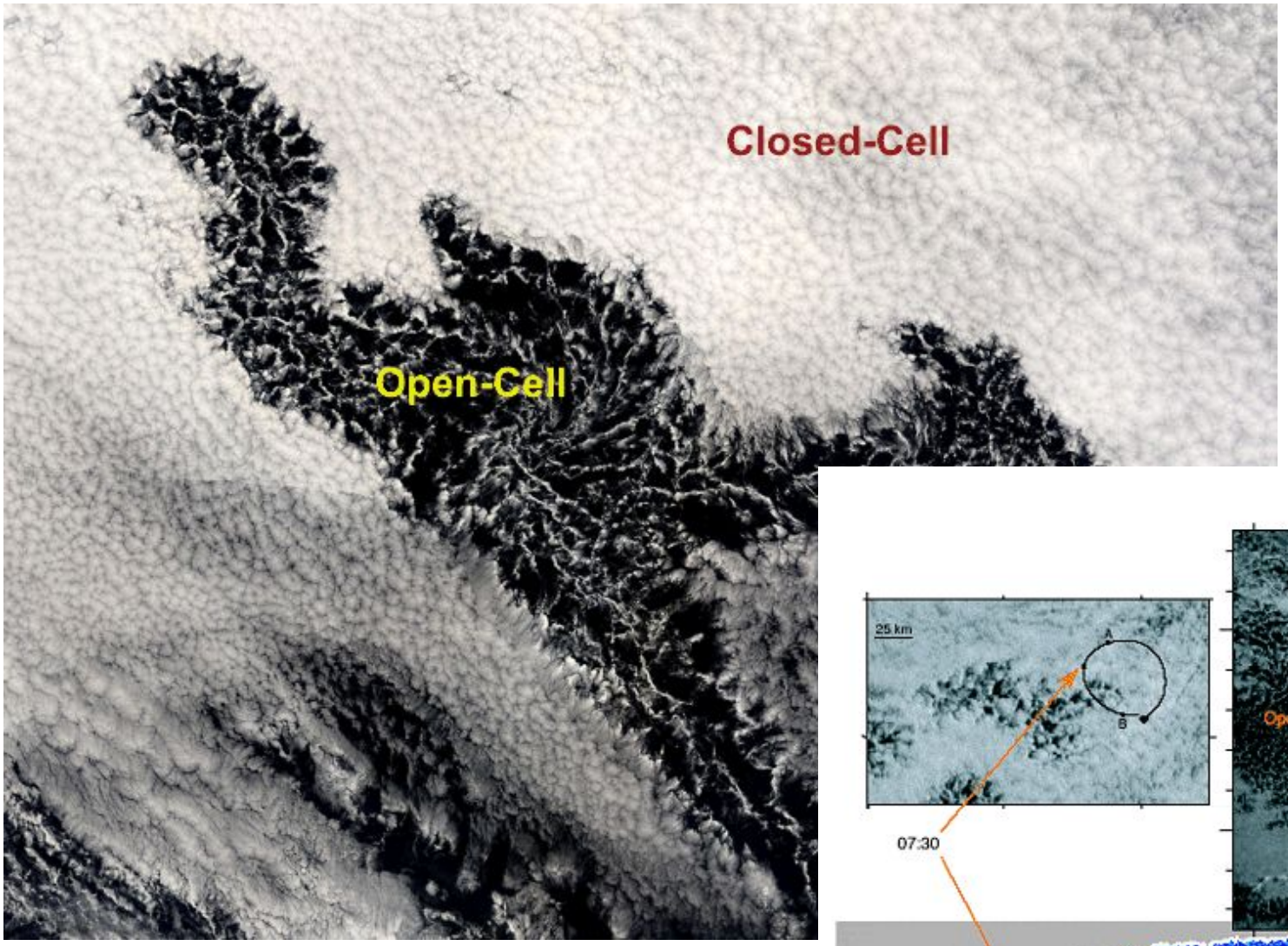

Stratocumulus morphology

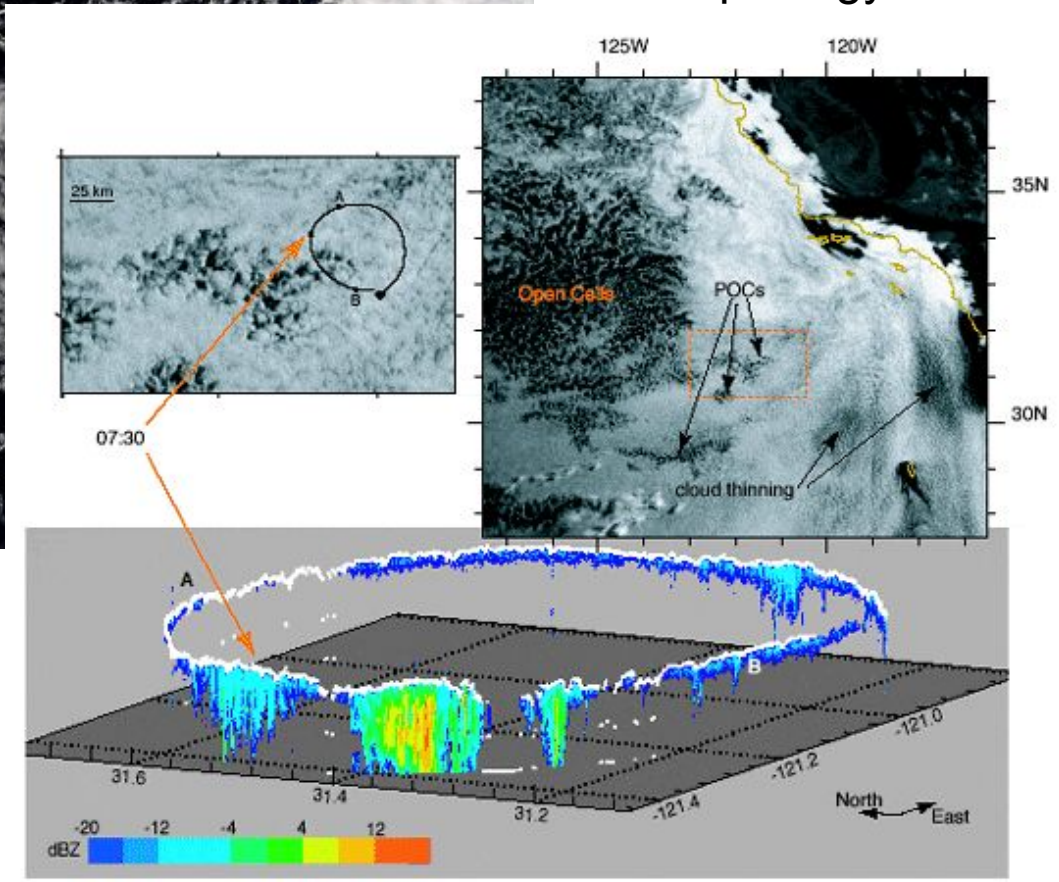

Cloud stew: slowly cooked from below, cooled from above

Wood 2012

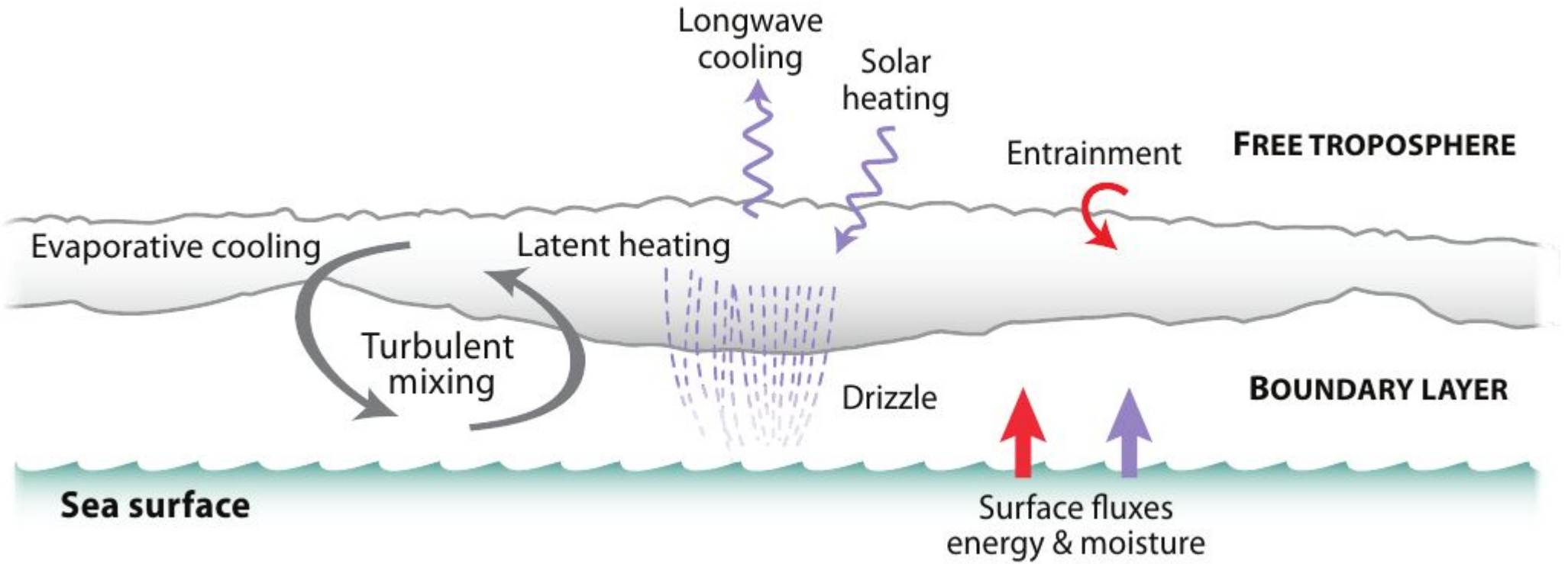

Notice strong inversion, almost a rigid lid!!!
Updrafts DO NOT penetrate inversion!!!

Stevens 2005

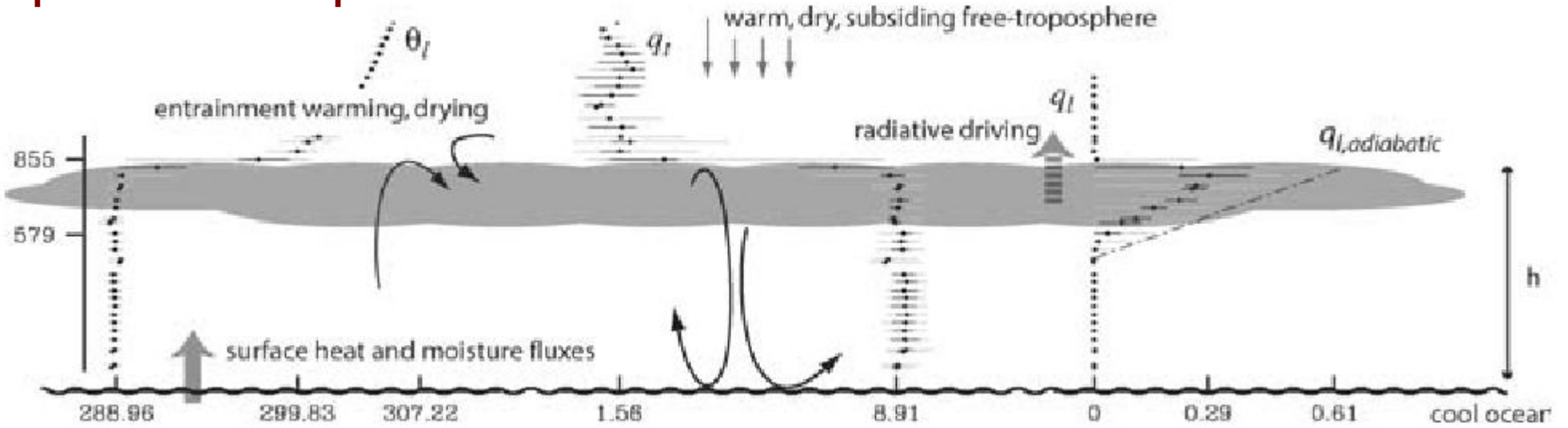

Stevens (2002) about Sc clouds :
"... We posed two questions: (1) how well do we really understand entrainment and (2) does it really matter? The answer to the first question is 'not very well'. The answer to the second question is yes."

In a review paper Wood (2012) writes:
"A major unresolved question in stratocumulus dynamics is how the entrainment rate we at the top of the STBL relates to STBL turbulent dynamics .... The extent to which entrainment is controlled by the large eddies ... as opposed to small scale mixing processes and direct non-turbulent radiative/evaporative cooling ... is not fully understood."

In-situ measurements in Stratocumulus clouds: DYCOMS II.

Stevens et al., 2003

DYCOMS-II Probe Locations

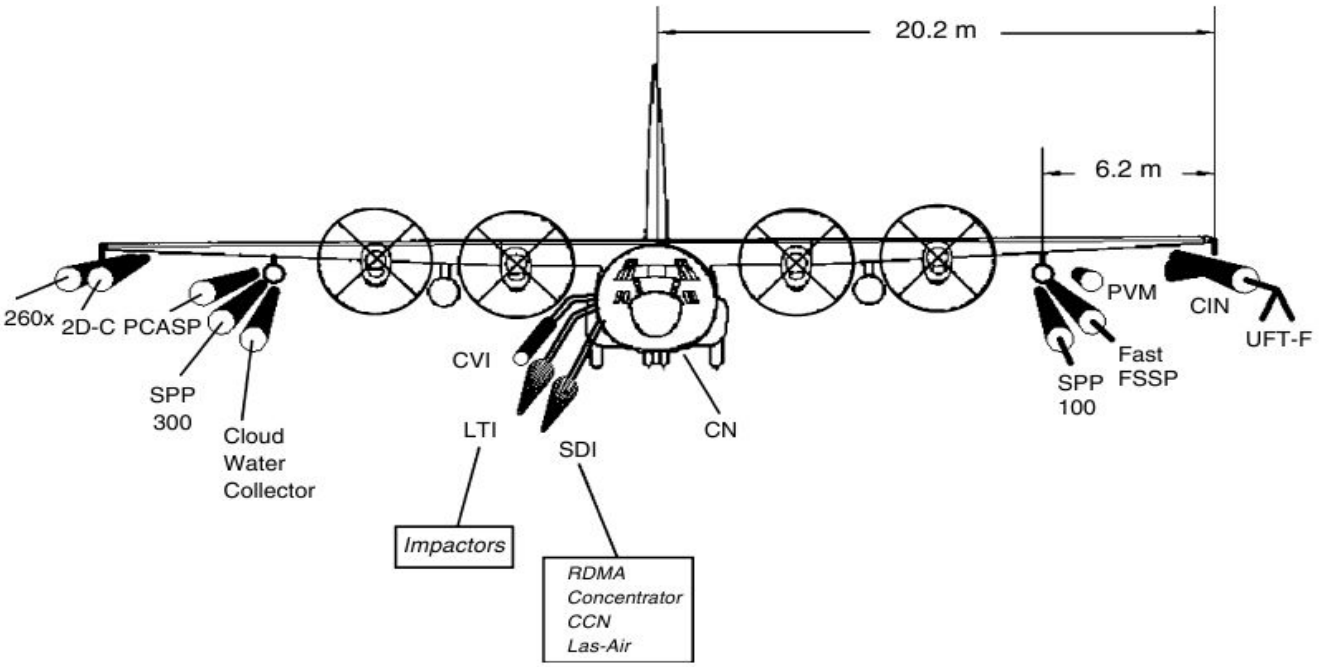

plus aerosol sampling with instruments inside aircraft

Penetration of the upper part of marine Sc cloud. 100Hz (1m resolution) data except for droplet spectra.

(Stevens et al., 2003, Gerber et al., 2005).

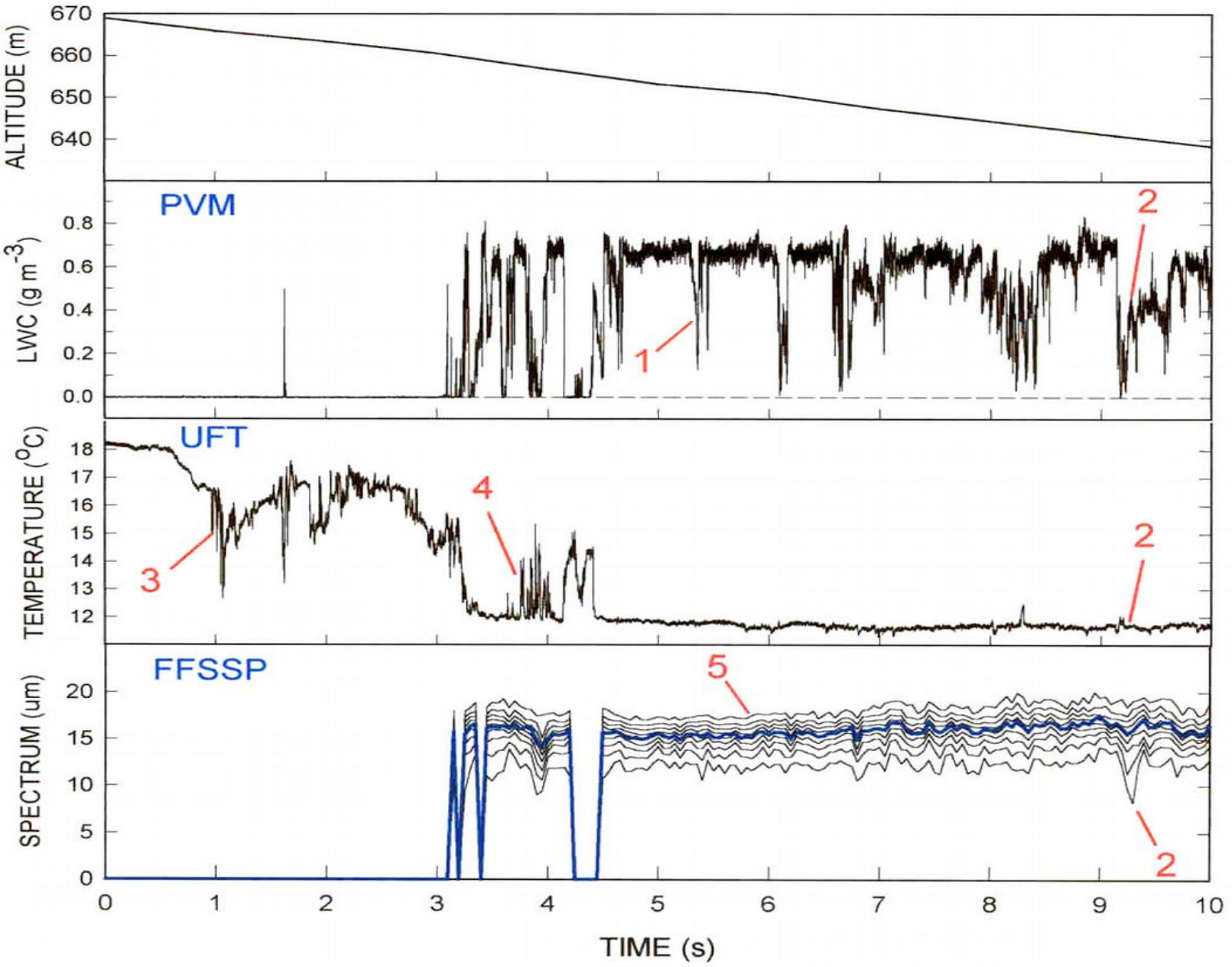

High-resolution measurements inside „cloud hole”:

LWC and water vapor mixing ratio (upper panel),

temperature and droplet density (middle panel),

droplet diameter (lower panel)

The red line helps to visualize effects of different location of the sensors and various response.

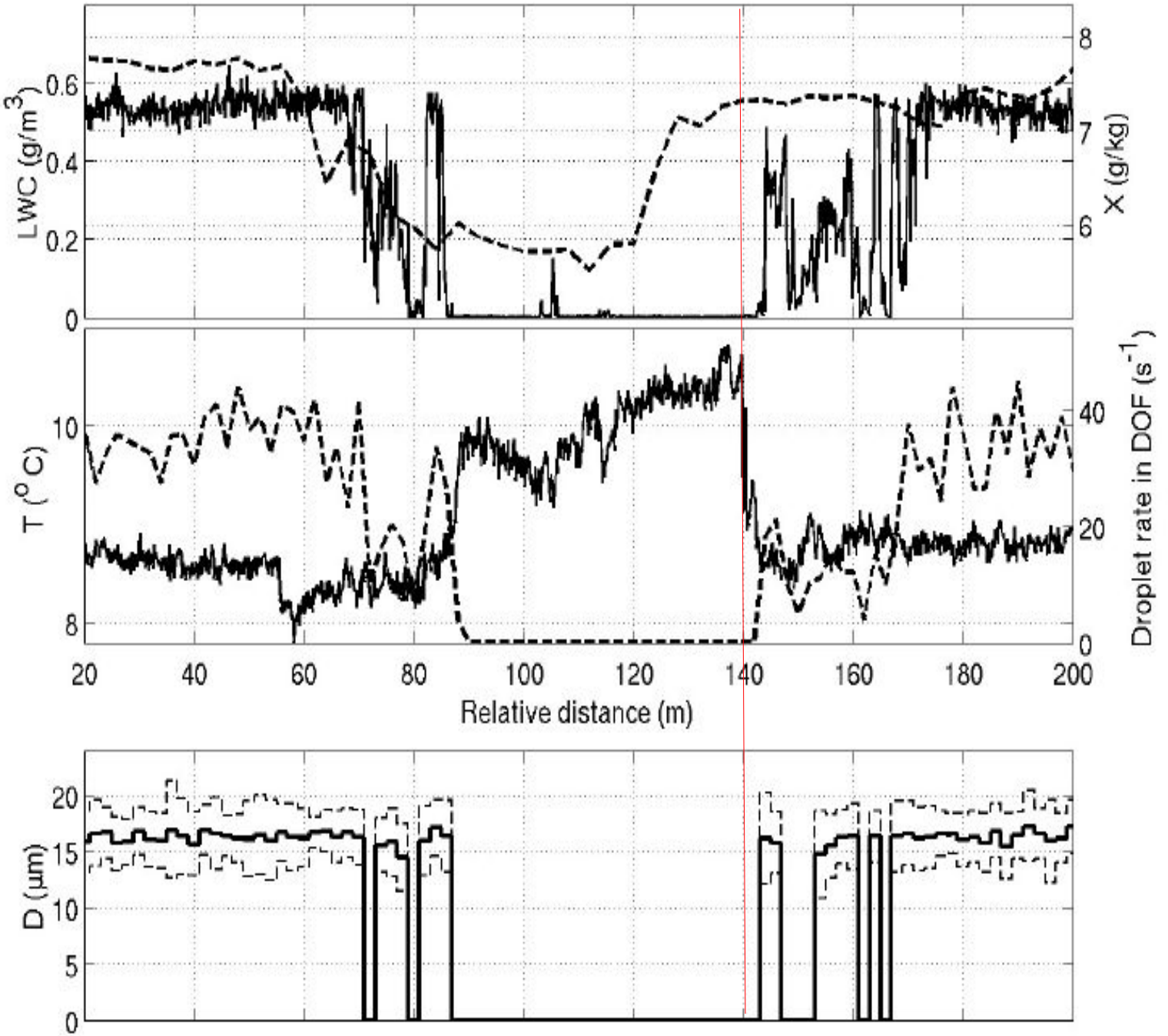

Haman et al., QJRMS, 2007

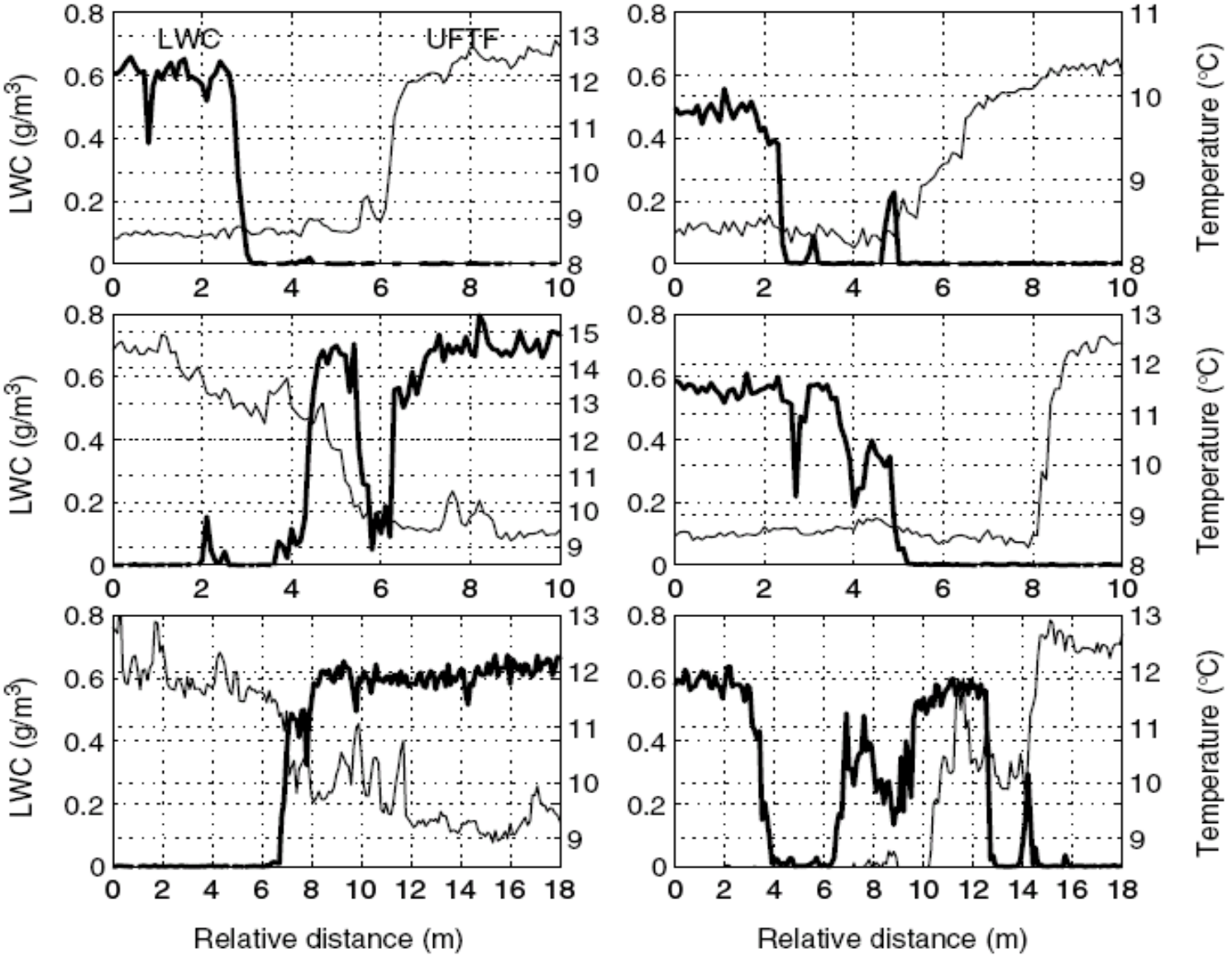

Examples of the cloud edge in 1000 Hz temperature (thin line) and LWC (thick line) records. Sharp jumps in LWC and temperature at distances of the order of 10 cm (data resolution) are currently observed.

Notice a shift between the temperature and LWC records resulting from the 6 m separation between the instruments and the low pitch angle of the aircraft with respect to the cloud clear air interface.

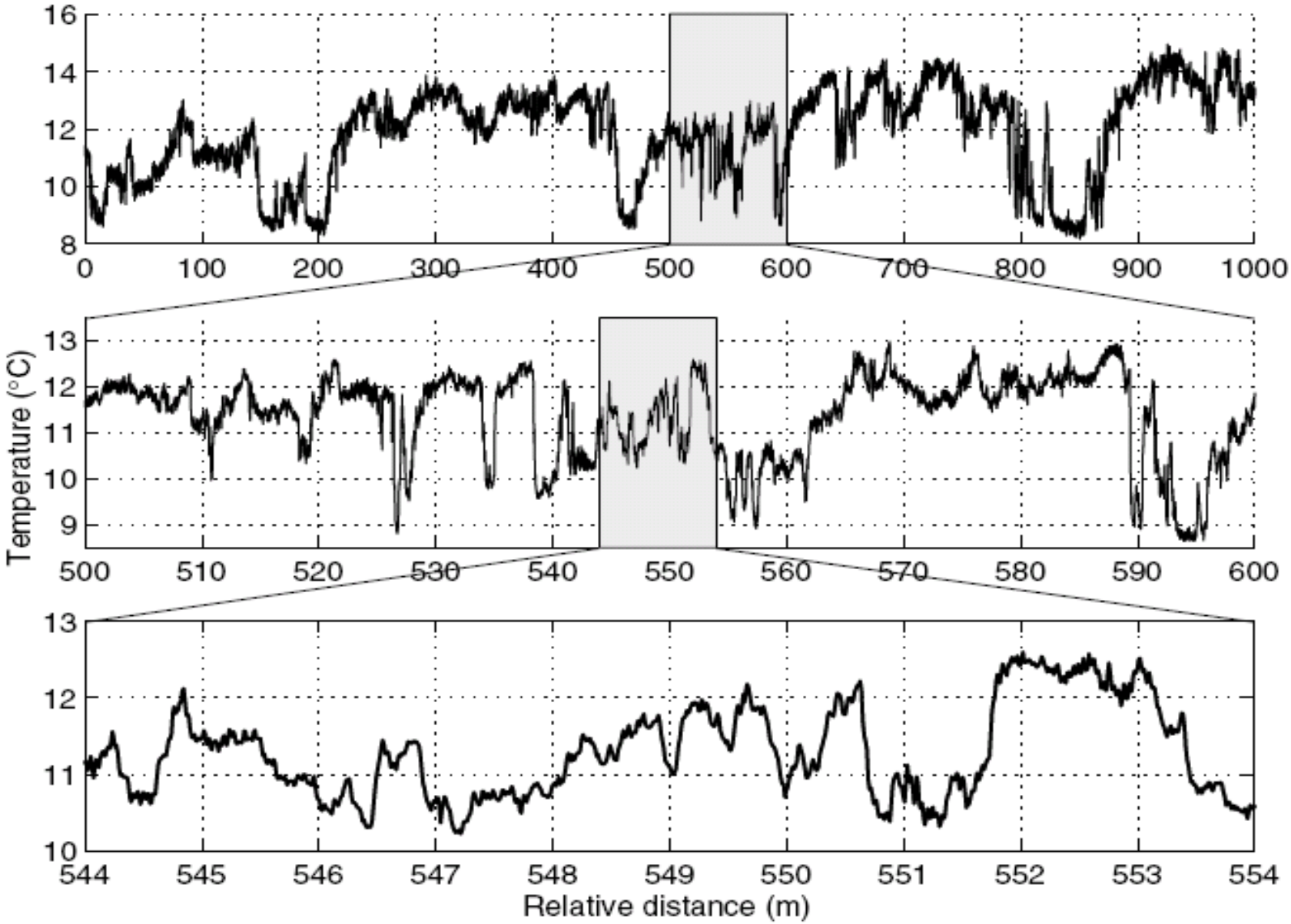

From the top to the bottom: successive ‘blow ups’ of 10 kHz temperature records showing self-similar structures – filaments of significantly different temperatures separated by narrow interfaces. The bottom panel presents the evidence for filaments of thickness of the order of 10 cm as well as for the steep gradients of temperature.

Notice that UFT-F in its present configuration and signal conditioning (low-pass filtering) is still too slow to resolve adequately all interesting small-scale features of the temperature field. Owing to the high amplitude of observed temperature fluctuations, the aerodynamic noise from the instrument (less than 0.3 °K) does not shade the high-resolution temperature fluctuations.

In-situ measurements: relative position of the top of inversion and the top of Sc cloud (Haman et. al., 2007)

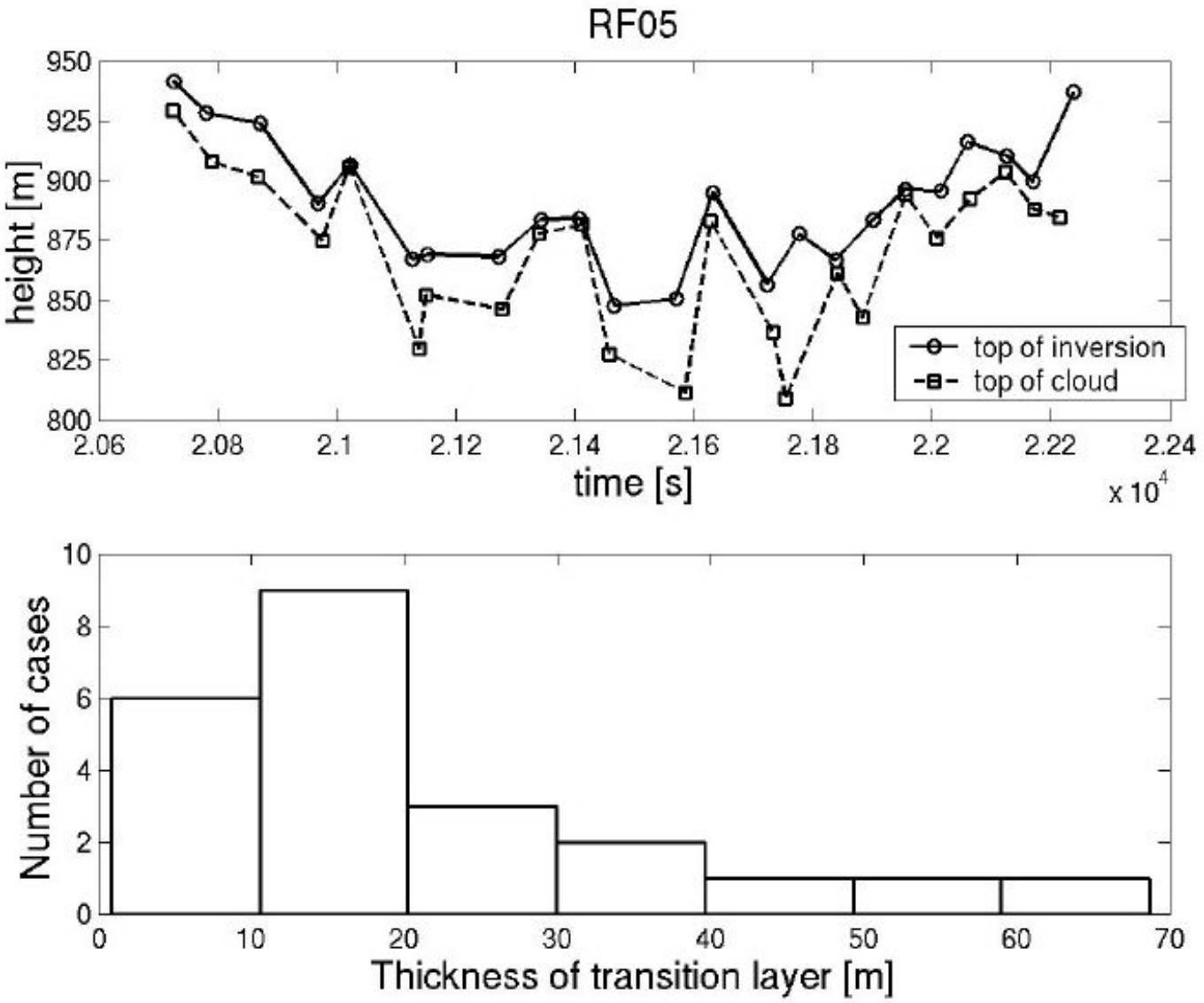

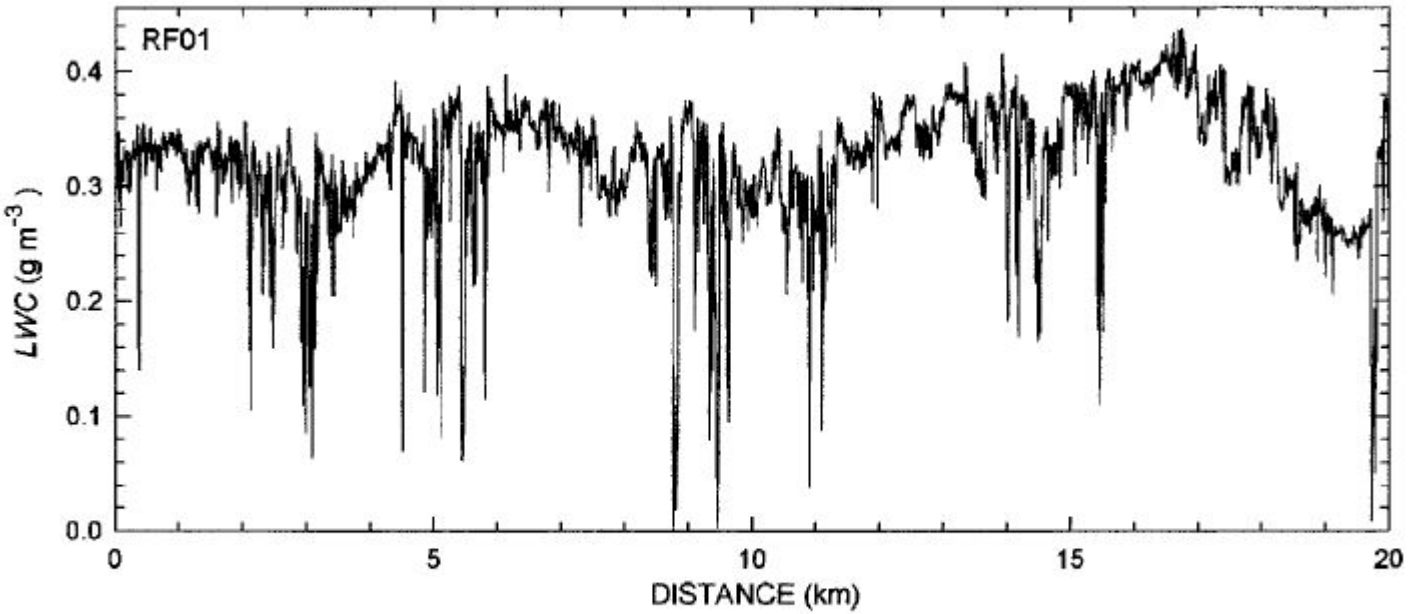

FIG. 1. LWC measured at 4-m resolution during horizontal flight of the NCAR C-130 aircraft 100 m below Sc top on flight RF01 of the DYCOMS-II study. Narrow regions of reduced LWC are interpreted as holes caused by the entrainment of air at cloud top.

„Cloud holes" – regions of depleted LWC during DYCOMS occurred to be negatively buoyant convective plumes.

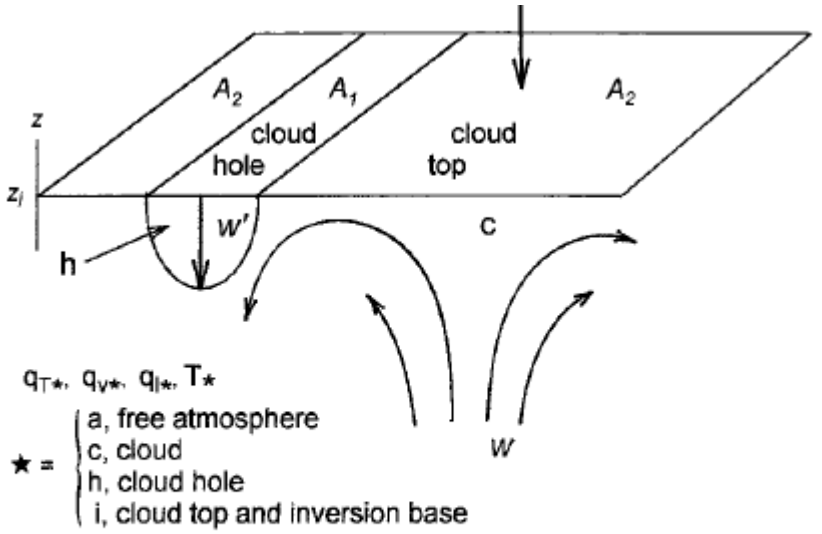

FIG. 2. Simplified schematic of a hole with depleted LWC′ at the Sc top, and associated vertical velocities w, water mixing ratios q, and temperature T.

Gerber et al., JAS 2005

In-situ measurements inside „cloud hole”:

LWC and water vapor mixing ratio (upper panel),

temperature and droplet density (middle panel),

droplet diameter (lower panel)

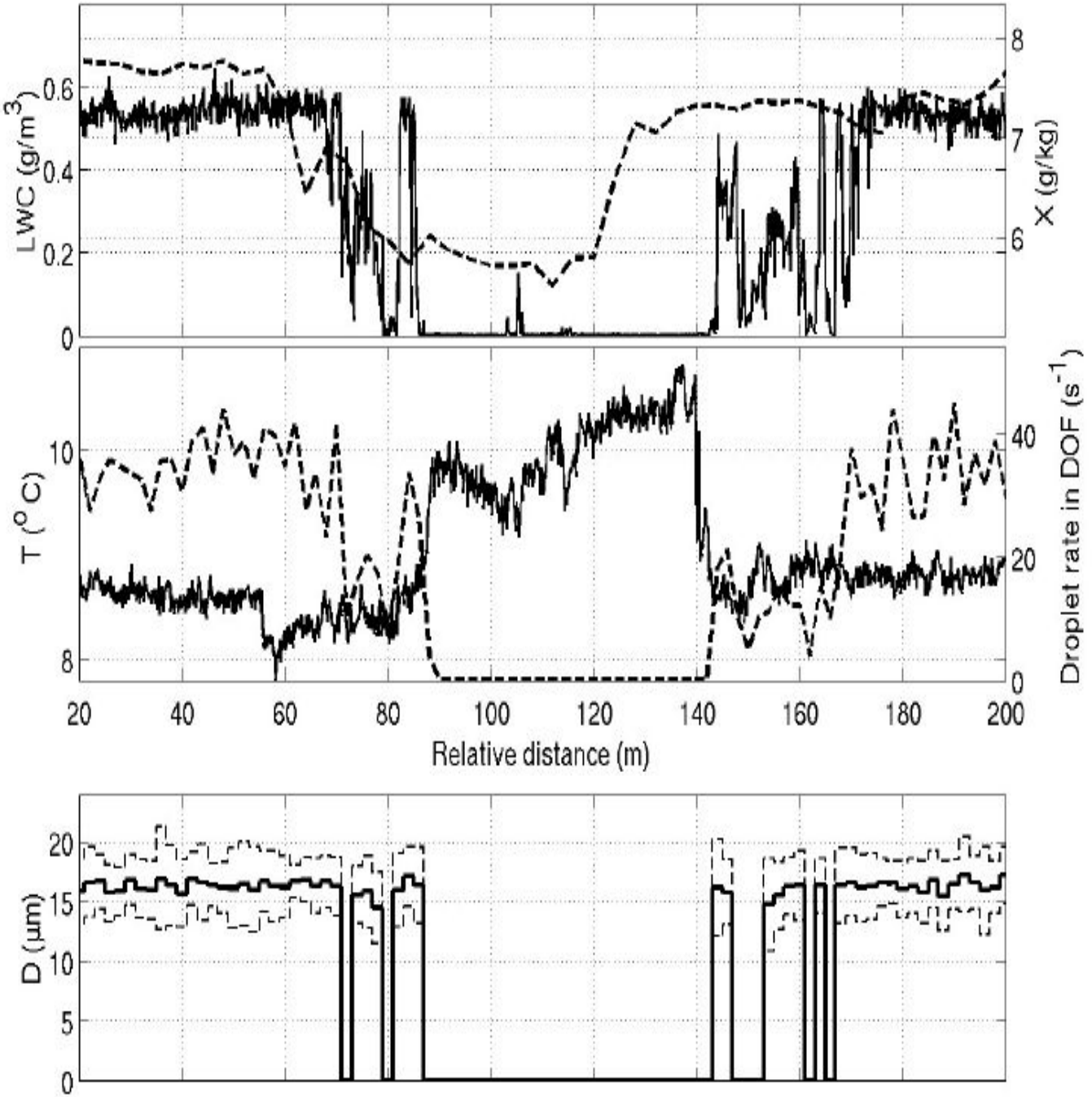

Numerical simulations:

- 3D anelastic semi-Lagrangian/Eulerian finite-difference model EULAG;
- setup to simulate nocturnal stratocumulus observed during the research flight RF01 of DYCOMS-II as in the model intercomparison study described in Stevens et al. (2005);
- drizzle processes are neglected, and the moist thermodynamics is limited to the condensation and evaporation of the cloud water;
- to maintain approximately steady-state conditions, large-scale subsidence, surface heat and moisture fluxes, and radiative cooling are all applied;
- the horizontal/vertical grid length is 35 m/5 m and the model time step is 0.6 s, the simulation is run for 6 hours.

Simulations:

temporal evolution of LWP

cloud cover fraction

TKE within the ABL

mean inversion height.

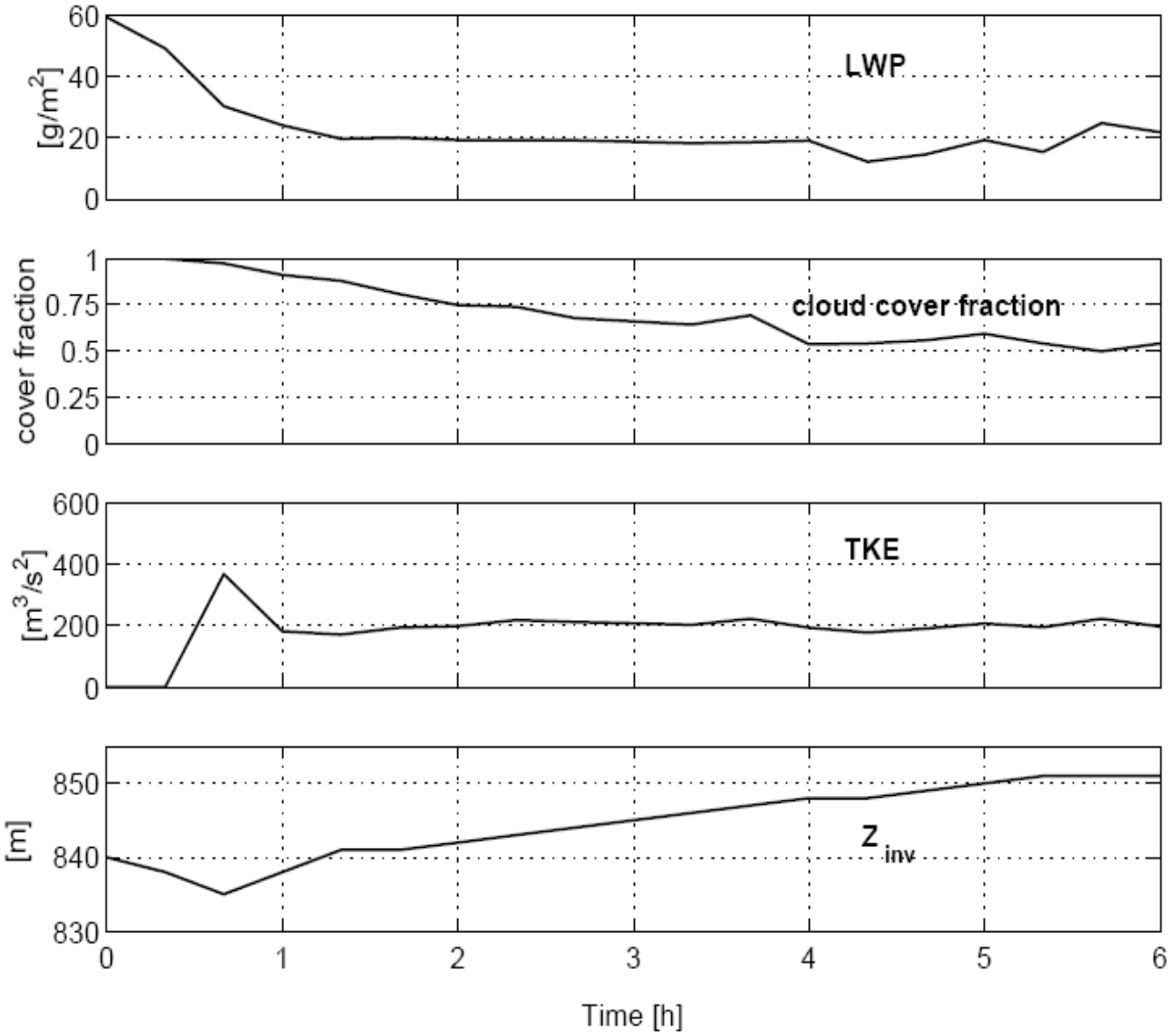

Mean profiles of:

total water content (left)

virtual potential temperature (middle)

enstrophy (right)

after 3,4 and 5 hours of simulations.

$< \omega^2 >$

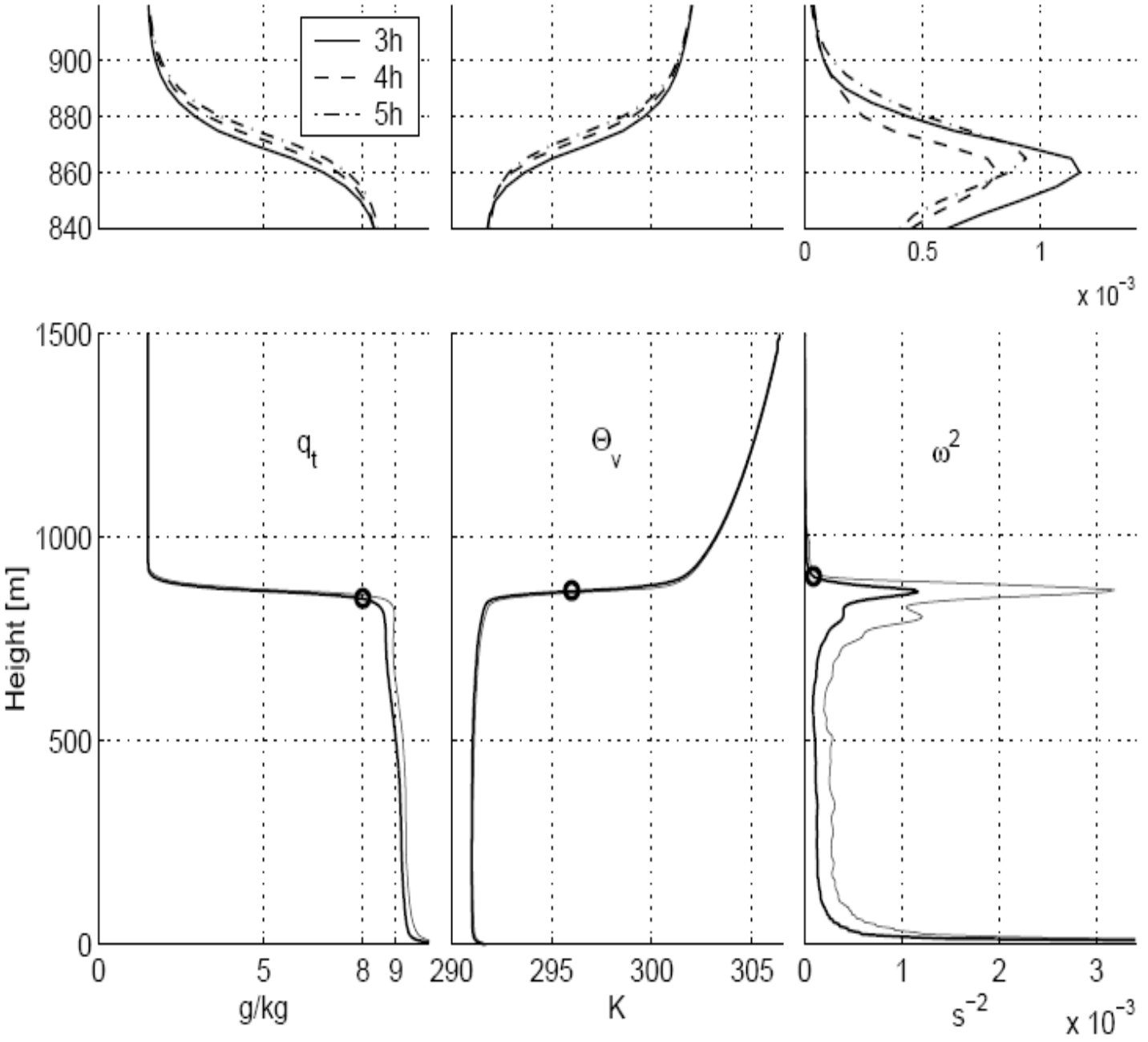

Below:
vertical velocities
in the model
columns;
time=3h

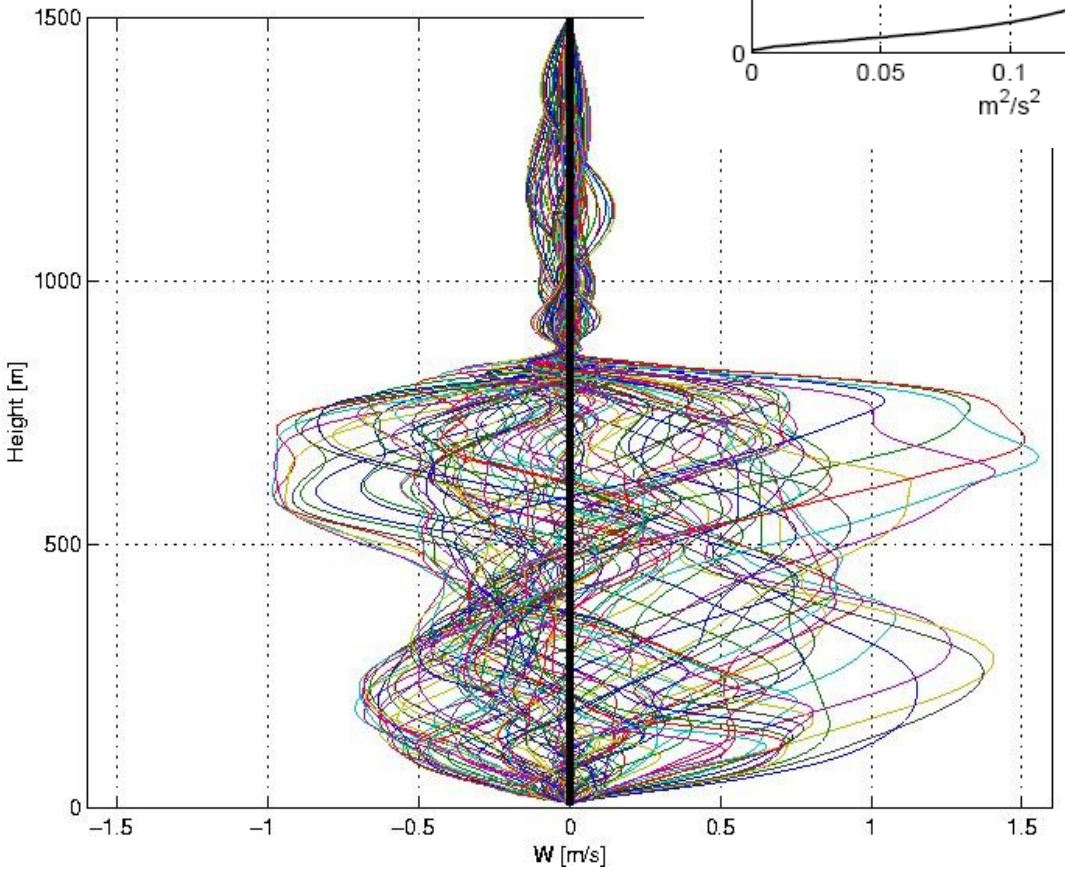

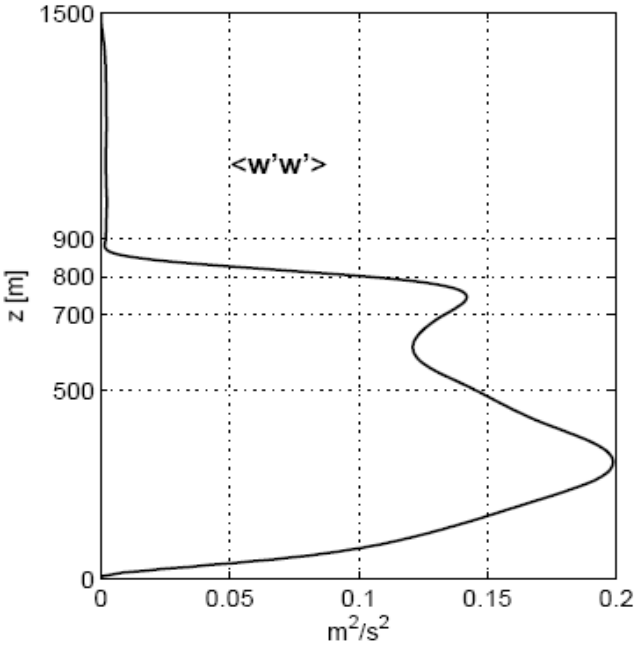

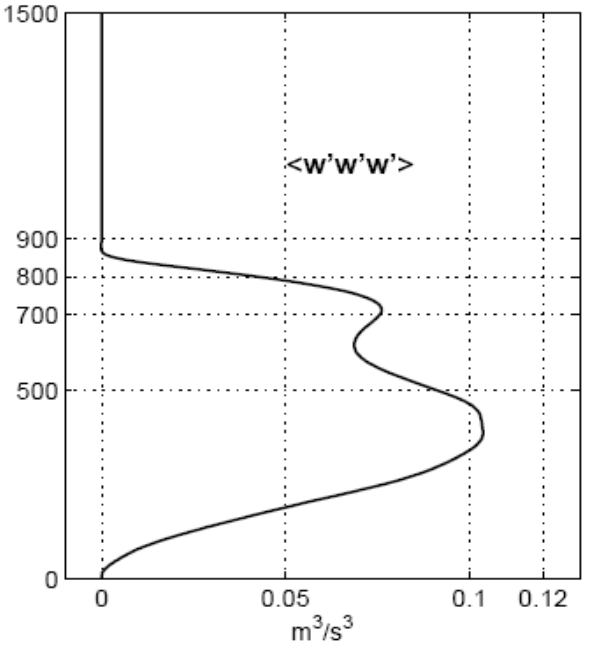

Above:
profiles of the vertical
velocity variance <w′w′>
and skewness <w′w′w′>,
time=3h

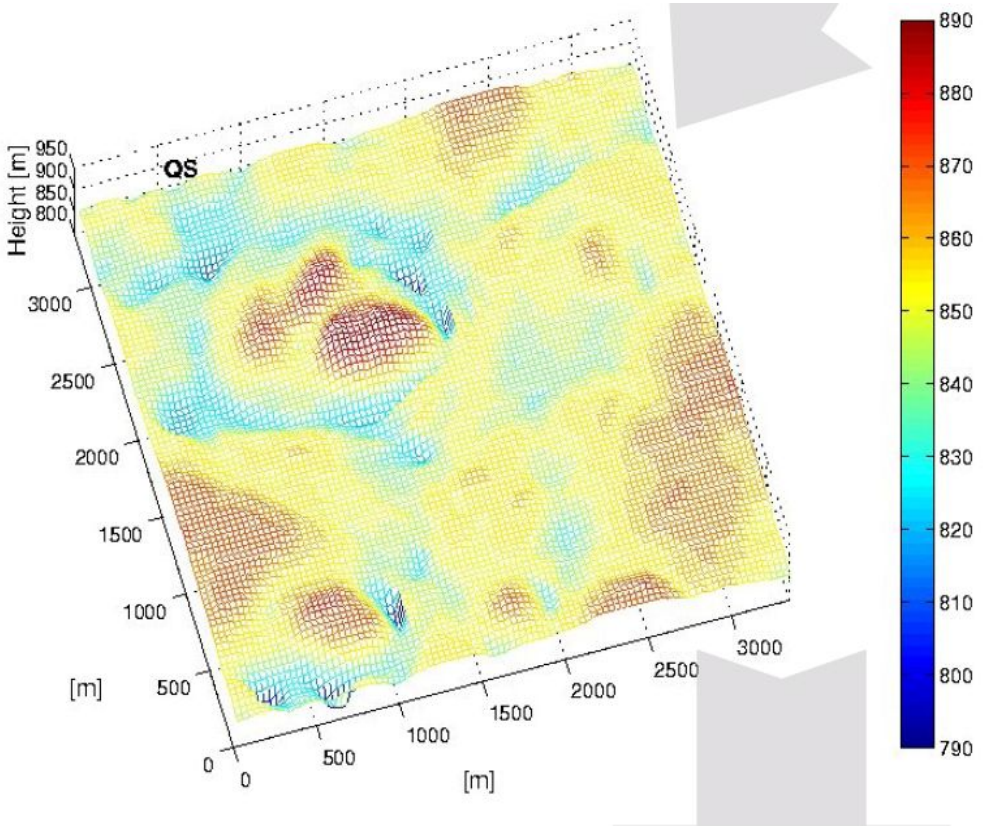

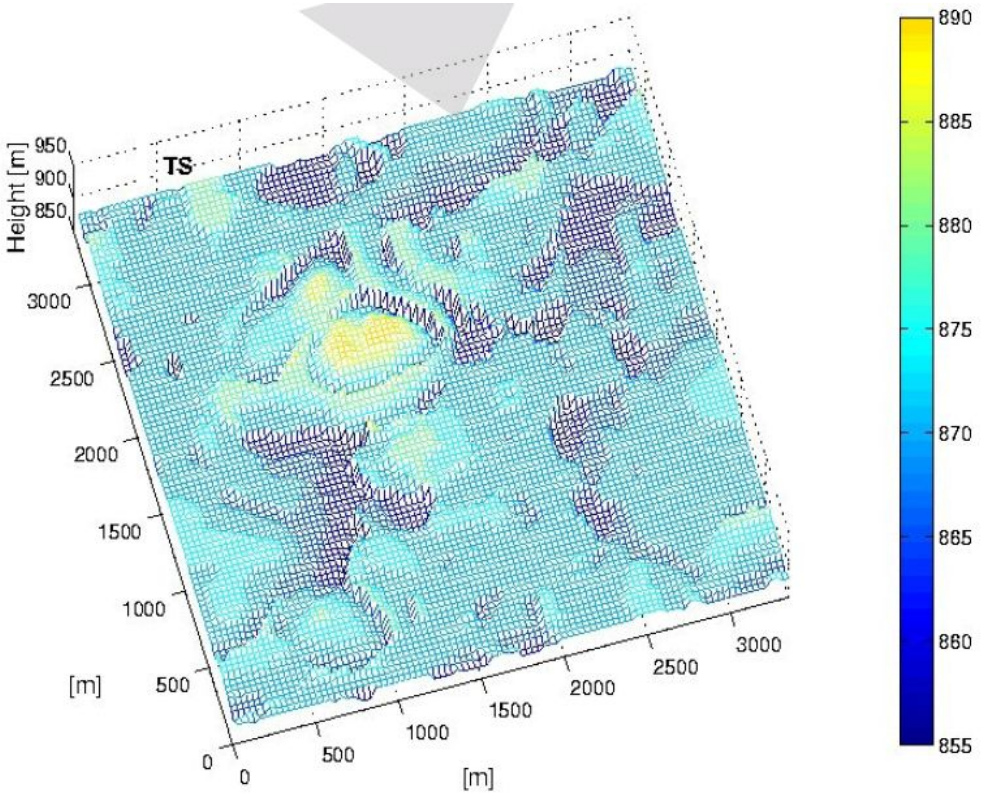

Upper panels: top of the cloud (left) and inversion surface (right) at time=3h.

Lower panel: a histogram of distances between the surfaces plotted above.

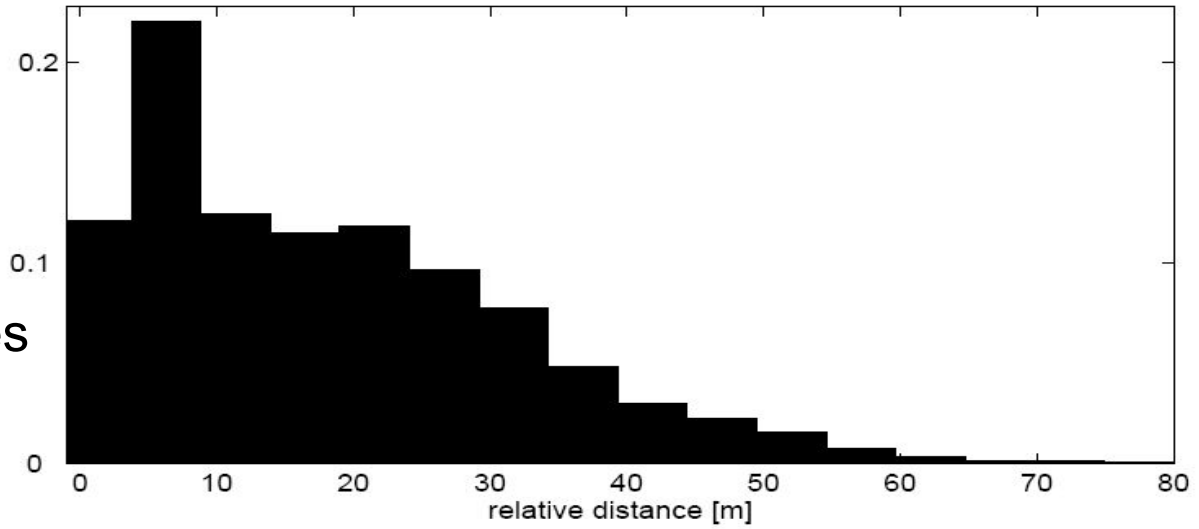

$$Ri = N^2/S^2$$

$$N^2 = (g/\theta_v)(\partial\theta_v/\partial z)$$

$$S^2 = \left(\frac{\partial U}{\partial z}\right)^2 + \left(\frac{\partial V}{\partial z}\right)^2$$

Dynamic stability (in terms of Richardson number **Ri)** and intensity of turbulence (in terms of **enstrophy)** on the inversion layer (**TS)** and top of the cloud (**QS**).

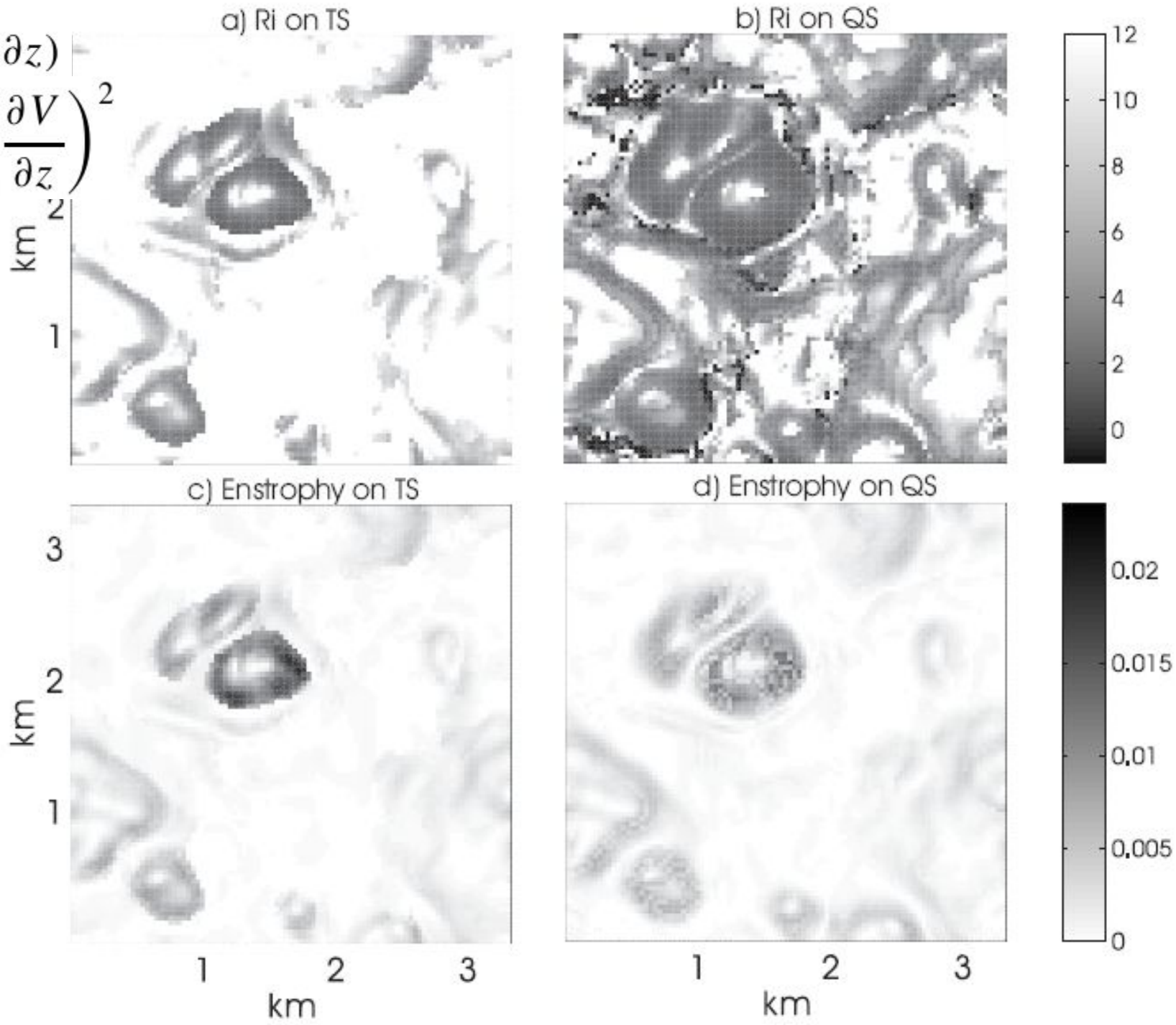

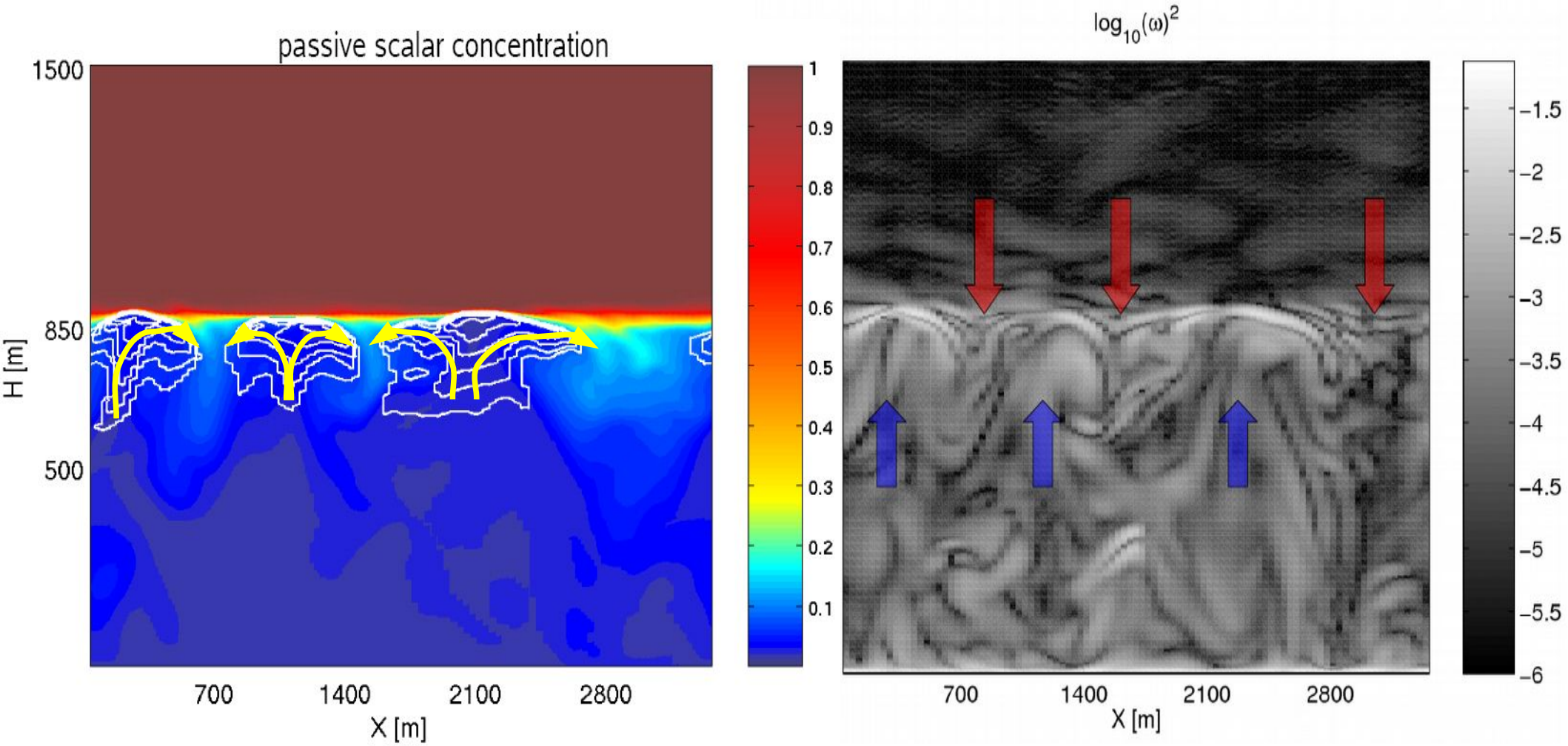

Passive scalar was added above inversion after 3 hours of simulation. Passive scalar concentration χ (left, cloud water contours shown by white lines) and enstrophy (right), at 6 hours of simulations.

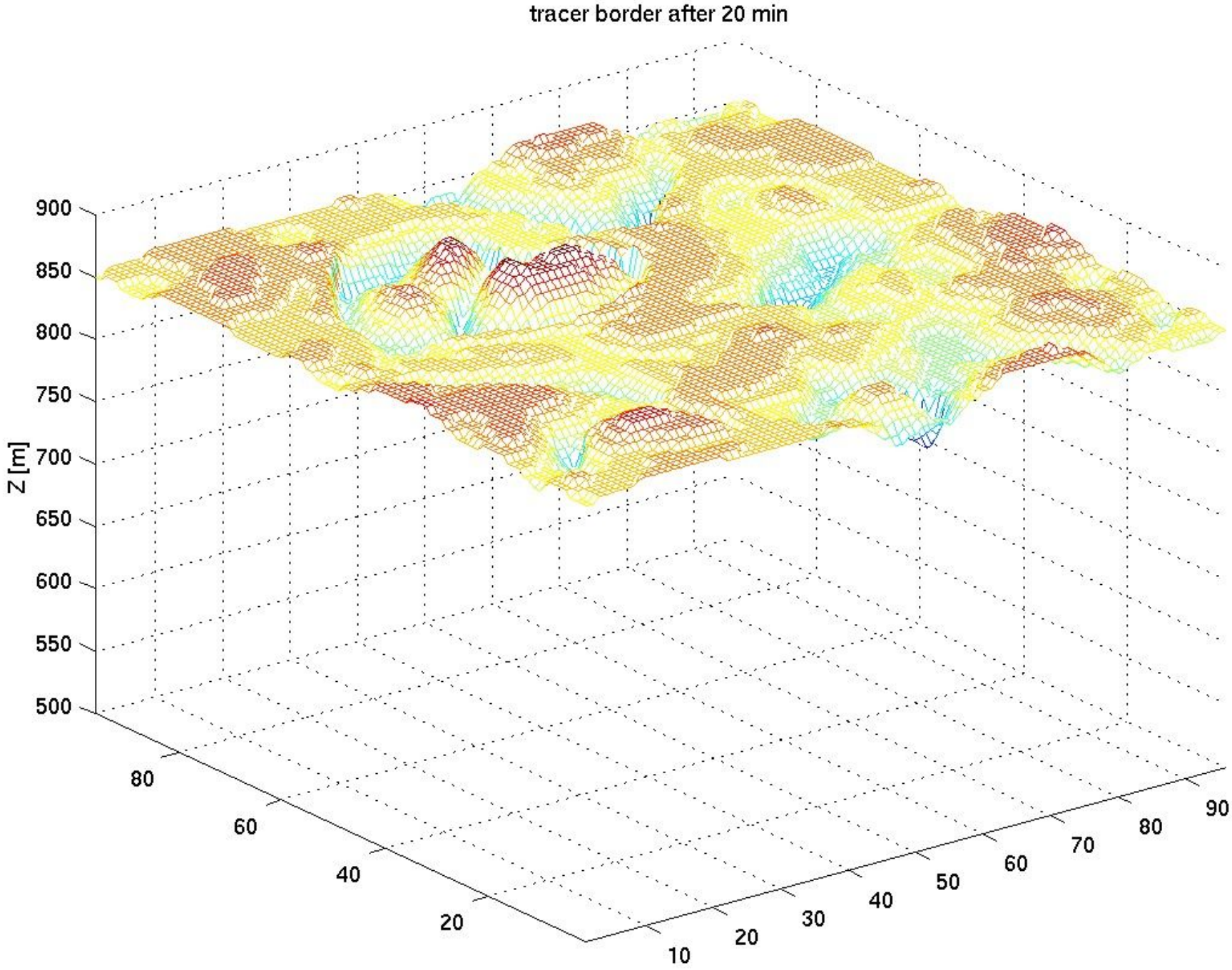
tracer border after 20 min
Z [m]
900
850
800
750
700
650
600
550
500
80
60
40
20
10
20
30
40
50
60
70
80
90

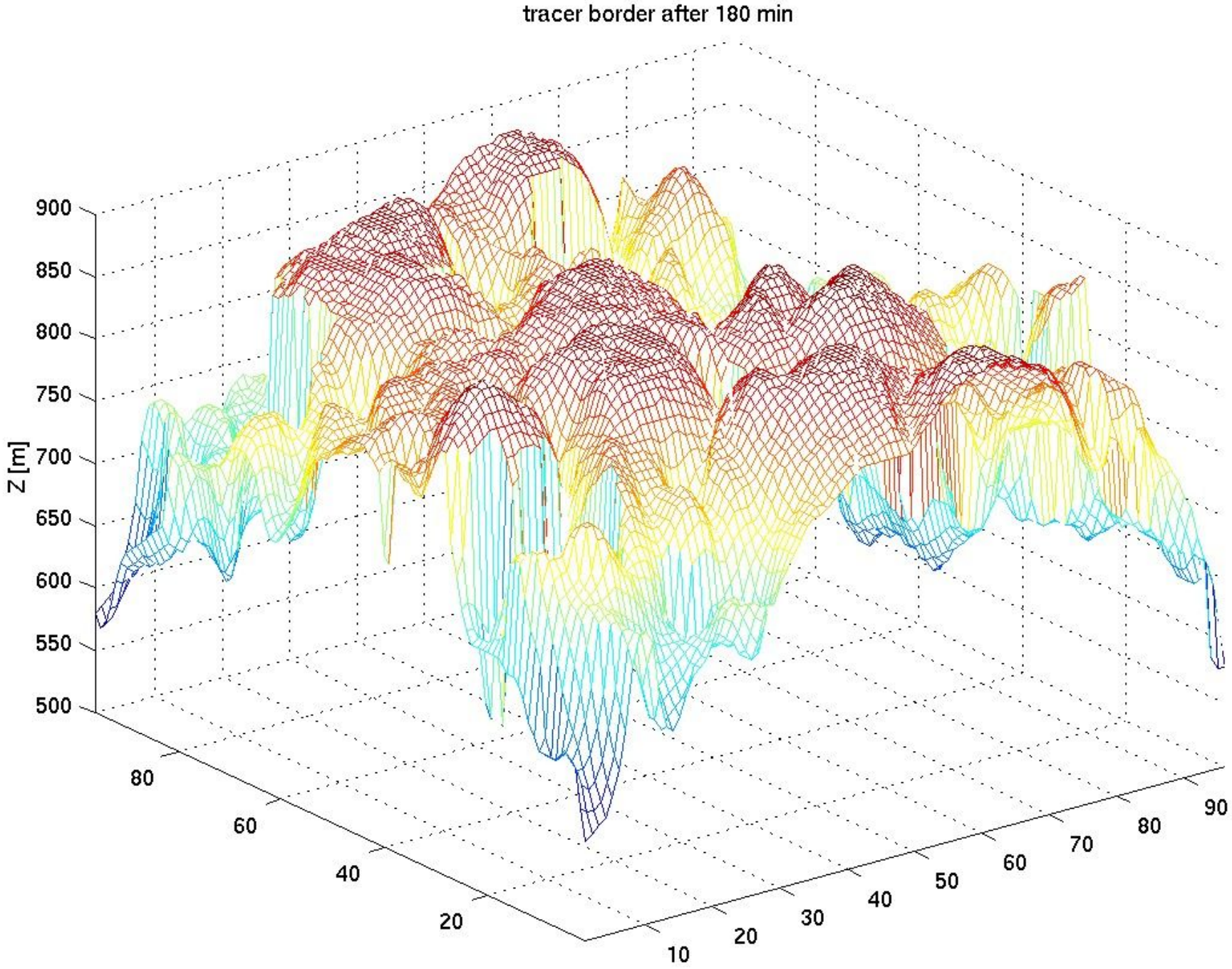
tracer border after 180 min
Z [m]
900
850
800
750
700
650
600
550
500
80
60
40
20
10
20
30
40
50
60
70
80
90

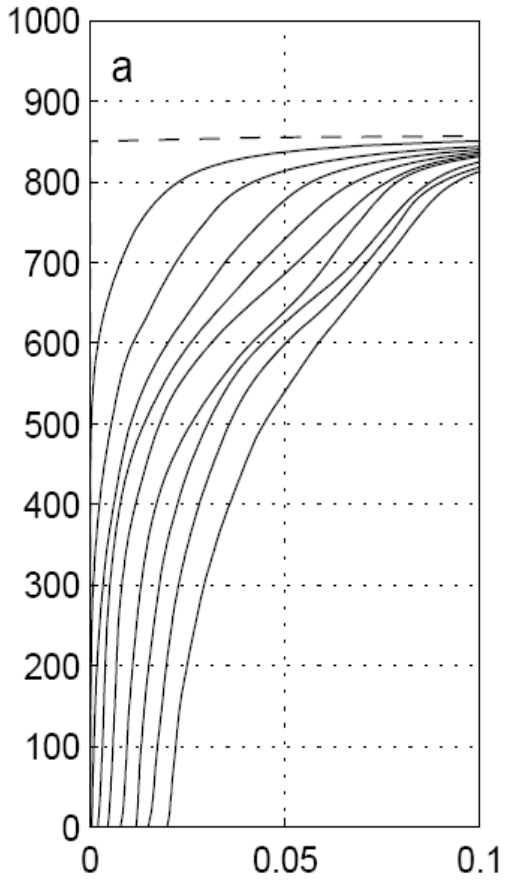

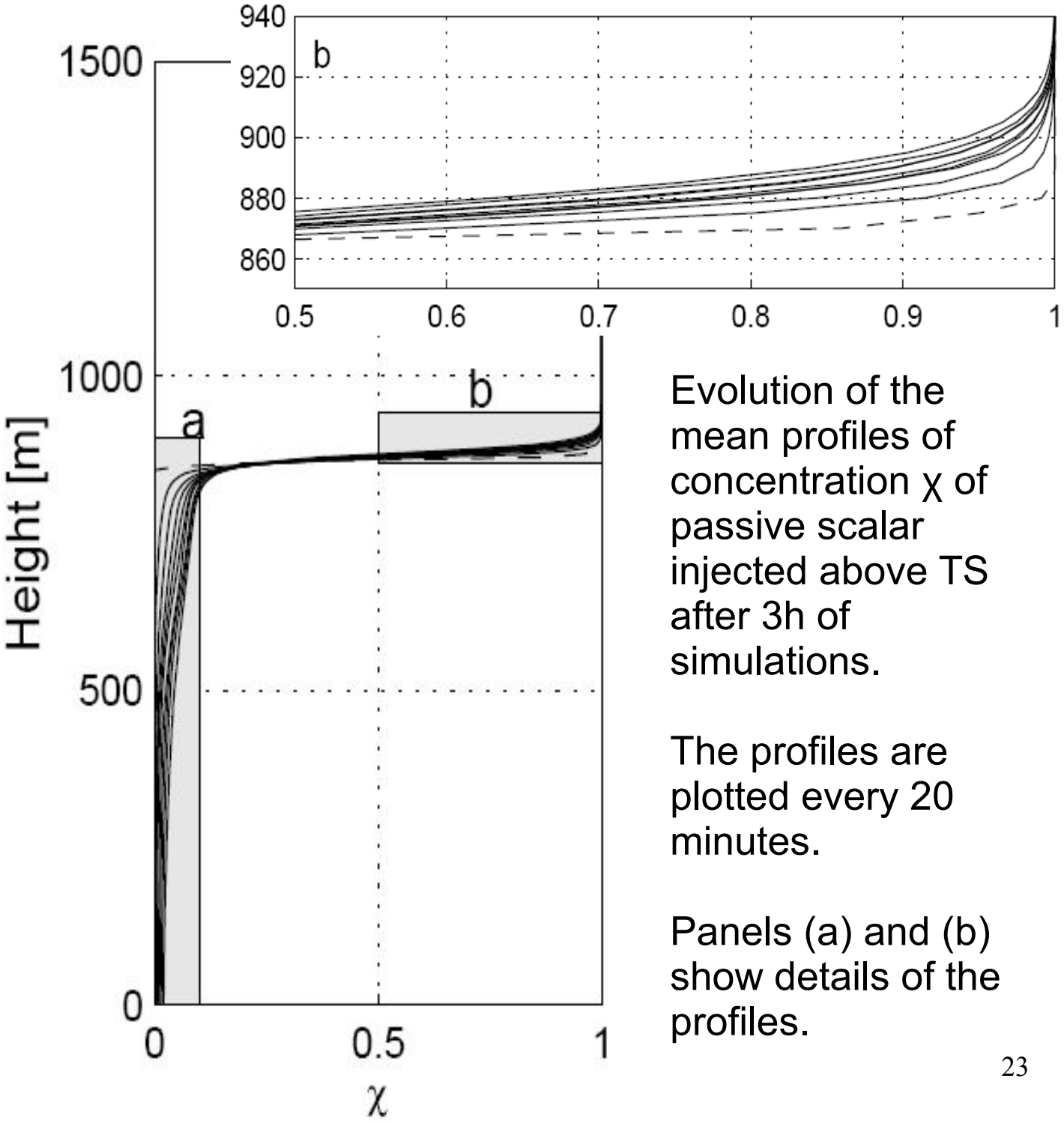

Evolution of the mean profiles of concentration χ of passive scalar injected above TS after 3h of simulations.

The profiles are plotted every 20 minutes.

Panels (a) and (b) show details of the profiles.

Mixing diagram showing buoyancy (density temperature) of mixture of cloud and free-tropospheric air (upper lines) and cloud and EIL air (lower lines).

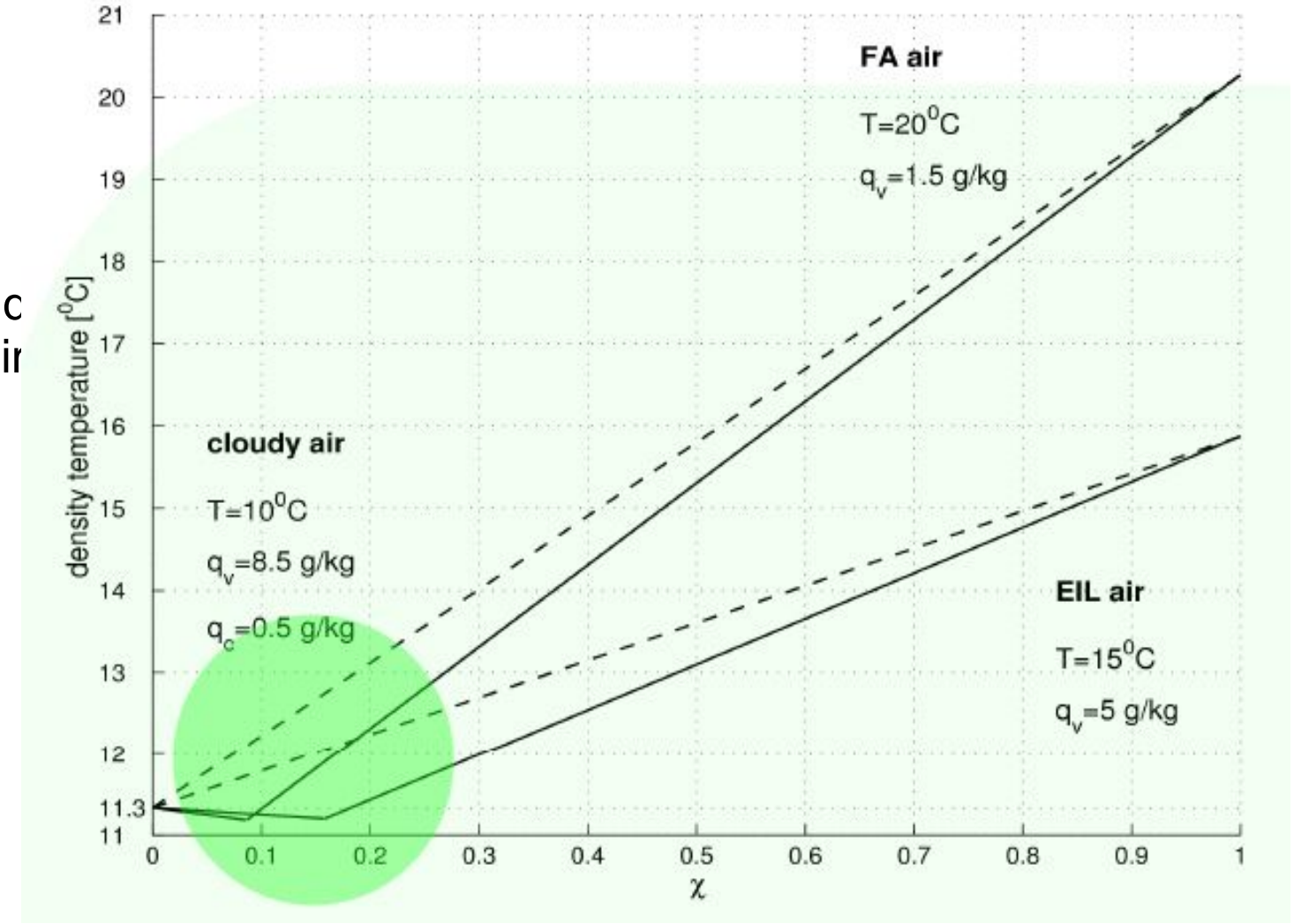

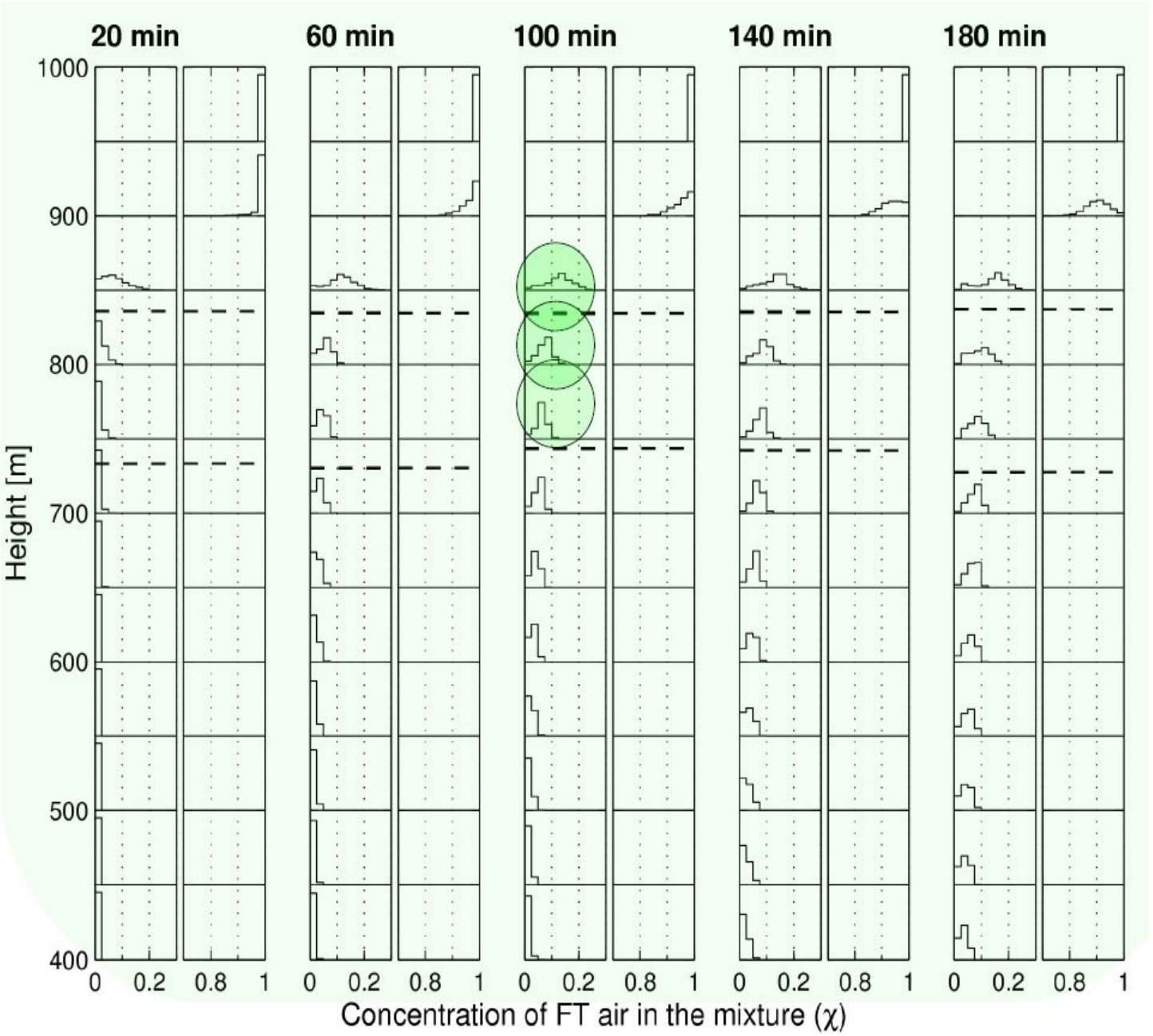

Histograms of passive scalar concentrations χ at different levels (every 50 m) and at selected times after initialization of the scalar.
The middle part of each histogram (for between 0.3 and 0.7) shows only zeros and thus it is removed.
The two horizontal dashed lines in each panel mark the mean cloud base and cloud top.

Conditional profiles (condition – concentration of passive scalar) of N-total lumber of gridboxes, Qc- cloud water content, qtot- total water content and w- vertical velocity at 20 minutes after injection of the scalar.

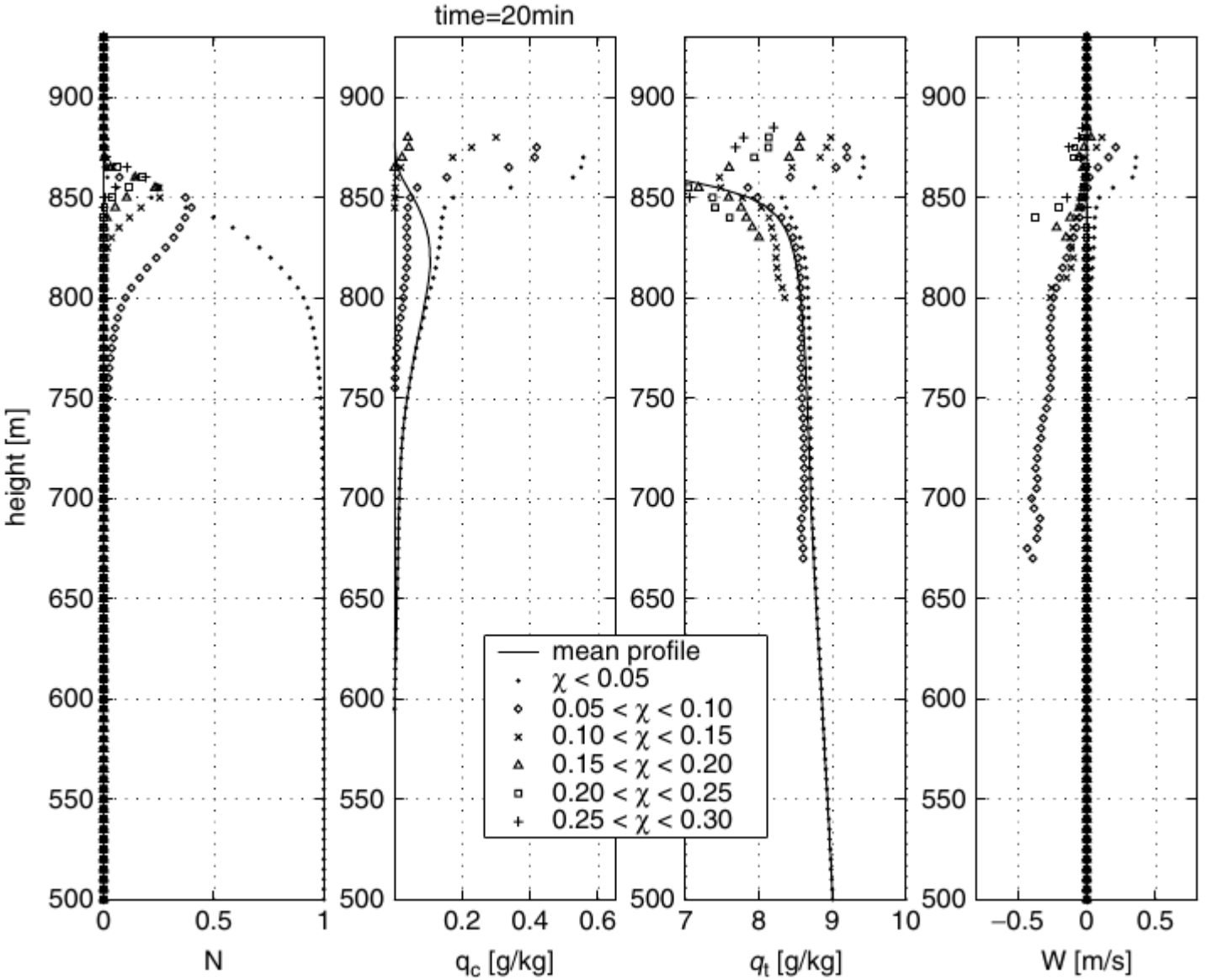

Conditional profiles (condition – concentration of passive scalar) of N-total lumber of gridboxes, Qc- cloud water content, qtot- total water content and w- vertical velocity at 60 minutes after injection of the scalar.

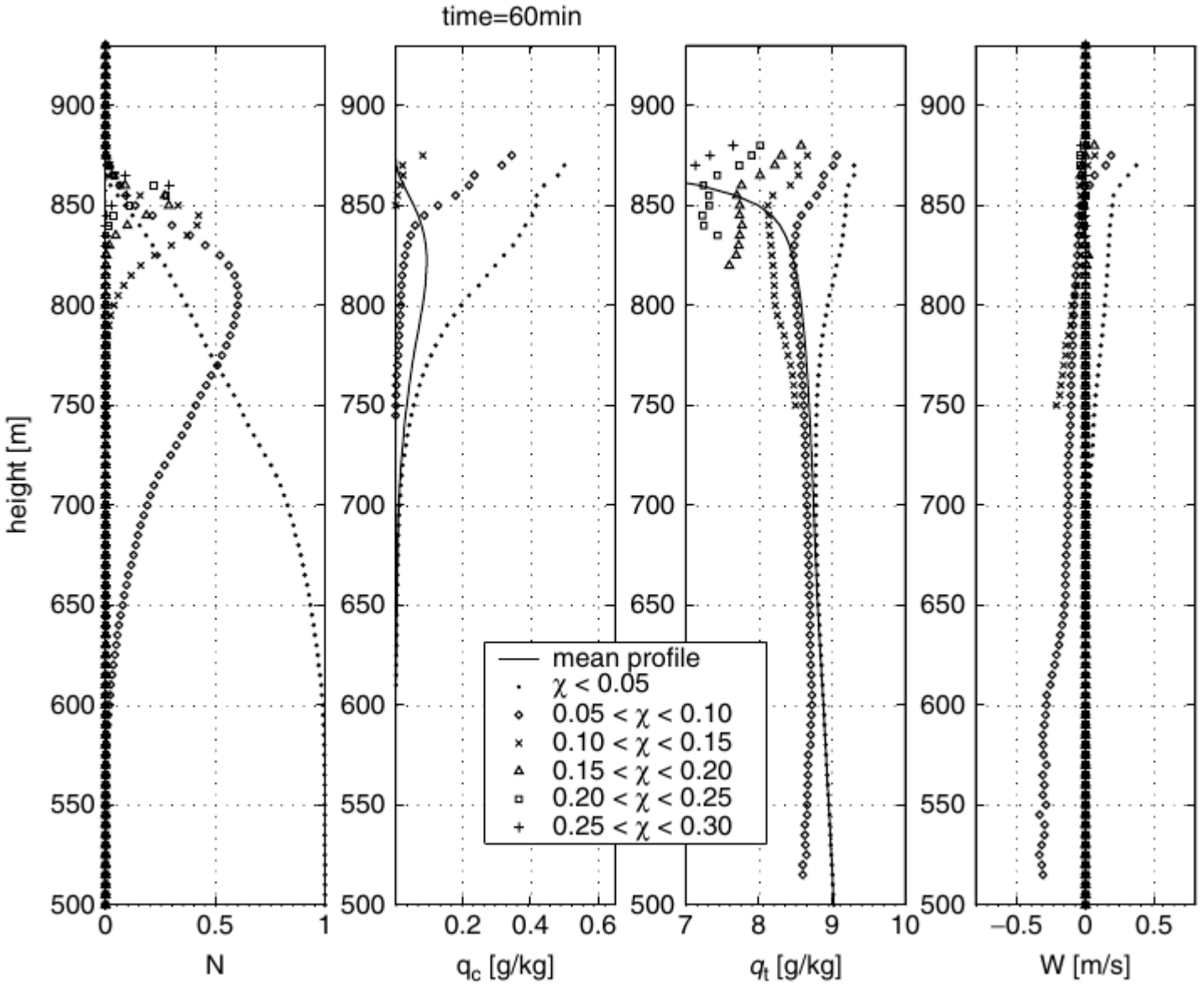

Conditional profiles (condition – concentration of passive scalar) of N-total lumber of gridboxes, Qc- cloud water content, qtot- total water content and w- vertical velocity at 180 minutes after injection of the scalar.

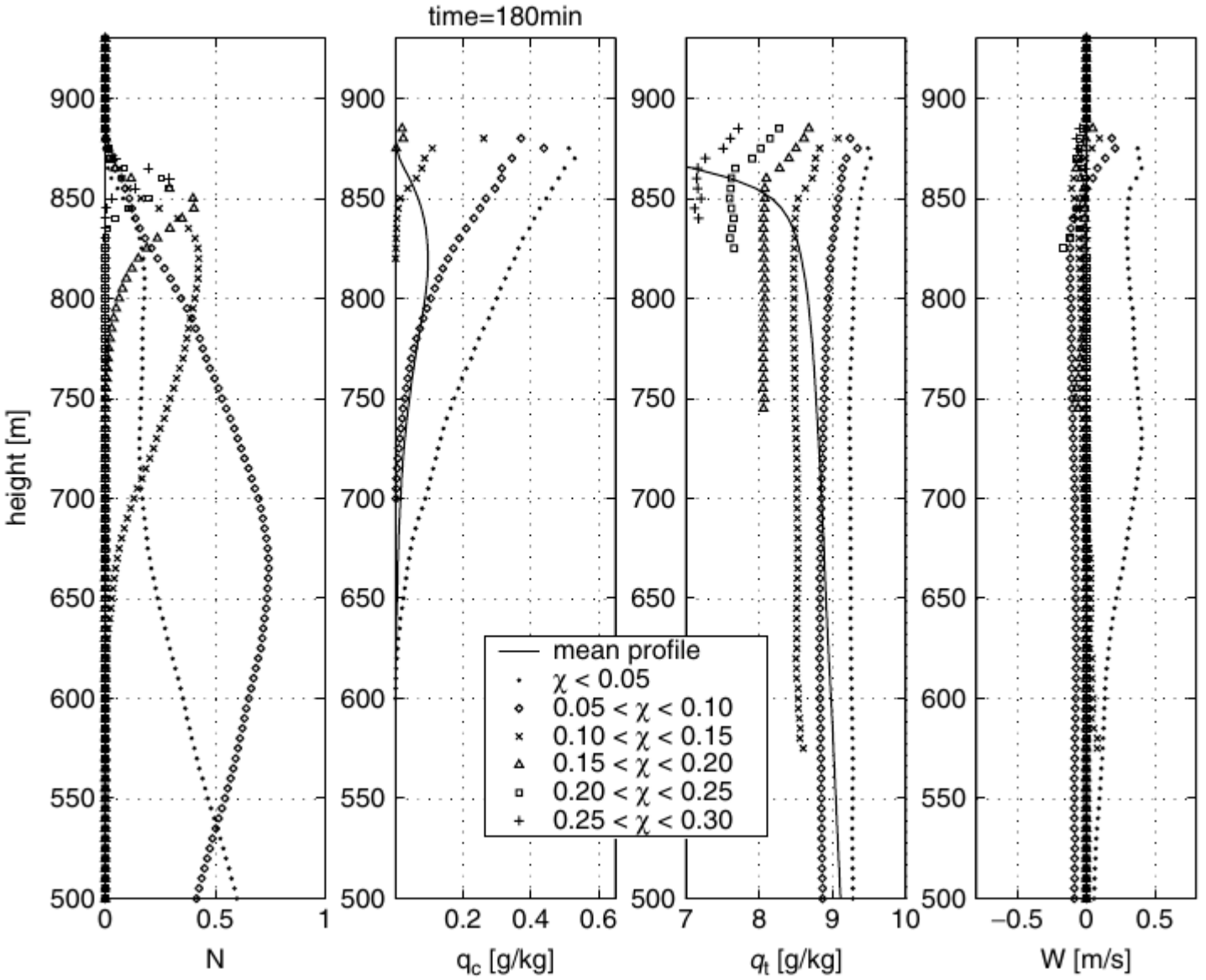

Conclusions:

- EIL (Entrainment Interface Layer) can be defined as a layer between the level of a threshold value of total water content (QS) and the level of maximum static stability (TS), its depth is typically between of few meters and a few tens of meters.

- The entrainment and mixing near the STBL top occurs at upper parts of updrafts forced to diverge under strong capping inversion. The divergence produces significant shears which can be large enough to initiate turbulent mixing as illustrated by the small Richardson number.

- Small mixing fraction χ (in range 0.08-0.16) of the air entrained from above the inversion results in a weakly negative buoyancy of the mixture.

- Such a mixture air sinks into STBL forming cloud holes,areas void of cloud water in shape of trenches or lines surrounding regions of diverging updraft circulations.

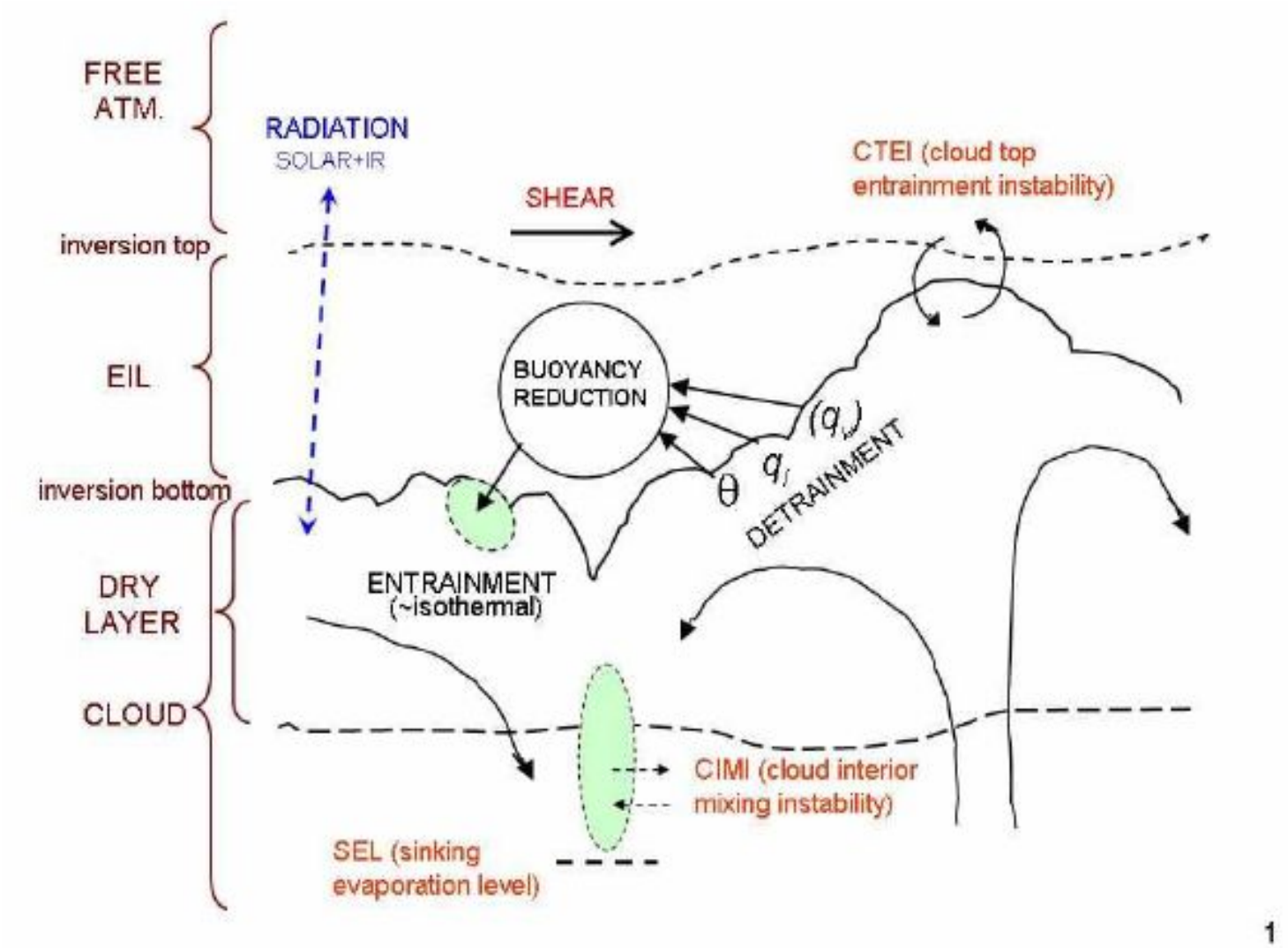

Figure 4 - Conceptual sketch of stratocumulus cloud top and the entrainment processes. EIL is the entrainment interface layer.

POST (Physics of Stratocumulus Top) - aircraft field study off the California Coast in 2008.
A single aircraft was used to primarily investigate unbroken stratocumulus clouds (Sc) near cloud top. The aircraft was instrumented with a full suite of probes for measuring state parameters of the atmosphere, drop spectra, CCN , irradiances, wind velocity and turbulence.

microphysics

aerosol (CCN)

droplet counting

FAST:

Turbulence

Humidity

LWC

Temperature

Measurement strategy

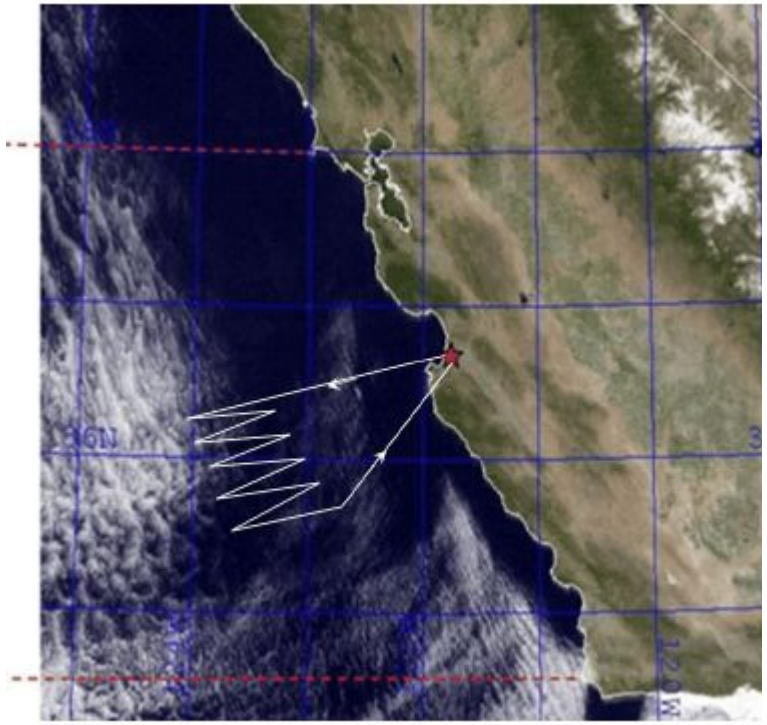

NexSat image (courtesy Naval Research Laboratory, Monterey) of CA and the Pacific Ocean showing the typical horizontal flight track used for each quasi Lagrangian Twin Otter flight. The red star indicates the Marina airport near Monterey Bay.

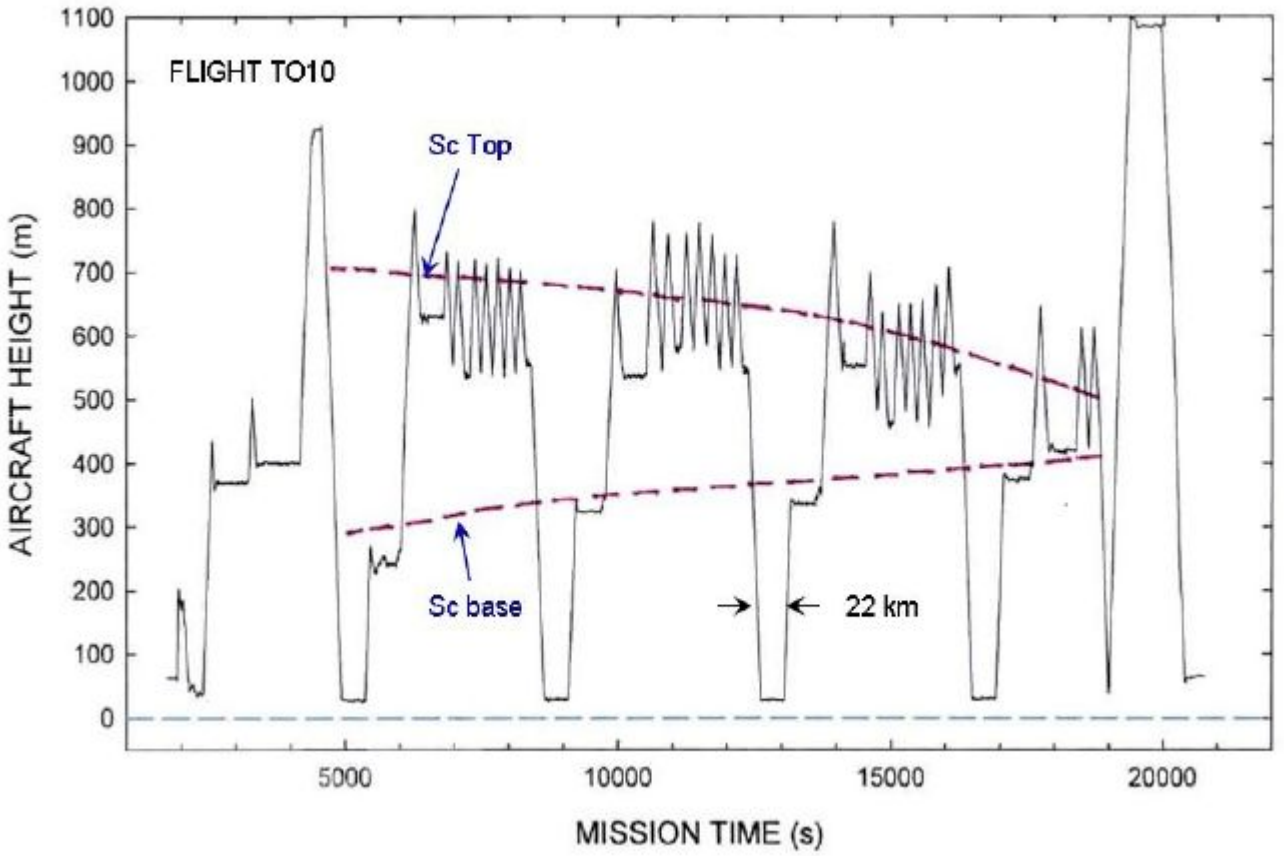

Typical vertical flight pattern of the Twin Otter during POST flights. Porpoising through cloud top is the dominant feature.
Notice that cloud deck does not have to be stable in course of flight.

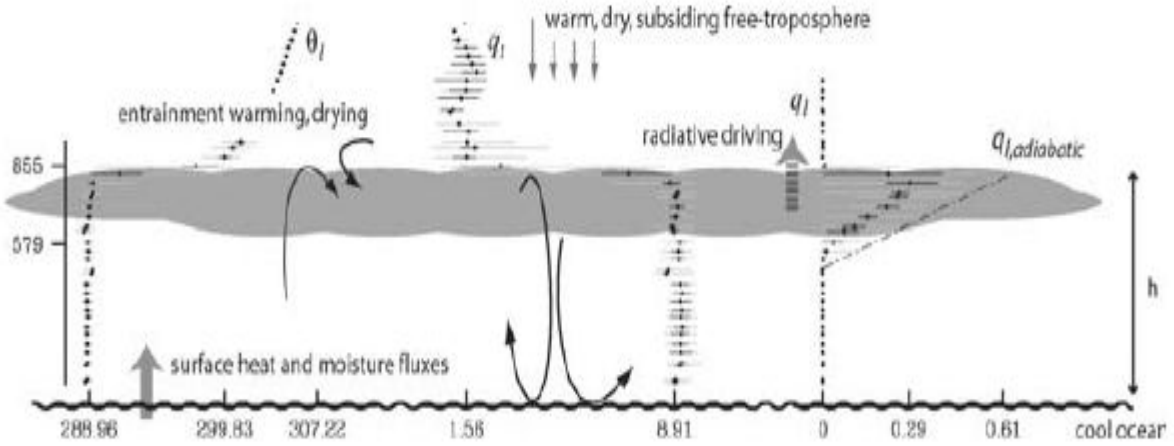

Figure 4 Cartoon of well-mixed, nonprecipitating, stratocumulus layer, overlaid with data from research flight 1 of DYCOMS-II. Plotted are the full range, middle quartile, and mean of θ_l, q_t, and q_l from all the data over the target region binned in 30-m intervals. Heights of cloud base and top are indicated, as are mixed layer values and values just above the top of the boundary layer of various thermodynamic quantities. The adiabatic liquid water content is indicated by the dash-dot line.

Stevens, 2005

Gerber et al., 2010

Classical

Day	*Night*
TO9	TO6
TO10	TO12
TO16	
TO17	

Non-Classical

Day	*Night*
TO1	TO3
TO2	TO5
TO7	TO13
TO8	TO14
	TO15

The difference between classical and non-classical cases is clearly the degree of turbulence and mixing in the Sc. The likely cause for strong turbulence is wind shear near cloud top. The neglect of this effect in the conditional sampling approach to calculate w_e may have caused errors in the previously published values of w_e using this approach.

Flight TOF-10, 2008/08/04 17:15 - 22:15 UTC
(daytime: local time = UTC -8)

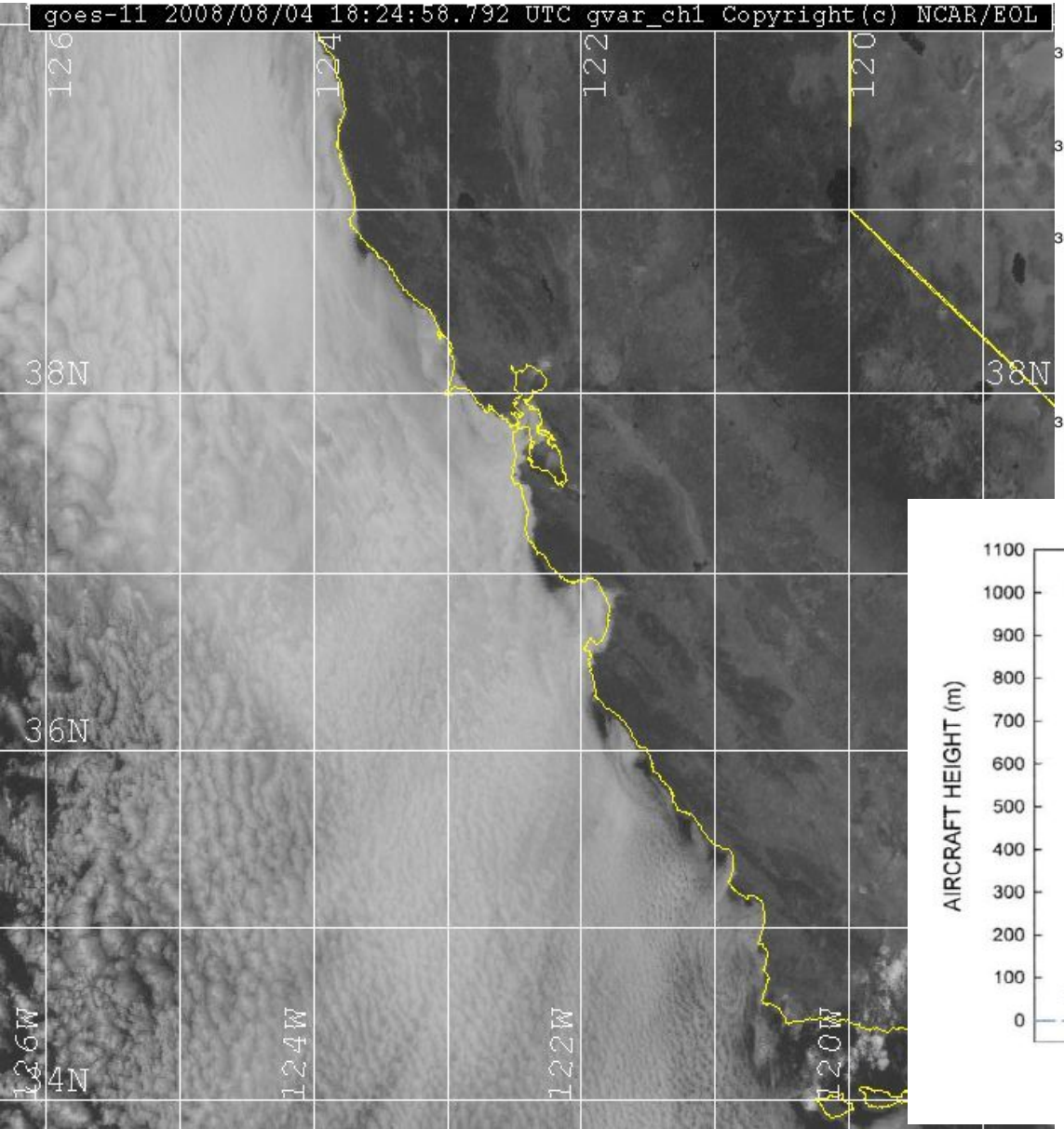

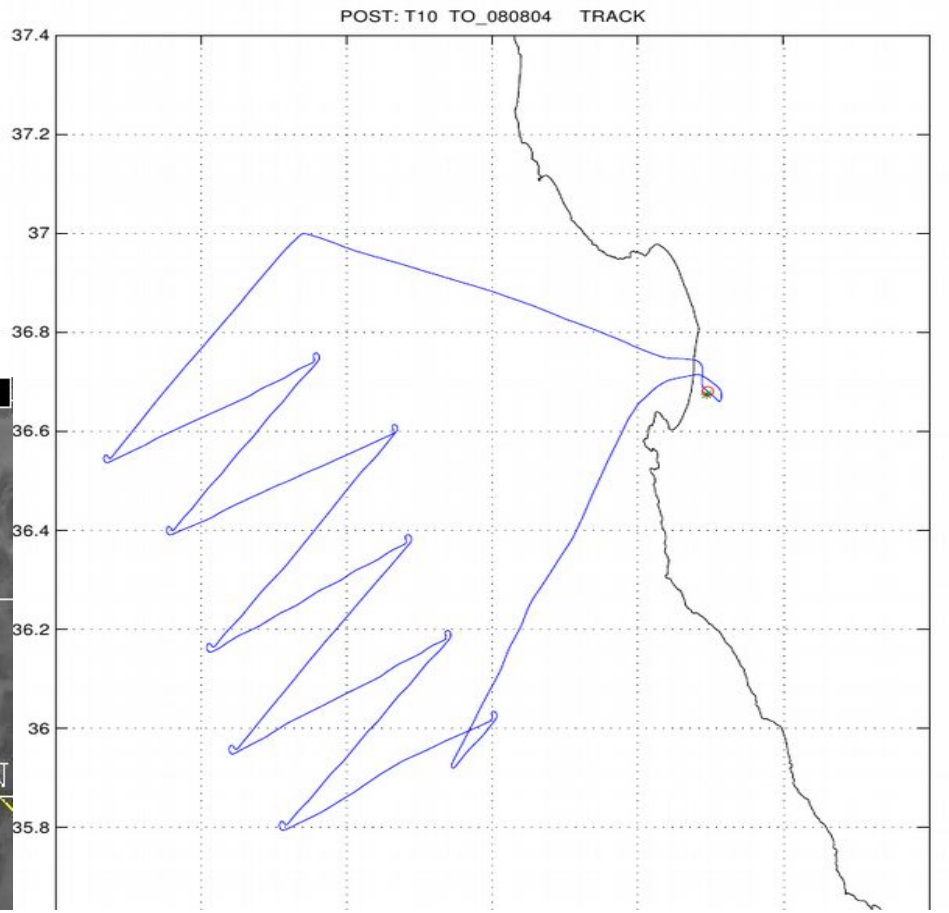

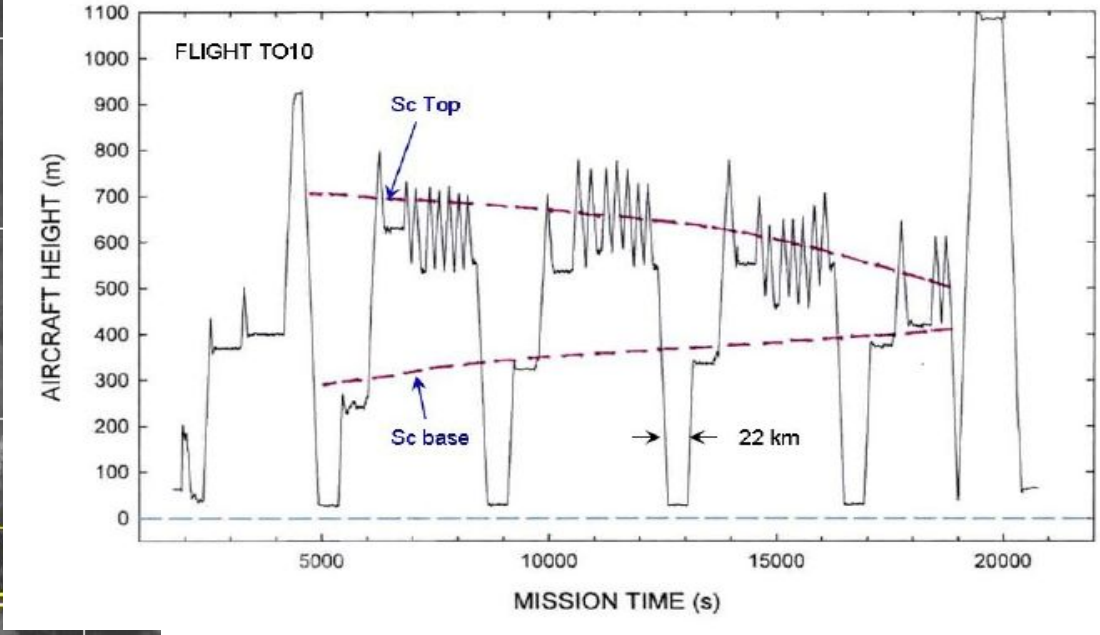

CLASSICAL

TOF10 – typical sounding: remarkable inversion (10K) and a shear layer just above the cloud top

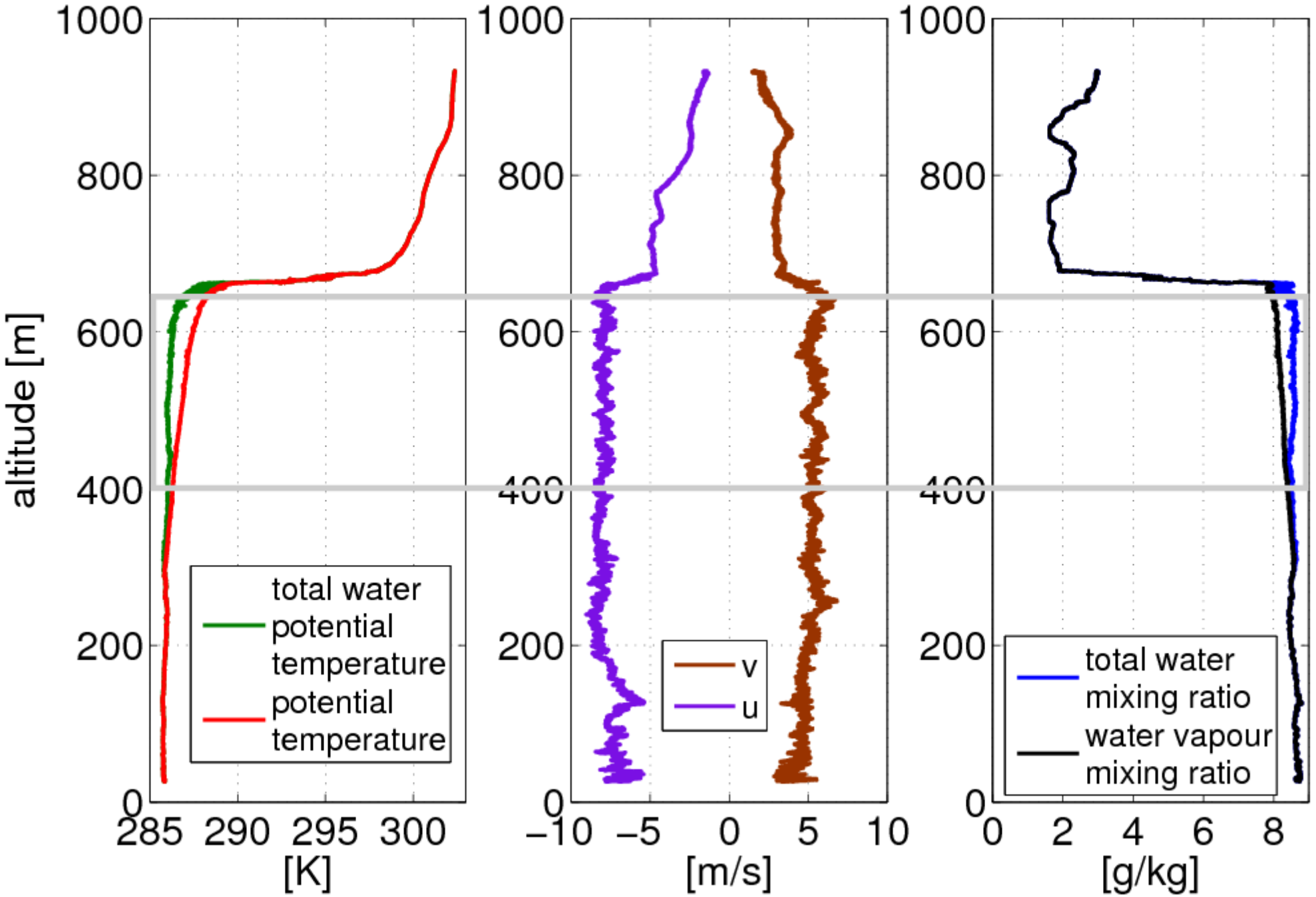

FT TIL CTML CTL

EIL

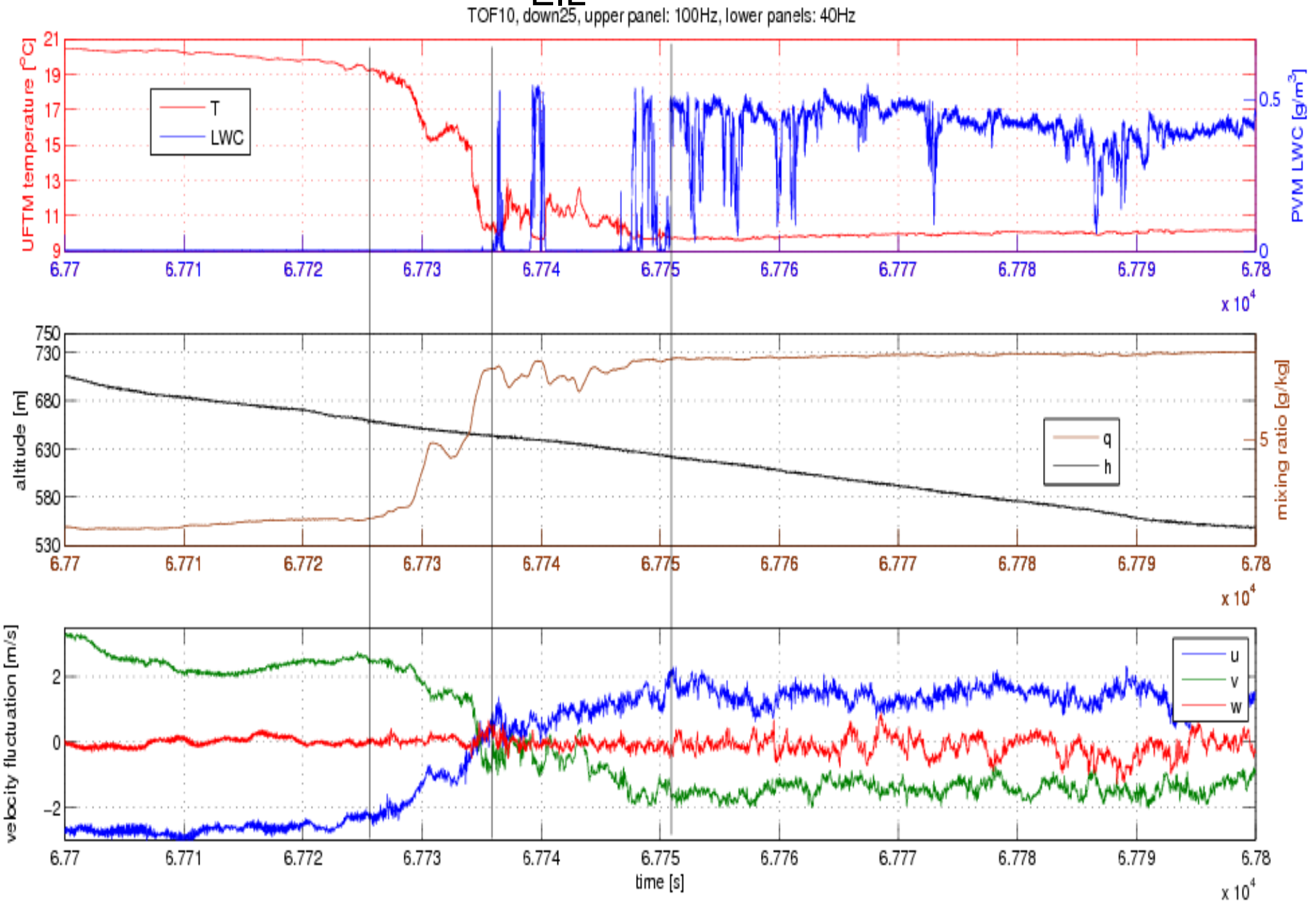

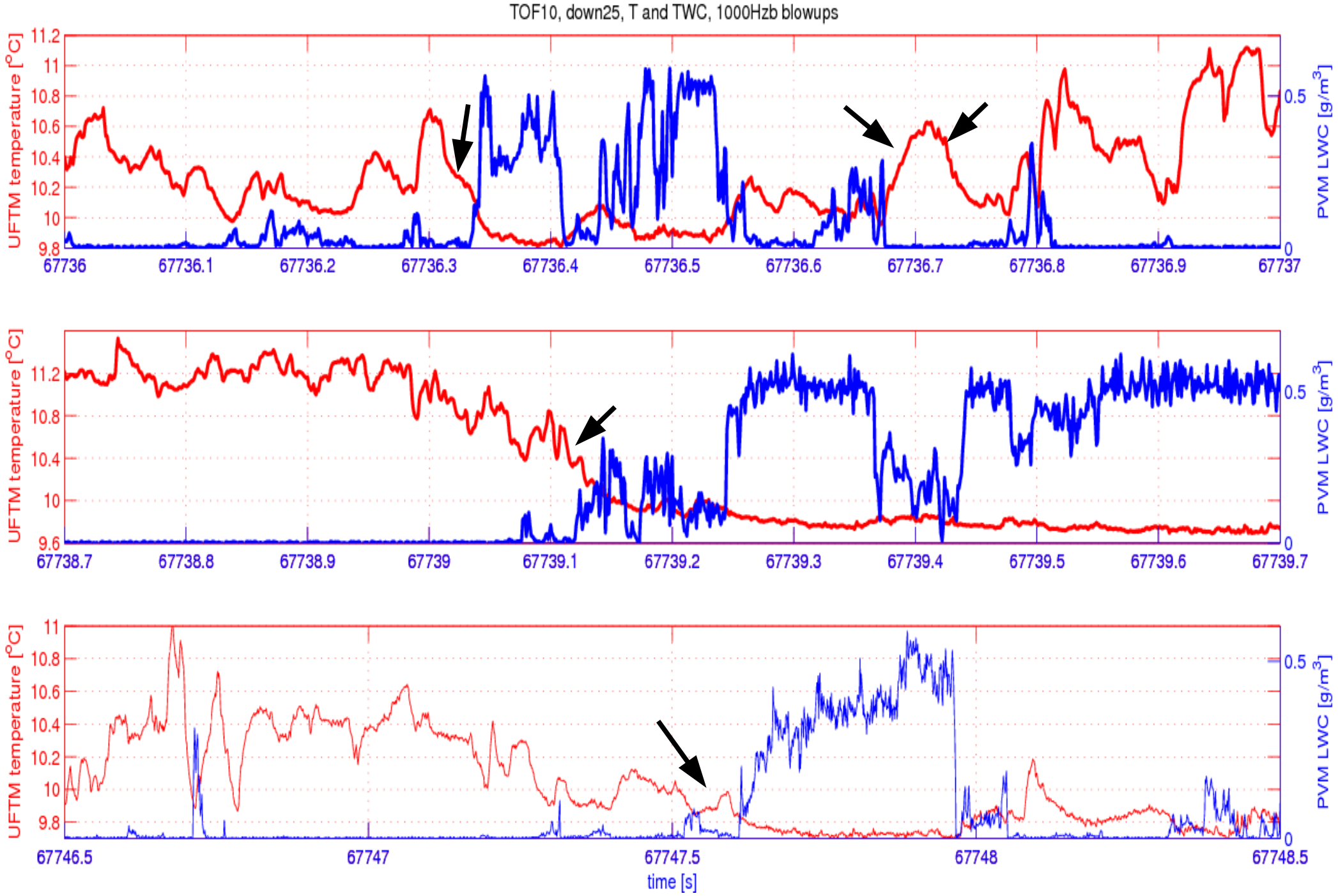
TOF10, down25, T and TWC, 1000Hzb blowups
UFTM temperature [°C]
PVM LWC [g/m3]
11.2
11
10.8
10.6
10.4
10.2
10
9.8
0.5
0
67736
67736.1
67736.2
67736.3
67736.4
67736.5
67736.6
67736.7
67736.8
67736.9
67737
UFTM temperature [°C]
PVM LWC [g/m3]
11.2
10.8
10.4
10
9.6
0.5
0
67738.7
67738.8
67738.9
67739
67739.1
67739.2
67739.3
67739.4
67739.5
67739.6
67739.7
UFTM temperature [°C]
PVM LWC [g/m3]
11
10.8
10.6
10.4
10.2
10
9.8
0.5
0
67746.5
67747
67747.5
67748
67748.5
time [s]

TOF10: LWC on ~1.2m long samples (40Hz):
maximum on the top, gradual decrease down except on dilution in mixing events

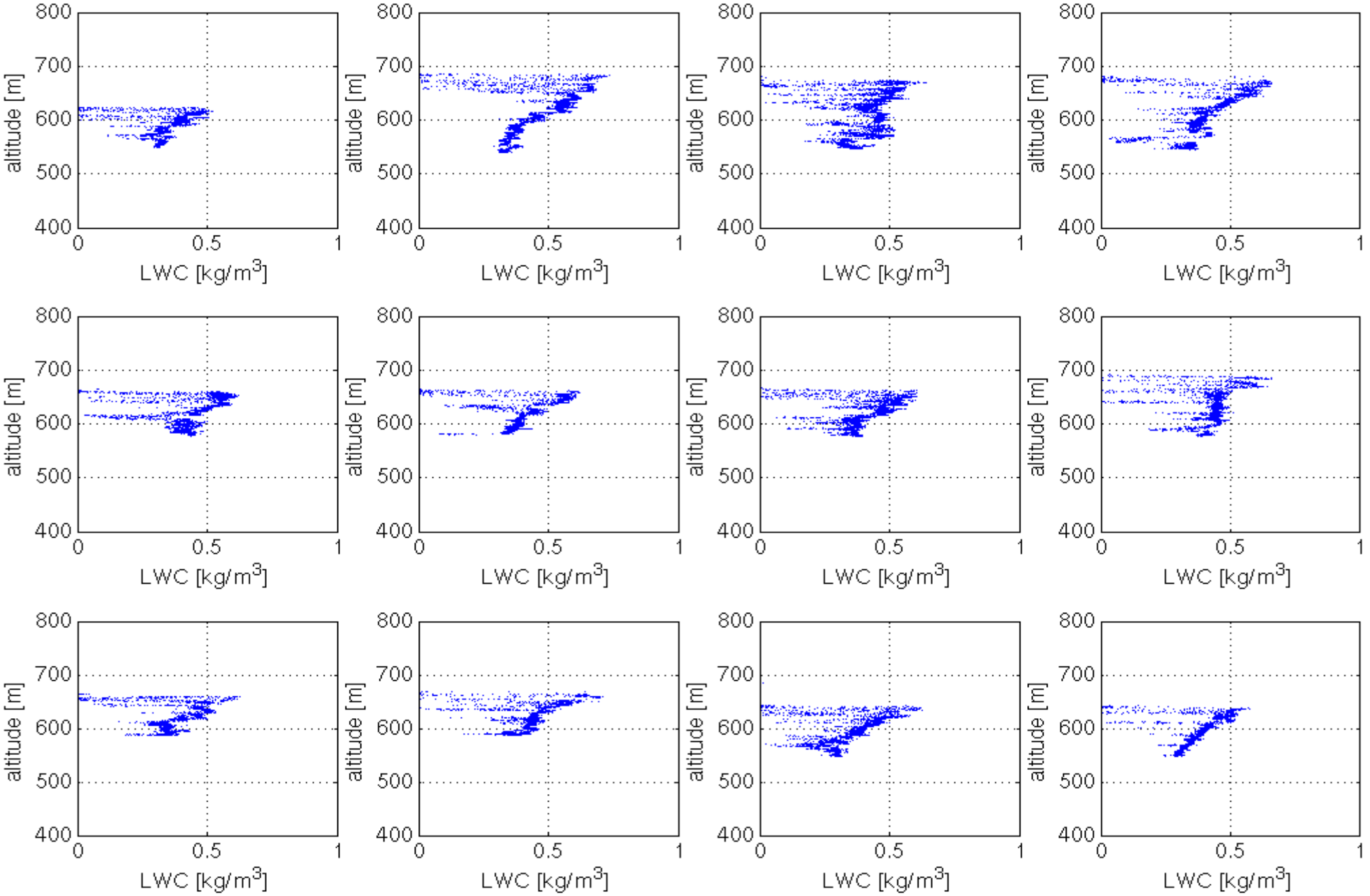

TOF 10: PDF's of LWC and droplet concentrations (courtesy Partick Chuang)

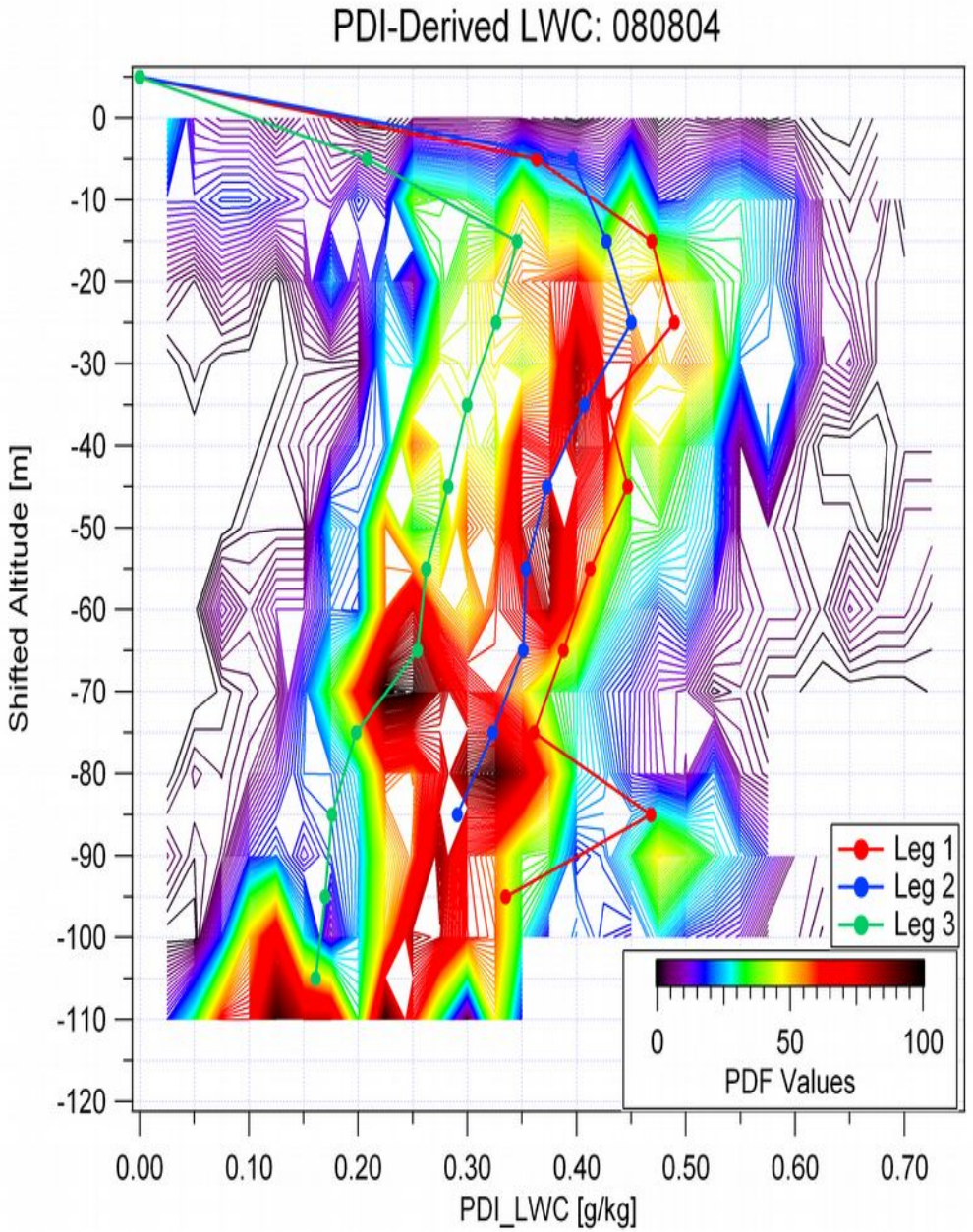

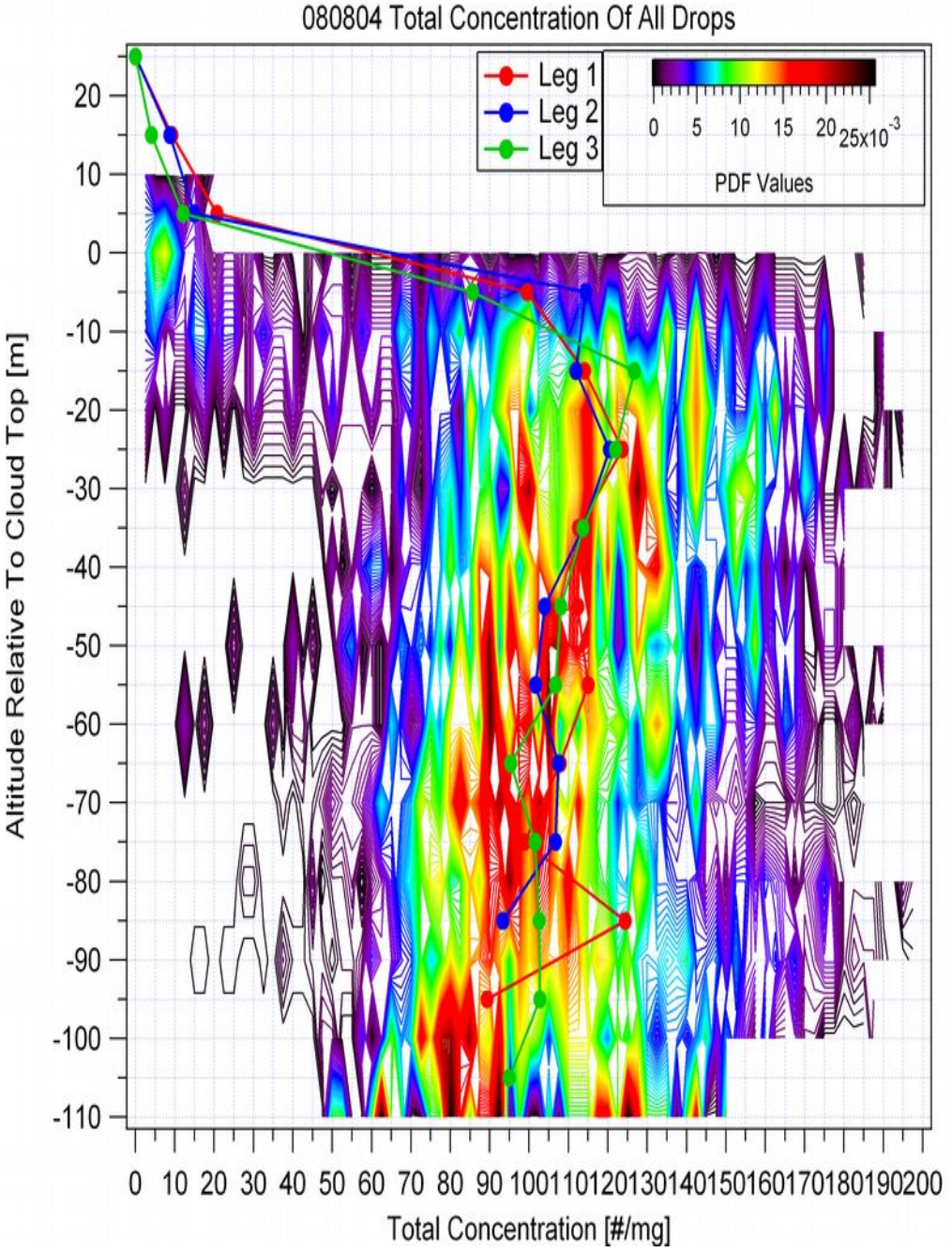

NON-CLASSICAL

Flight TOF-13, 2008/08/09 00:52 – 06:00 UTC (evening)

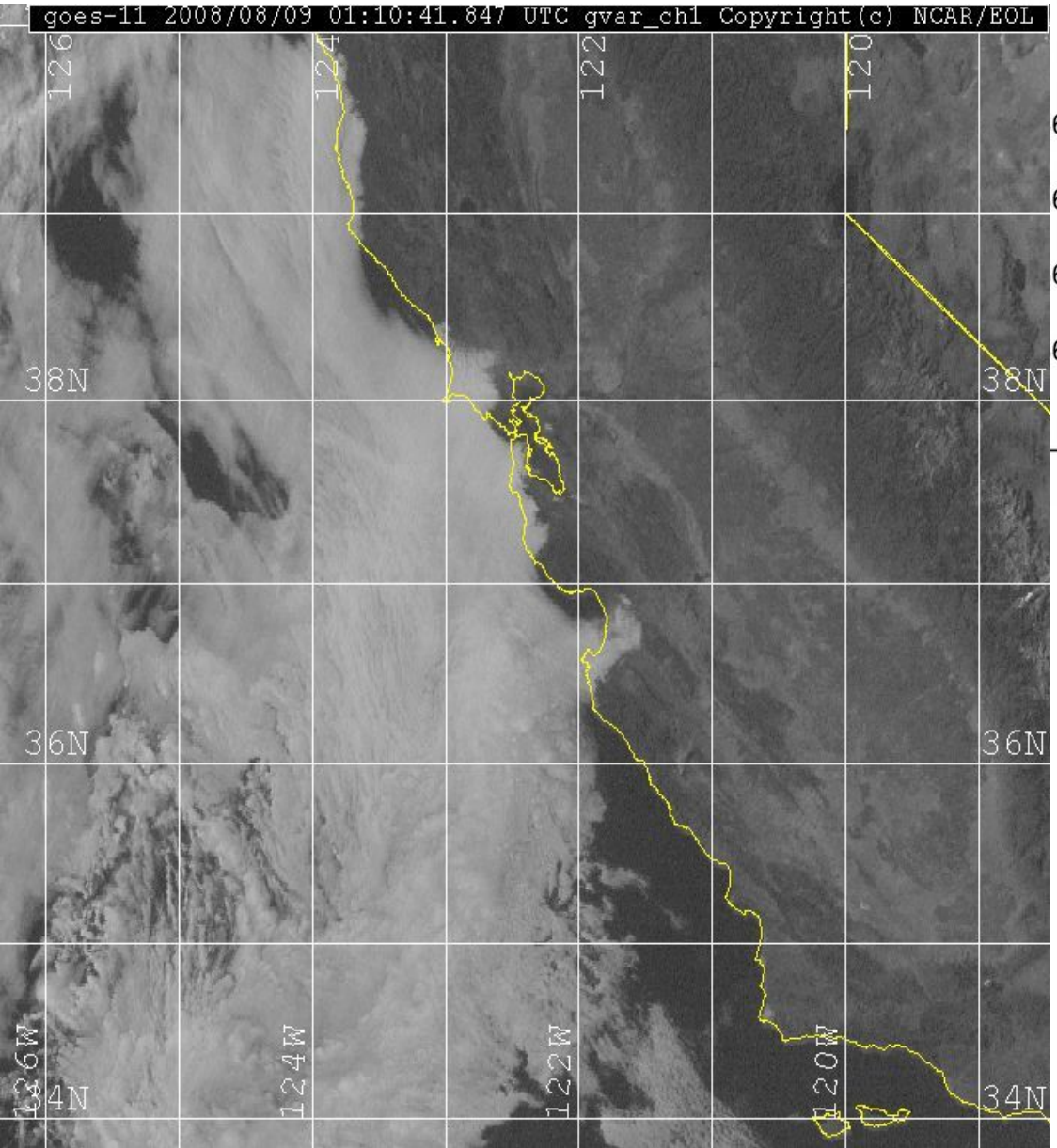

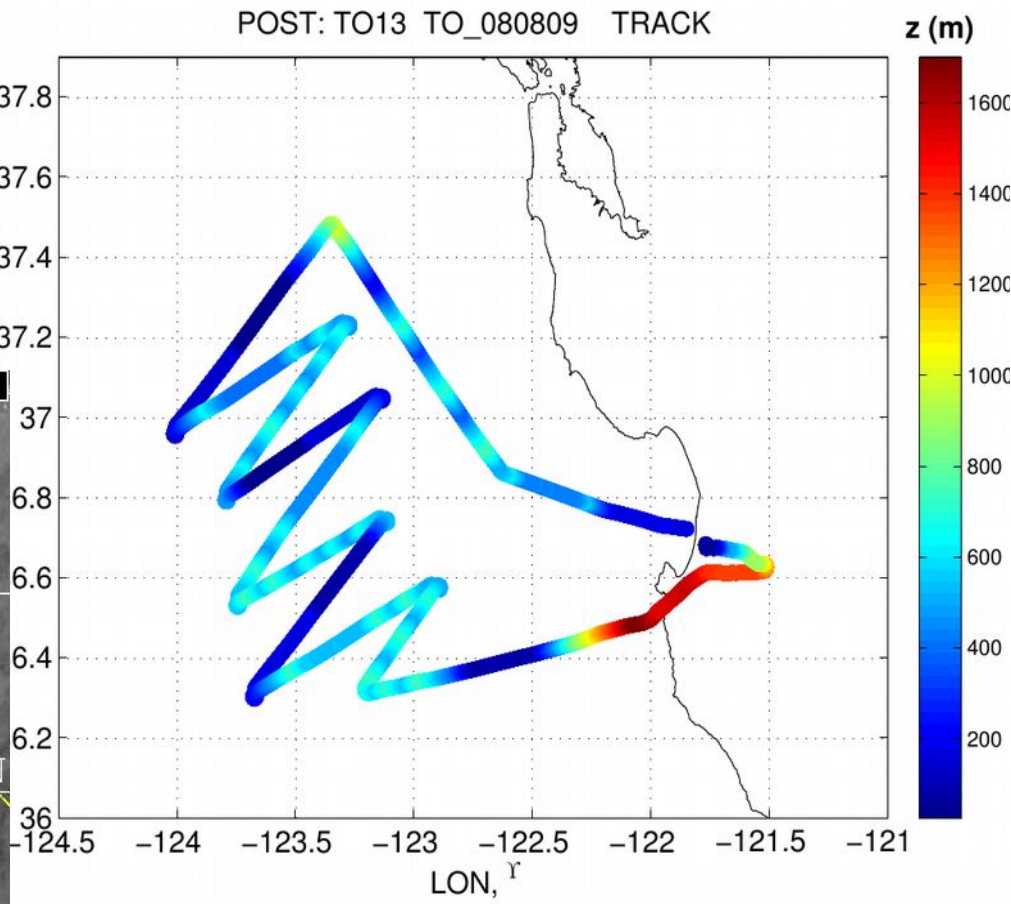


TO13 Photo.
Observer comment:
'cloud top looks like moguls'
Data from POST available at http://www.eol.ucar.edu/projects/post/

No, just heterogeneity. General conditions in the cloud-top region: weak inversion, weak wind shear, high humidity.

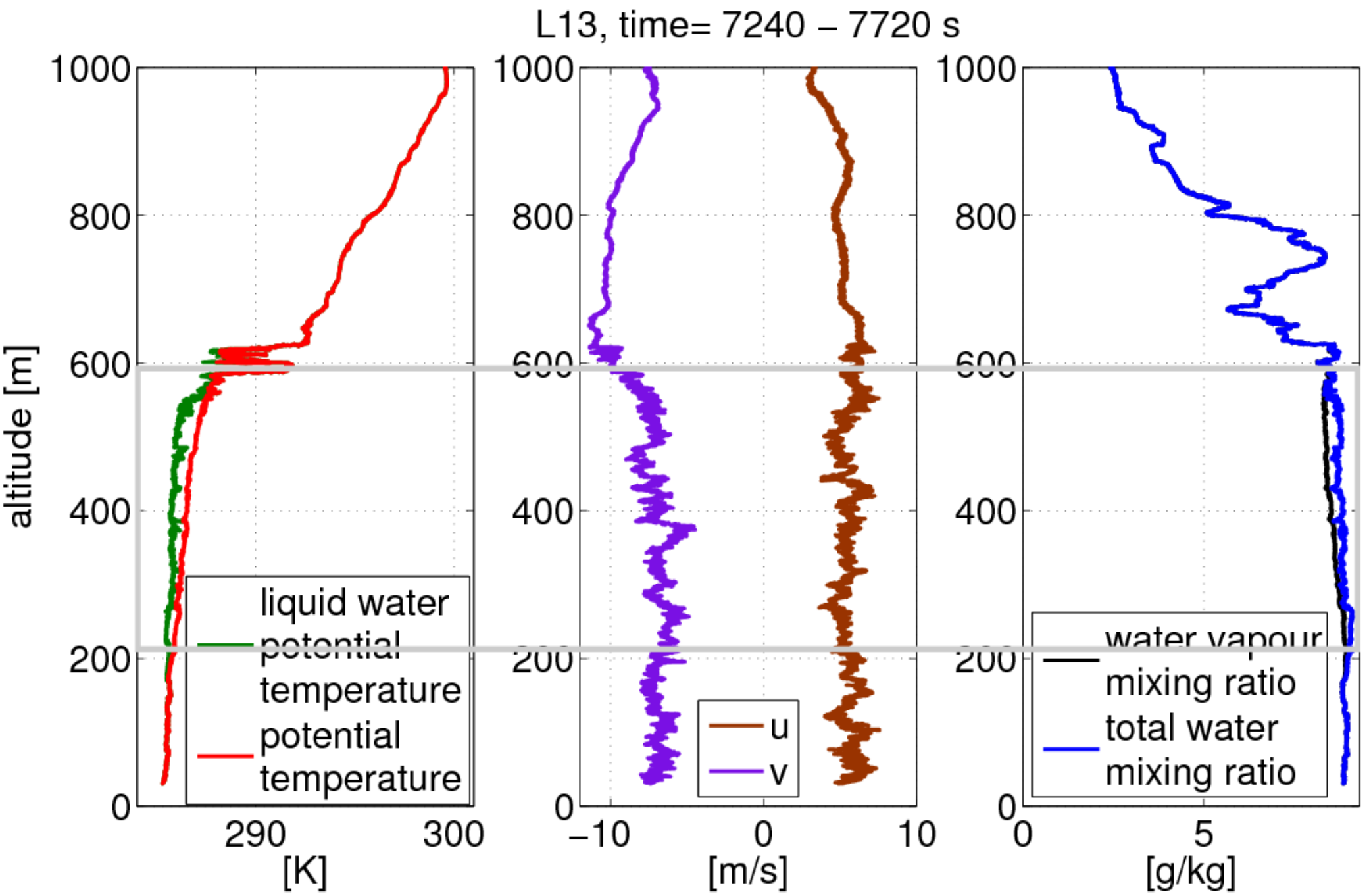

FT TIL CTML CTL

EIL

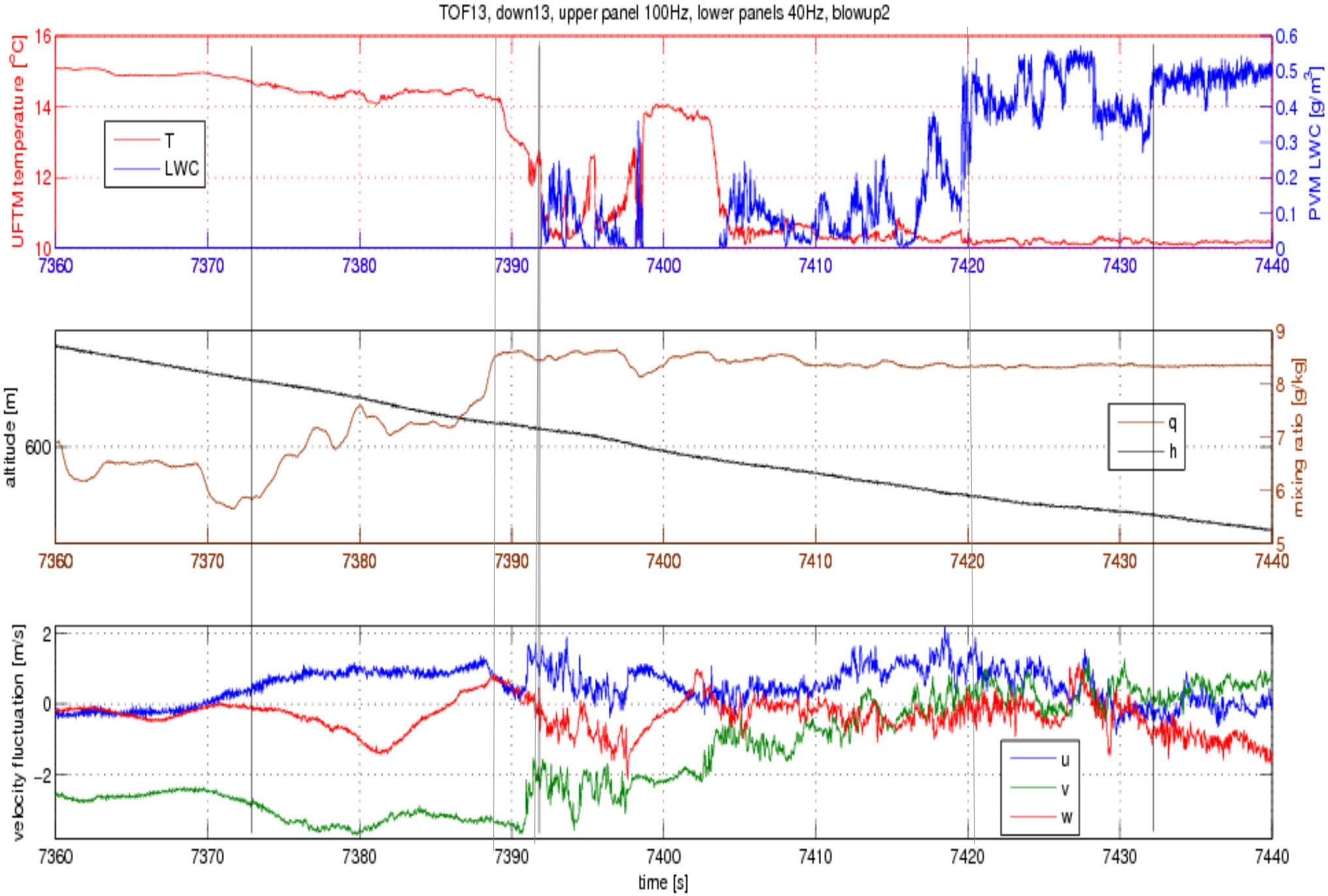

Notice steep temperature jumps: sharp edges of filaments (compared to TOF10)

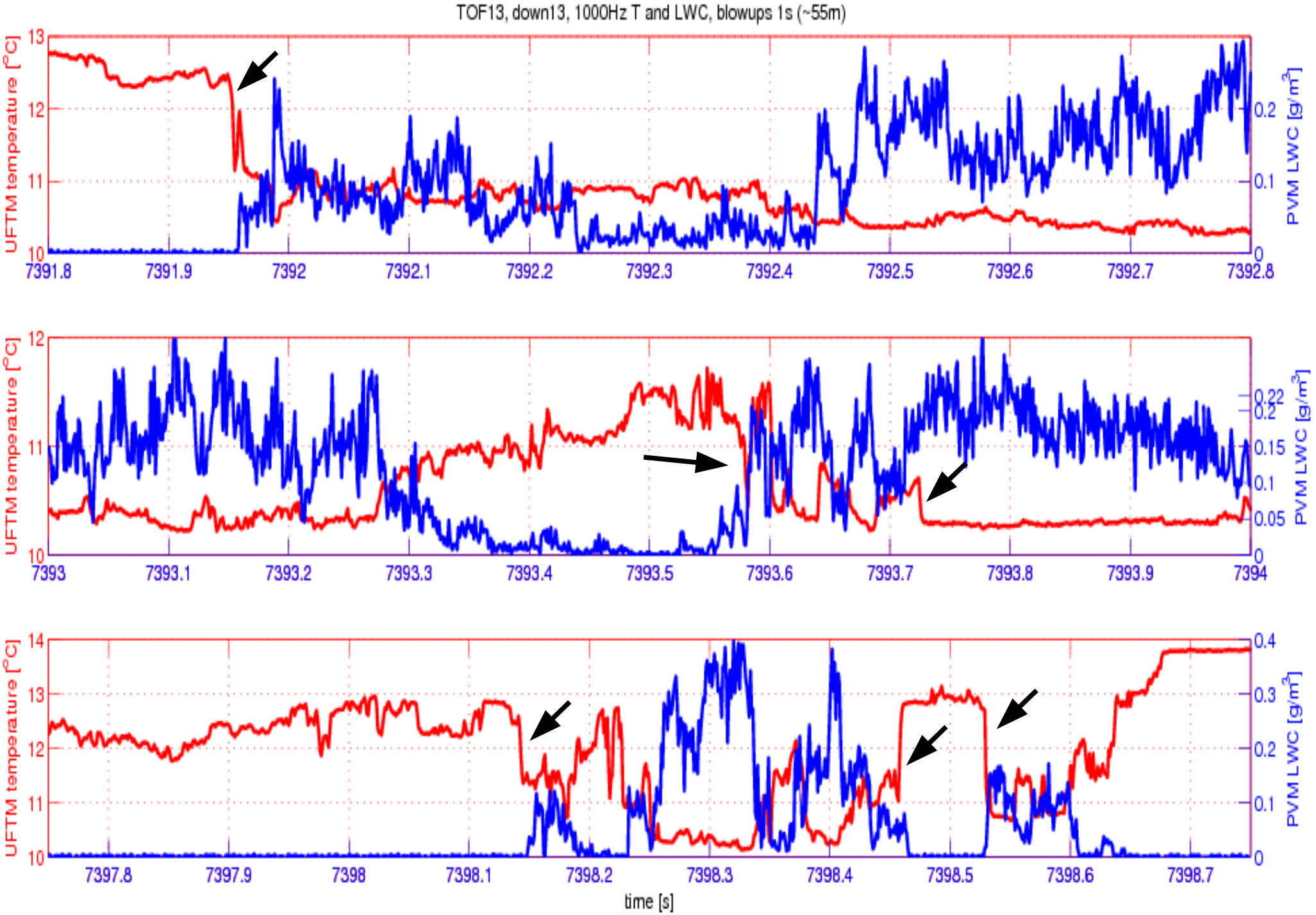

TOF 13: PDF's of LWC and droplet concentrations (courtesy Partick Chuang)

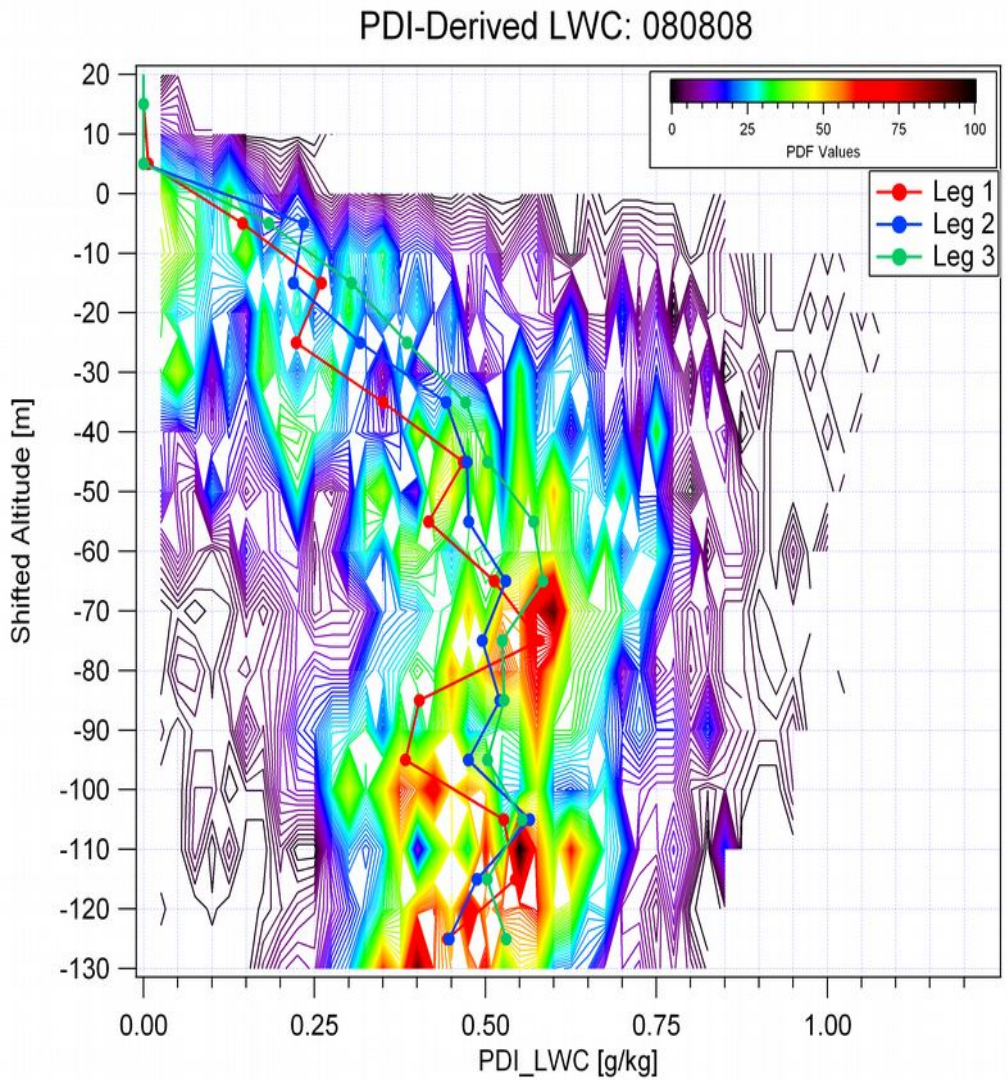

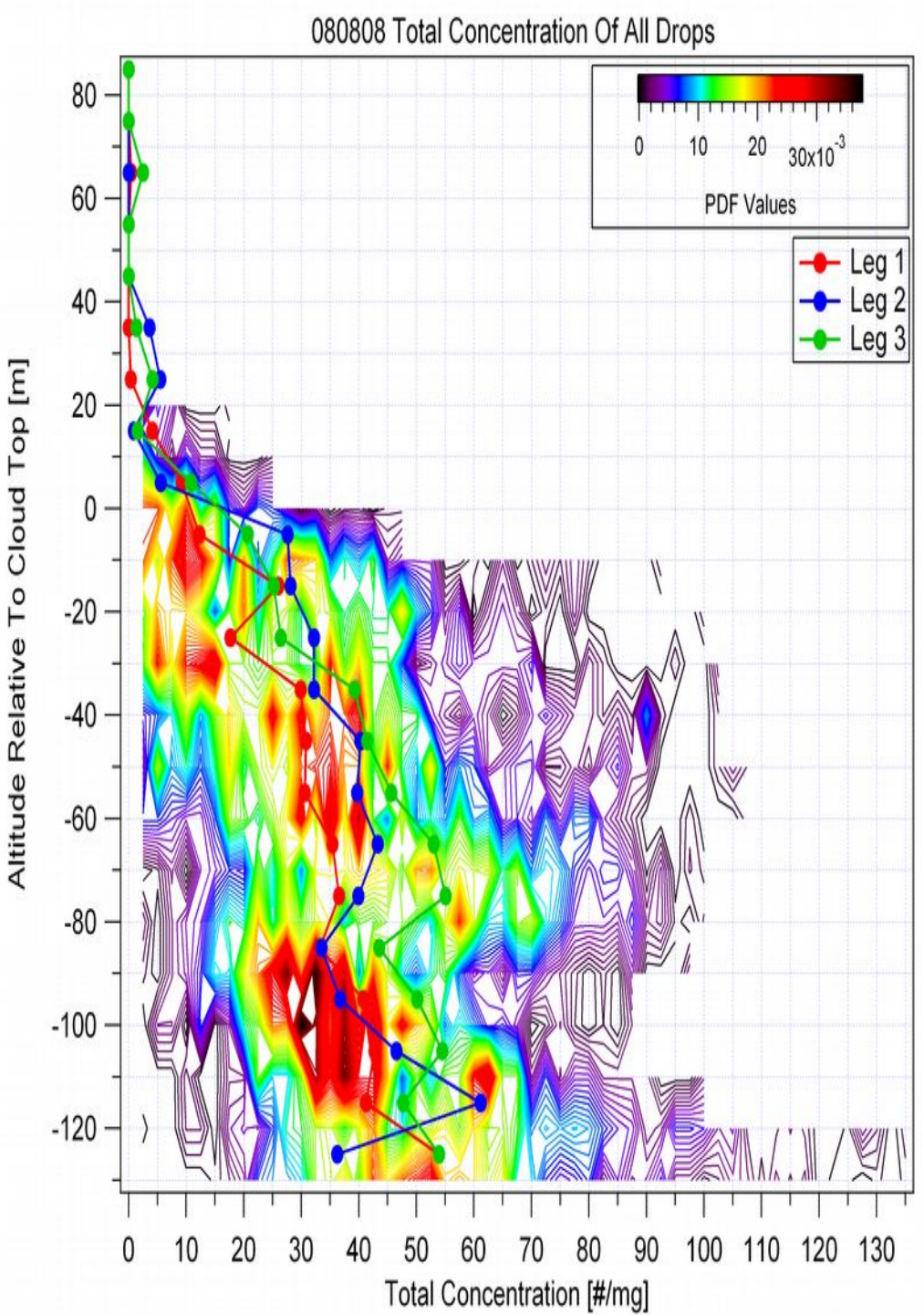

TOF13: LWC on ~1.2m long samples (40Hz):
Stronlgly diluted, no maximum on the top.

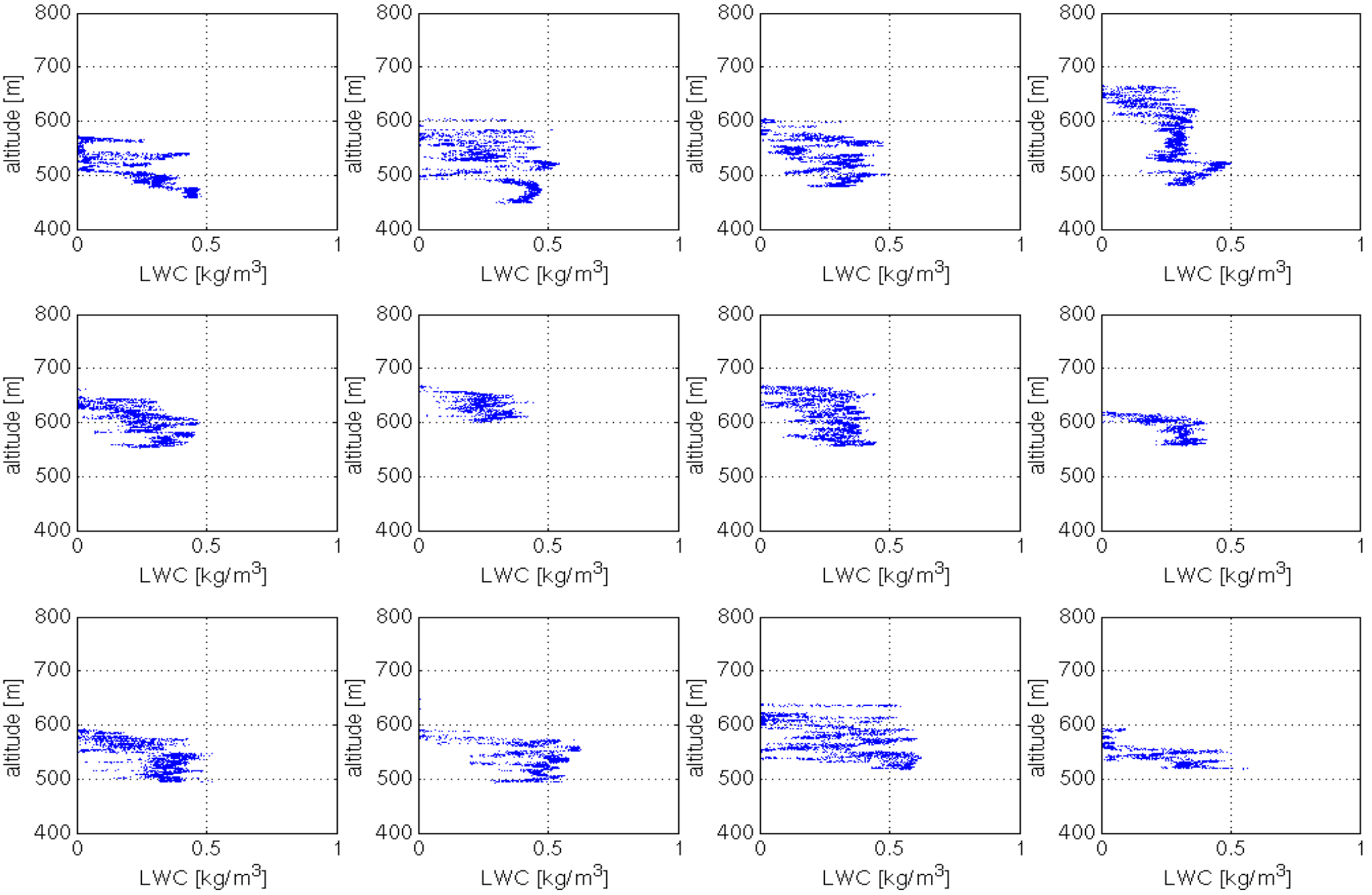

Is stratocumulus top structure observed in TOF13 unique???

NO!!! See e.g. Roode and Wang 2007, FIRE, RF08B:

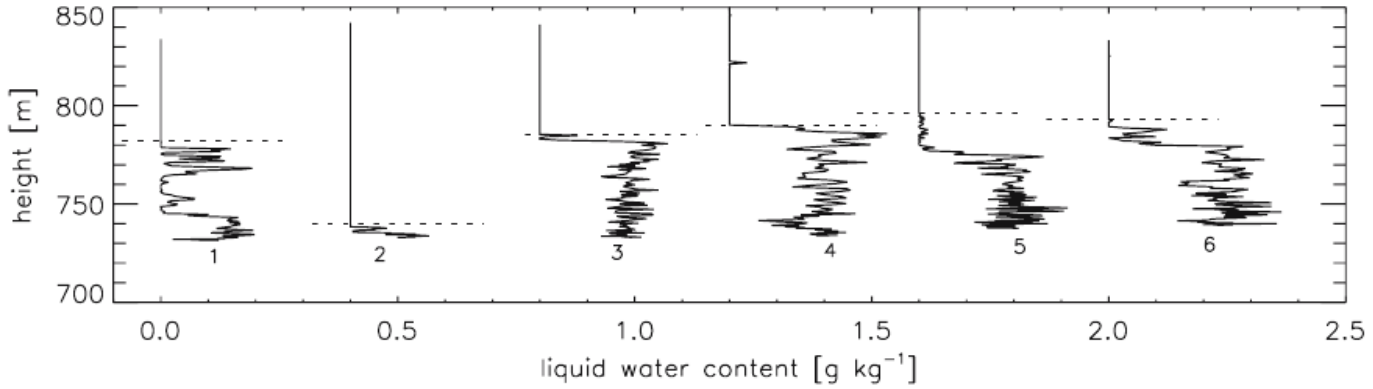

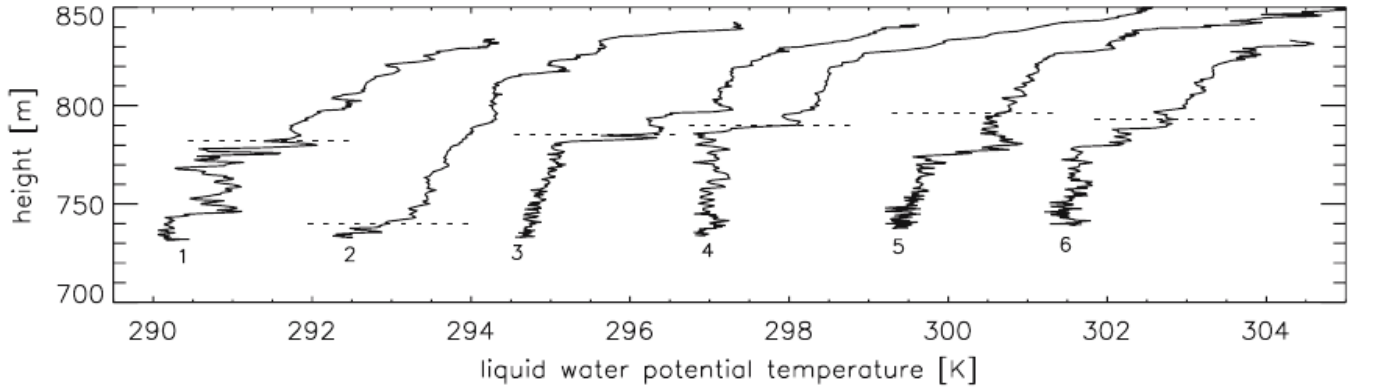

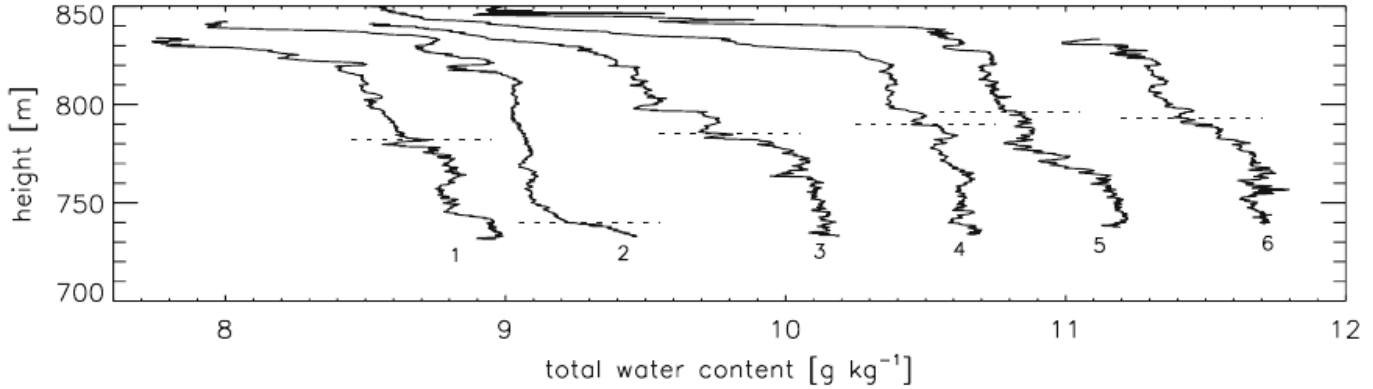

Also Katzwinkel, Siebert and Shaw, 2011
- similar picture from helicpoter-borne measurements

Layer Division

- Divide each up/down flight segment through cloud top

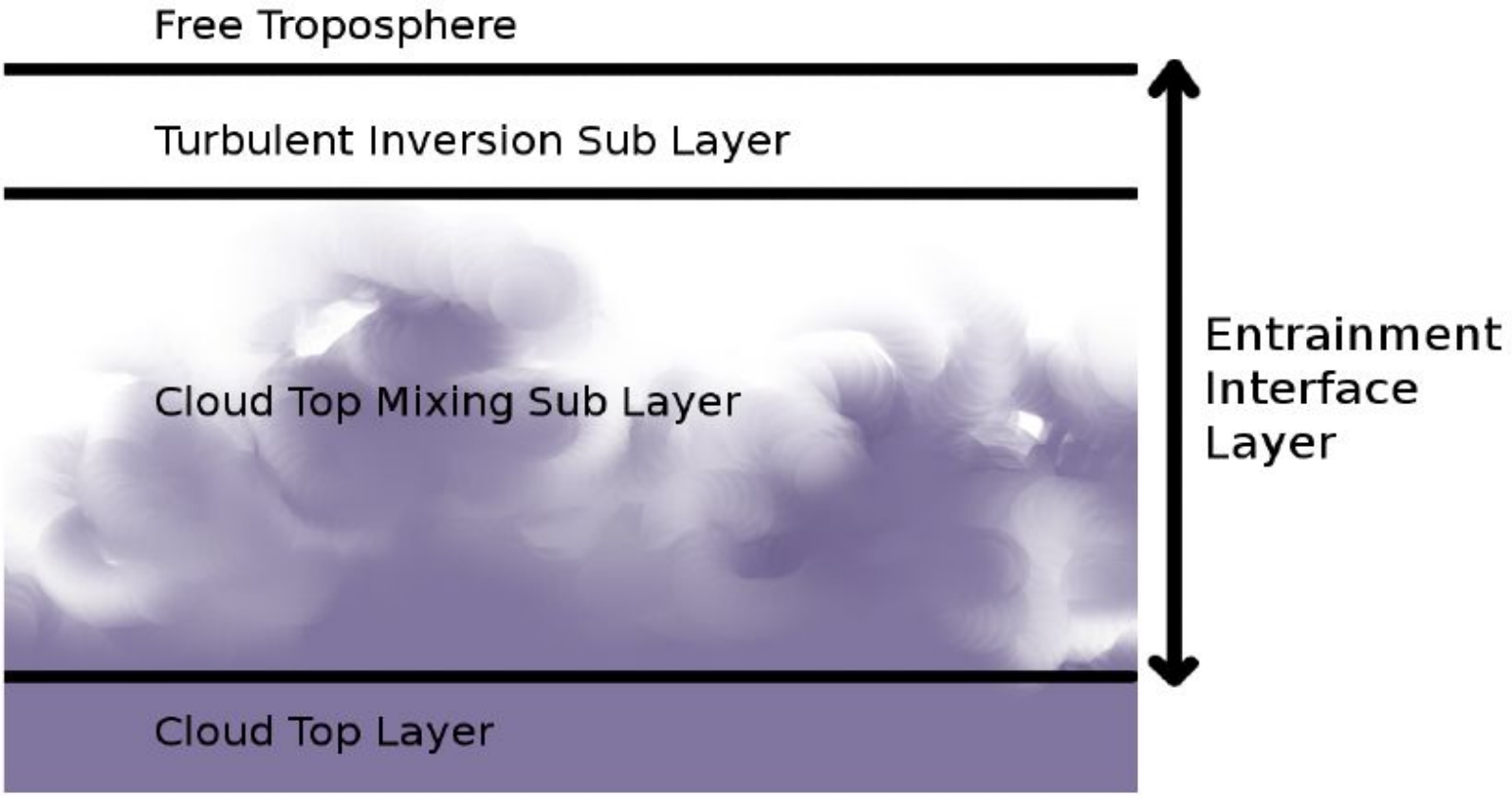

[K. Nurowska, Diploma Thesis]

Layer Division

- Establish systematic layer division using 300 point moving averages of 40 Hz data, corresponding to 450 m resolution vs. 100 m large turbulent eddies
- Free Troposphere (FT) / Turbulent Inversion Sublayer
  - Highest point where turbulent kinetic energy $\geq 0.01\ m^2/s^2$ and grad $\theta_L \geq 0.2\ K/m$
- TISL / Cloud Top Mixing Sublayer
  - Highest point where LWC $\geq 0.05\ g/m^3$
- CTMSL / Cloud Top Layer
  - Highest point where horizontal wind shear $\Delta u^2 + \Delta v^2$ reaches 90% max
- Entrainment Interface Layer (EIL): TISL + CTMSL

Flight Segments

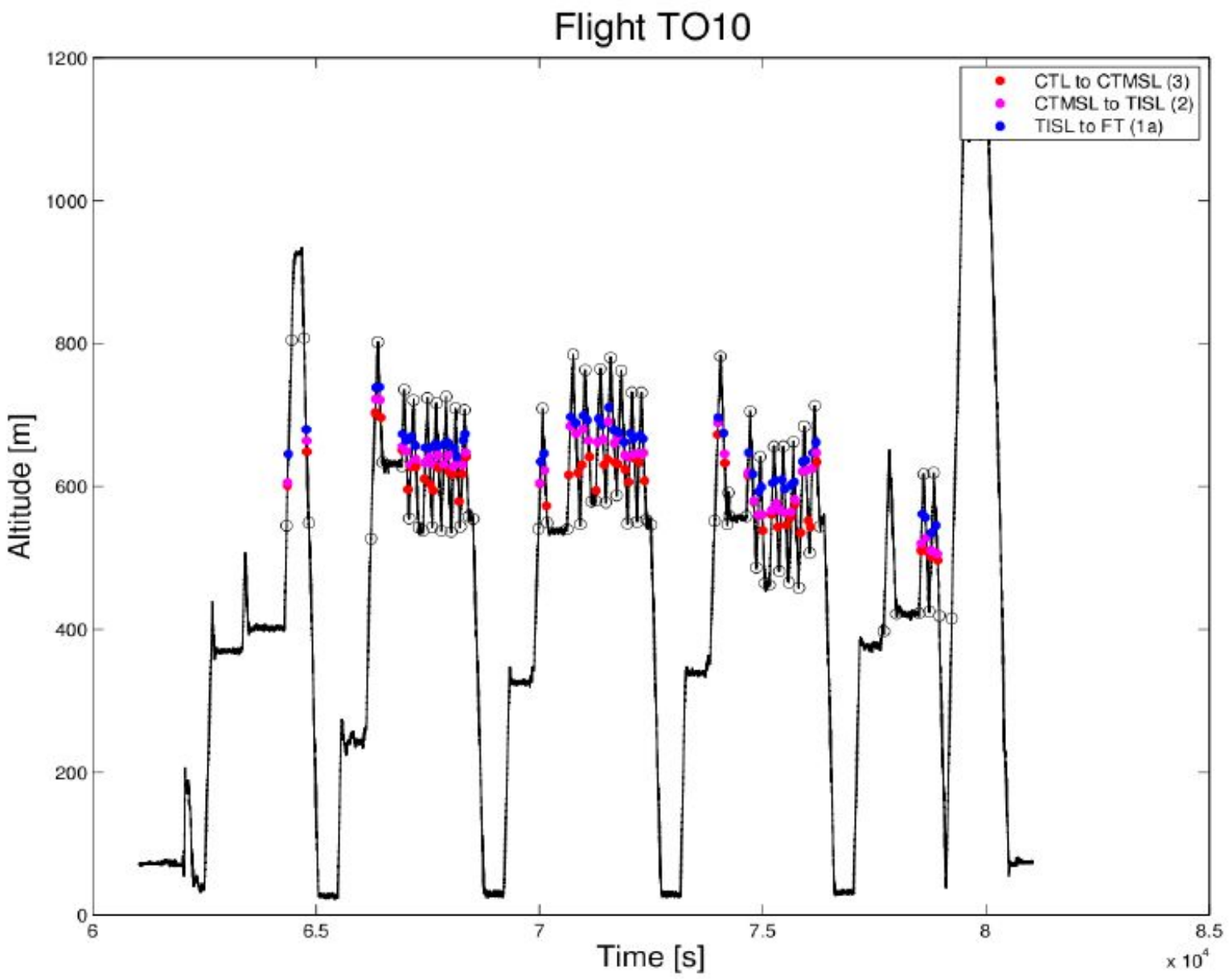

Many non-classical cases were observed.
Pink rectangles show either weak inversion or humid layer above.

Flight	Date (UTC)	z_i (m)	$z_i - z_o$ (m)	Δz (m)	dz_i/dt (cm/s)	T_i (^{0}C)	ΔT (^{0}C)	LWC$_i$ (g/m^3)	q_{vi} (g/kg)	Δq_v (g/kg)	U_i (m/s)	U_s (1/s)	$U_{\theta i}$ (deg.)	$U_{\theta s}$ (deg.)
TO1[1] D	7/16	560	365	34	-.17	10.6	5.9	.48	8.66	+2.02	8.40	.056	336	+22
TO2[1] D	7/17	529	219	32	-.49	9.8	7.4	.33	7.99	-2.72	11.0	.119	336	-23
TO3[1] N	7/19	500	264	52	+.35	10.3	10.1	.46	8.29	-3.65	14.5	.183	333	+14
TO5[1,2] N	7/28	486	253	41	+.76	10.8	2.8	.30	8.70	-.71	11.6	.352	335	+2
TO6[1] N	7/29	638	275	20	-1.32	9.4	7.5	.50	7.88	-5.94	9.50	.151	331	-1
TO7 D	7/30	375	282	50	+.01	12.7	2.9	.33	9.06	-.27	13.2	.108	330	+9
TO8[1,2] D	8/1	413	82	43	-.68	12.8	3.5	.22	9.73	-.83	17.4	.133	340	+8
TO9[3] D	8/2	182	127	57	+.08	11.4	8.3	.21	8.61	-.88	12.7	.092	324	+5
TO10 D	8/4	635	269	34	-2.30	9.7	8.7	.39	8.04	-5.70	9.9	.183	331	+3
TO12 N	8/8	760	329	29	-.62	9.0	8.9	.50	7.81	-4.67	6.5	.235	320	-24
TO13[2] N	8/9	654	409	59	+.93	10.4	2.3	.29	8.50	-.49	10.9	.190	328	+2
TO14 N	8/12	545	416	31	-.08	11.7	6.4	.59	9.22	-1.47	13.9	.069	333	+6
TO15 N	8/13	495	314	62	+.79	10.5	9.5	.30	9.00	-1.30	14.6	.141	341	+13
TO16[4] D	8/14	457	326	70	+.38	11.5	10.2	.42	9.00	-3.04	7.6	.099	325	+5
TO17 D	8/15	454	329	59	+.08	11.8	6.8	.47	9.12	+.21	9.3	.093	330	-7
POST Mean		513	284	45		10.8	6.7	.39	8.64	-1.96	11.4	.145	332	+2
DYCOMS-II Mean		756	360	23		11.6	8.2	.67	9.36	-5.93				

[1] some deviation from Lagrangian flight pattern
[2] uncertainty in Δ jumps
[3] not Lagrangian, N-S flight along coast
[4] no UFT data

Gerber et al, 2013

Richardson Number

- Use layer division to characterize stability for each region of thickness Δz using Richardson number

$$R_i = \frac{\frac{g}{\theta}\left(\frac{\Delta\theta}{\Delta z}\right)}{\left(\frac{\Delta u}{\Delta z}\right)^2 + \left(\frac{\Delta v}{\Delta z}\right)^2}$$

- Generally expect Ri > 1 stable, non-turbulent; 0.25 < Ri < 1 some turbulence; 0 < Ri < 0.25 turbulent; Ri < 0 unstable
- Uncertainty includes cloud top variation over horizontal distance traveled; consider distribution for many penetrations

Richardson Number: Classical

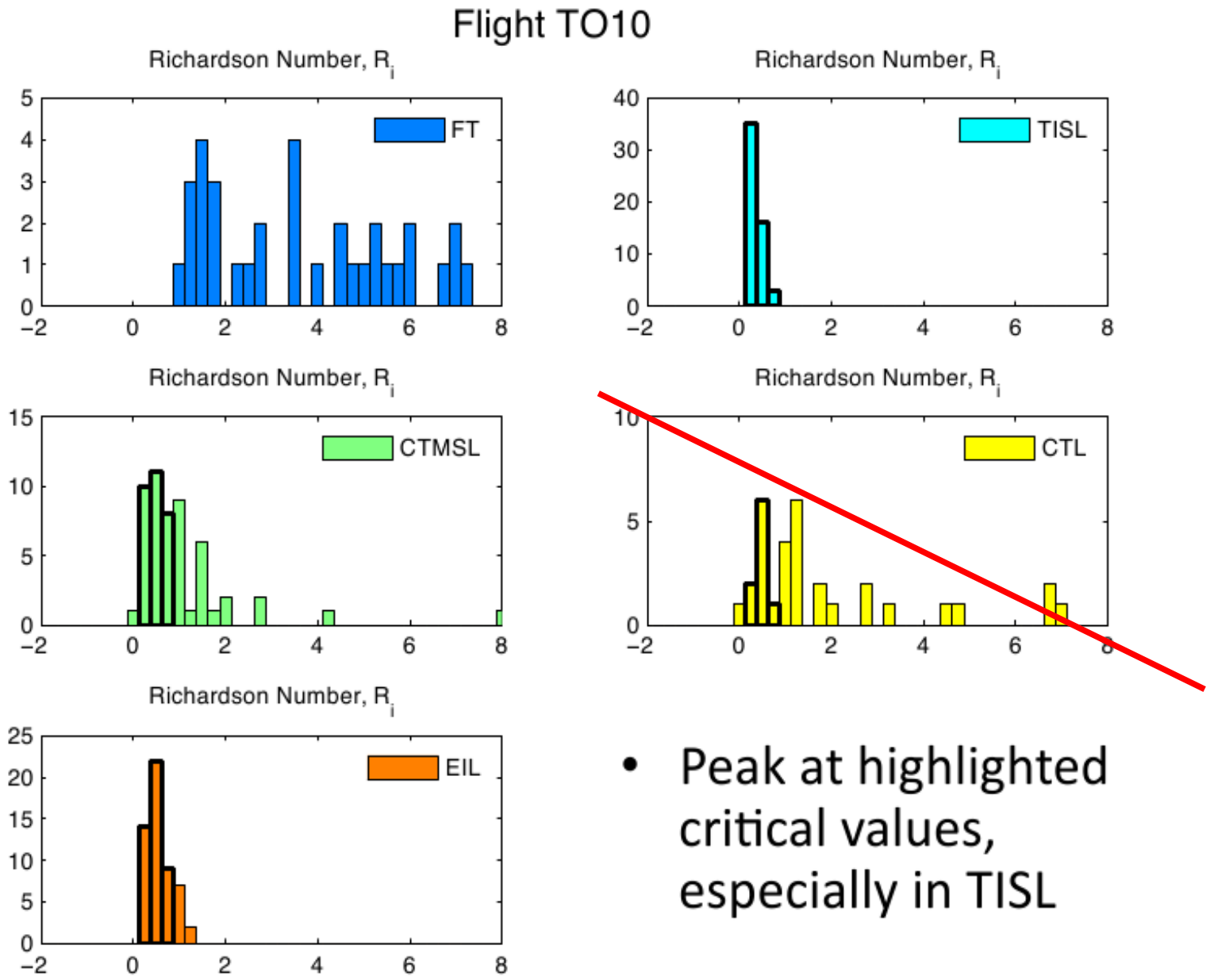

- Peak at highlighted critical values, especially in TISL

Richardson Number: Non-Classical

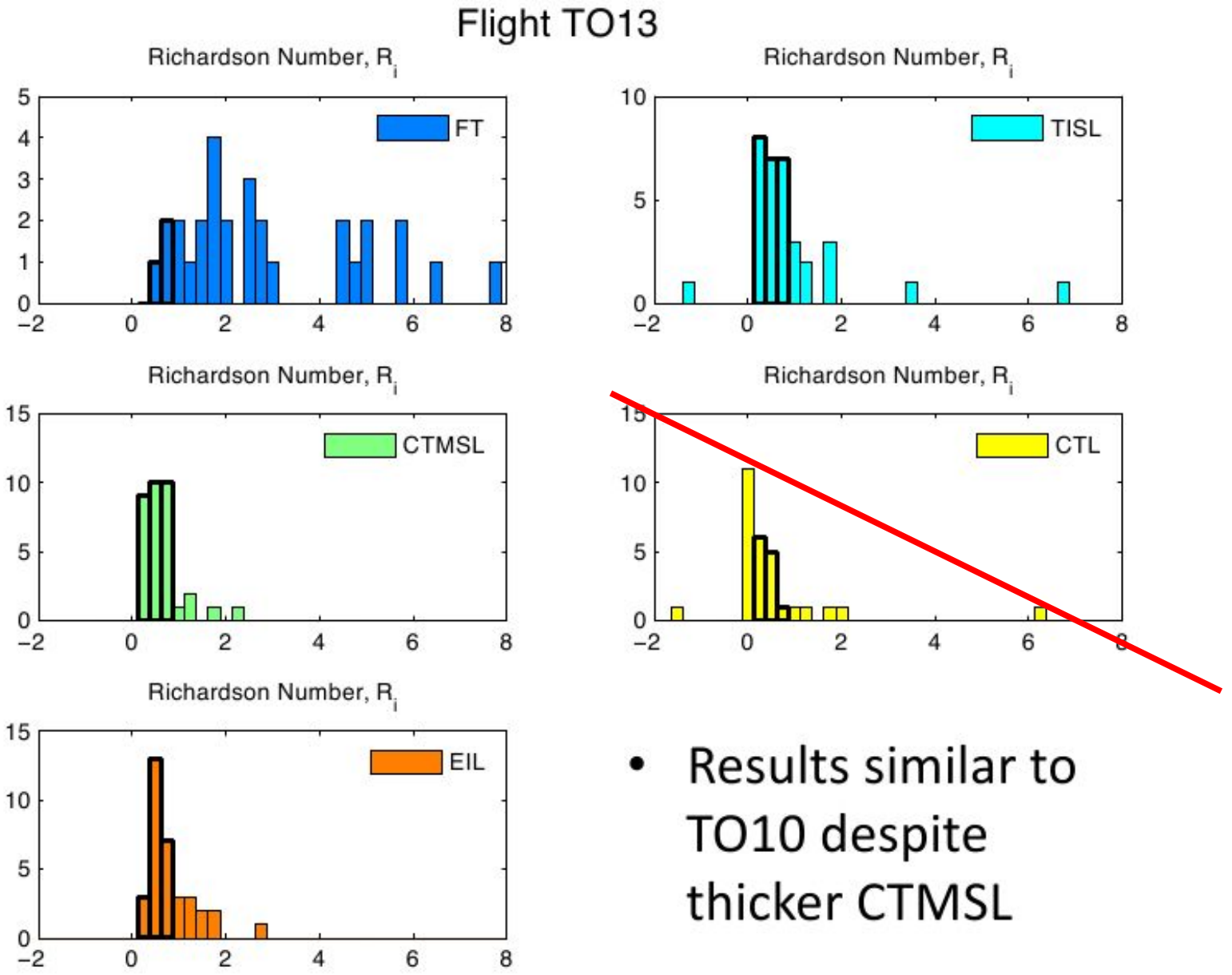

- Results similar to TO10 despite thicker CTMSL

Mixing diagram showing buoyancy (density temperature) of mixture of cloud and free-tropospheric air (upper lines) and cloud and EIL air (lower lines).

Negative buoyancy – below the blue line.

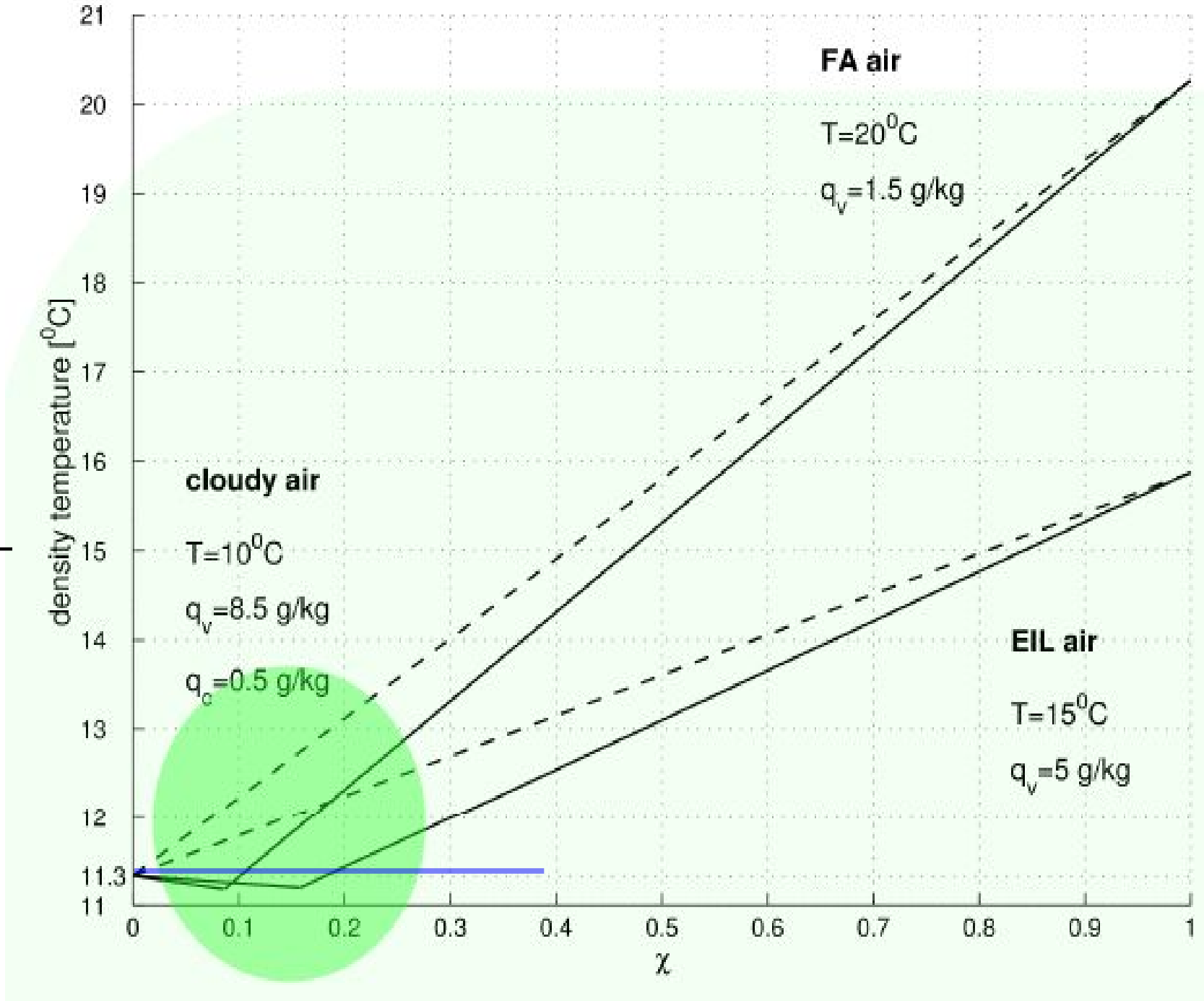

Similar and Different

- Two very different cases show remarkably similar behavior when characterized by Richardson number
- How might this occur? Local layer thickness Δz can adapt to forcings [Katzwinkel et al, Boundary Layer Met. 2011]

$$R_i = \left(\frac{g}{\theta}\right)\frac{\Delta\theta}{\Delta u^2 + \Delta v^2}\Delta z$$

Classical

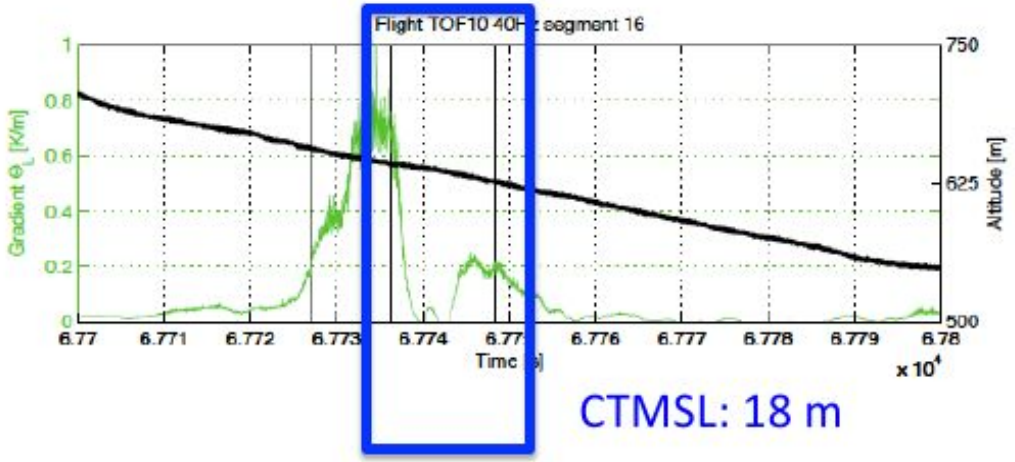

Non-Classical

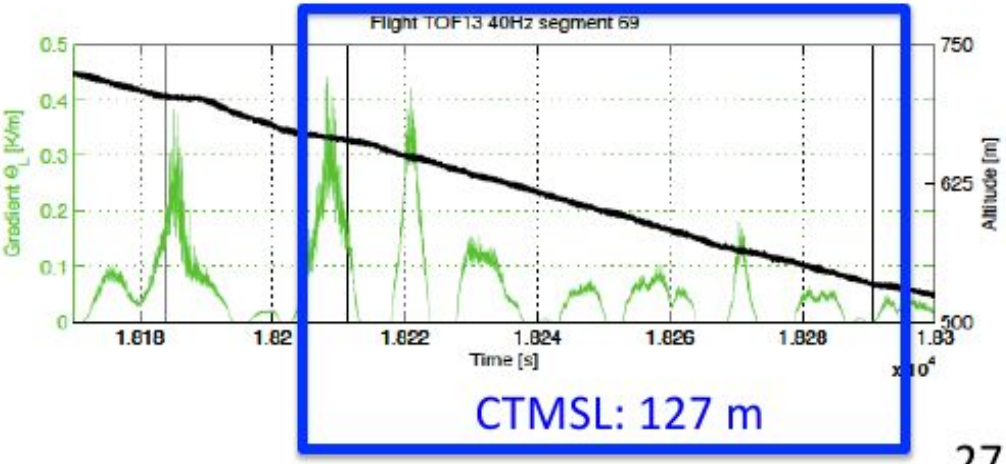

Summary

High-resolution measurements in POST allow to investigate fine-scales of mixing at SC top.

Preliminary data analysis suggests different dynamics of entrainment/mixing in two investigated cases:

TOF10 – typical case - narrow Entrainment Interfacial Layer (EIL), capped with strong inversion and thin shear layer, CTEI permitted.

TOF13 – diluted case - decreased LWC and total water in the cloud top region,

capped with the weaker inversion and a thick layer of relatively weak shear and increased humidity, CTEI not permitted

Capping inversion TURBULENT (CTL) despite the remarkable static stability.

HYPOTHETICAL PICTURE of entrainment at Sc top.

1. Marginal dynamic stability (Ri close to critical) in EIL – governs EIL thickness and mass exchange.

2. Thermodynamic structure of the cloud top dependent on properties of FT and CTL (whether CTEI permitted or not).

3. Coupling/.decoupling of Sc top to the mixed layer in ABL depends on thermodynamic properties of entrained/mixed air.

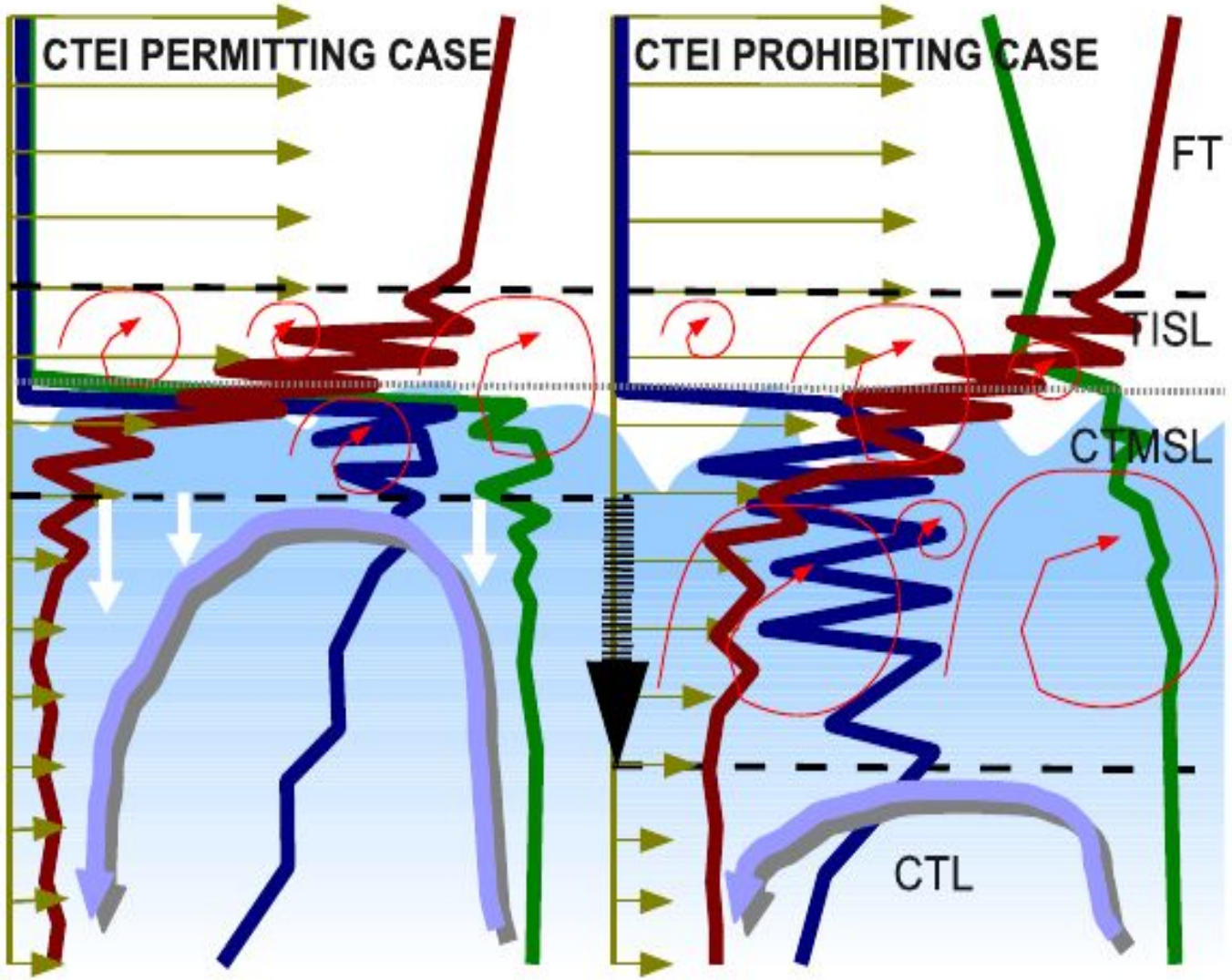

Fig. 16. Cartoon summarizing the main physical mechanisms of mixing in stratocumulus top in CTEI permitting and preventing si uations. FT – free troposphere, TISL – turbulent inversion sublayer, CTMSL – cloud top mixing sublayer, CTL – cloud top laye EIL = TISL + CTMSL – entrainment interface layer, between black dashed lines. Straight brown arrows – mean wind, thin spiral brow arrows – turbulent eddies due to shear, double violet-grey lines - convective circulations in STBL, green and blue lines – θ_l and LWC profile from airborne measurements. White arrows in the left panel indicate removal of negatively buoyant parcels fron the EIL in CTEI permittin case, while black dashed arrow indicates buildup of CTMSL in CTEI prohibiting case.

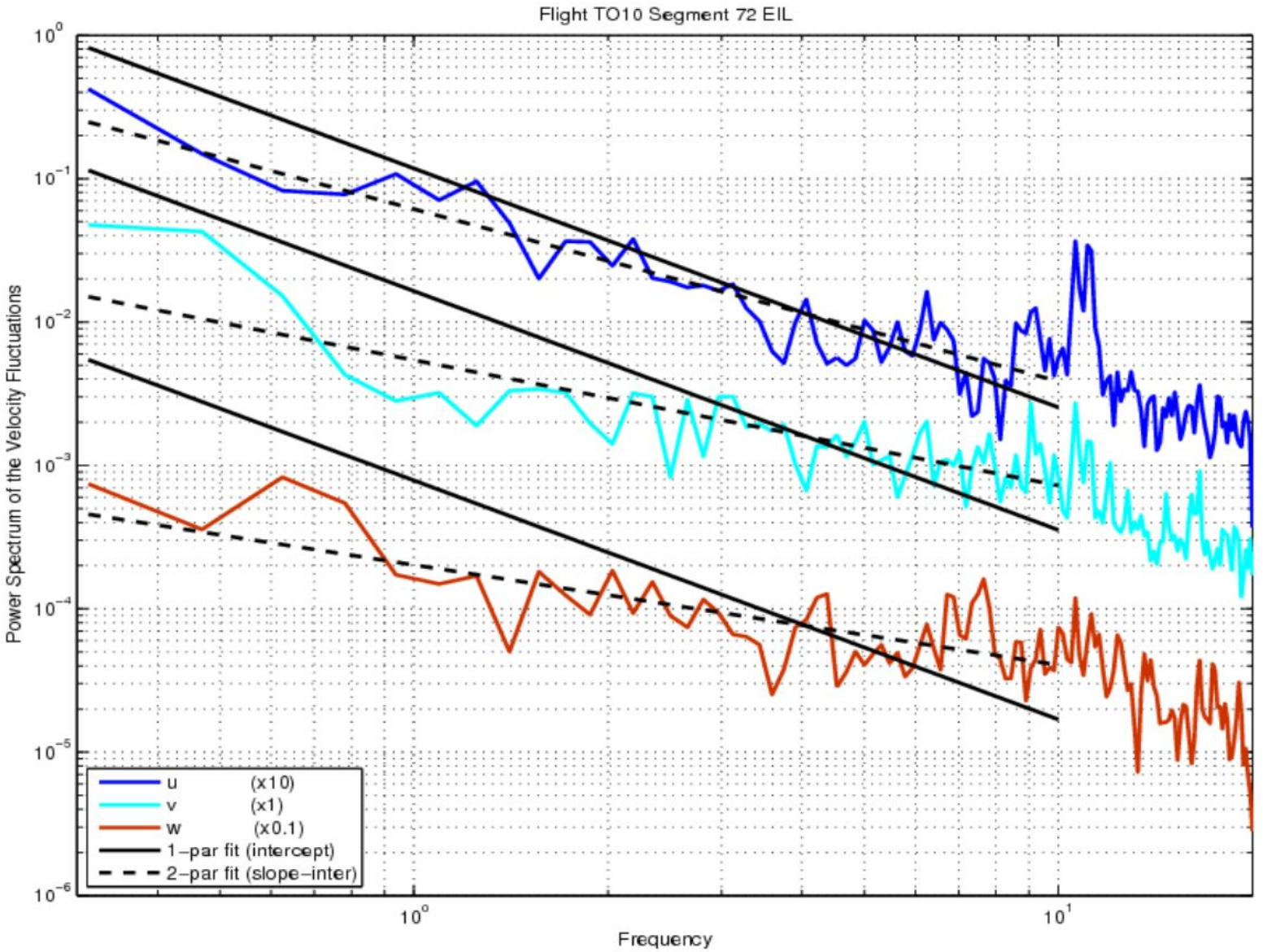

$$\overline{\varepsilon} = \frac{2\pi}{\overline{U}} \left(\frac{f^{\frac{5}{3}} S(f)}{\alpha} \right)^{\frac{3}{2}}$$

The line of slope −5/3 is shown by the solid line fits in the figure. The frequency range is limited to 0.3 to 10 Hz, removing the higher frequency features attributed to interaction with the plane and lower frequency artifact of the Welch method.
As an additional check, the data are also fit with two free parameters, the linear slope and intercept, as indicated by the dashed lines. Segments where the slope obtained in this way differs from −5/3 by more than 50% are rejected.

TKE DISSIPATION RATE

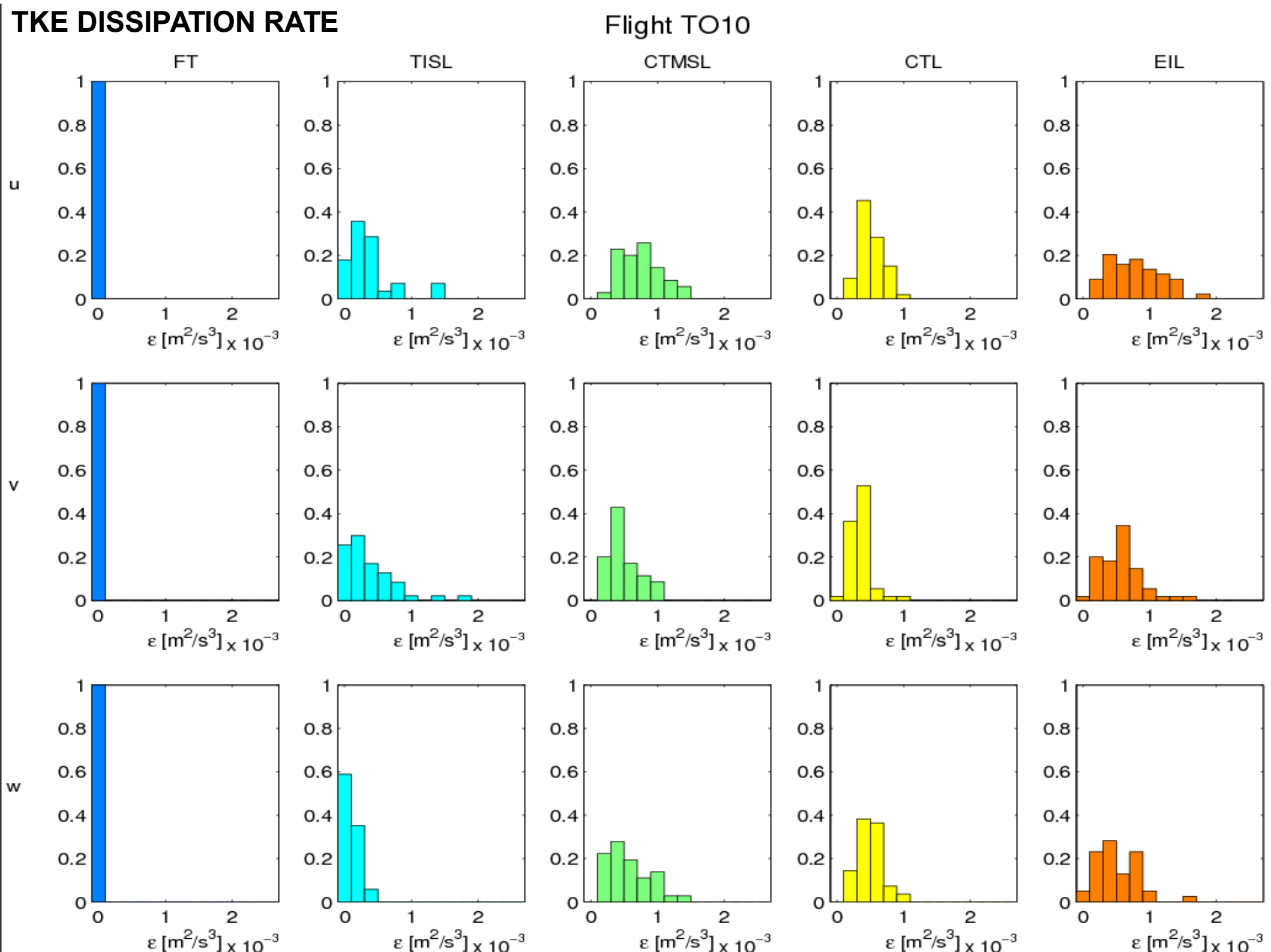

TKE DISSIPATION RATE

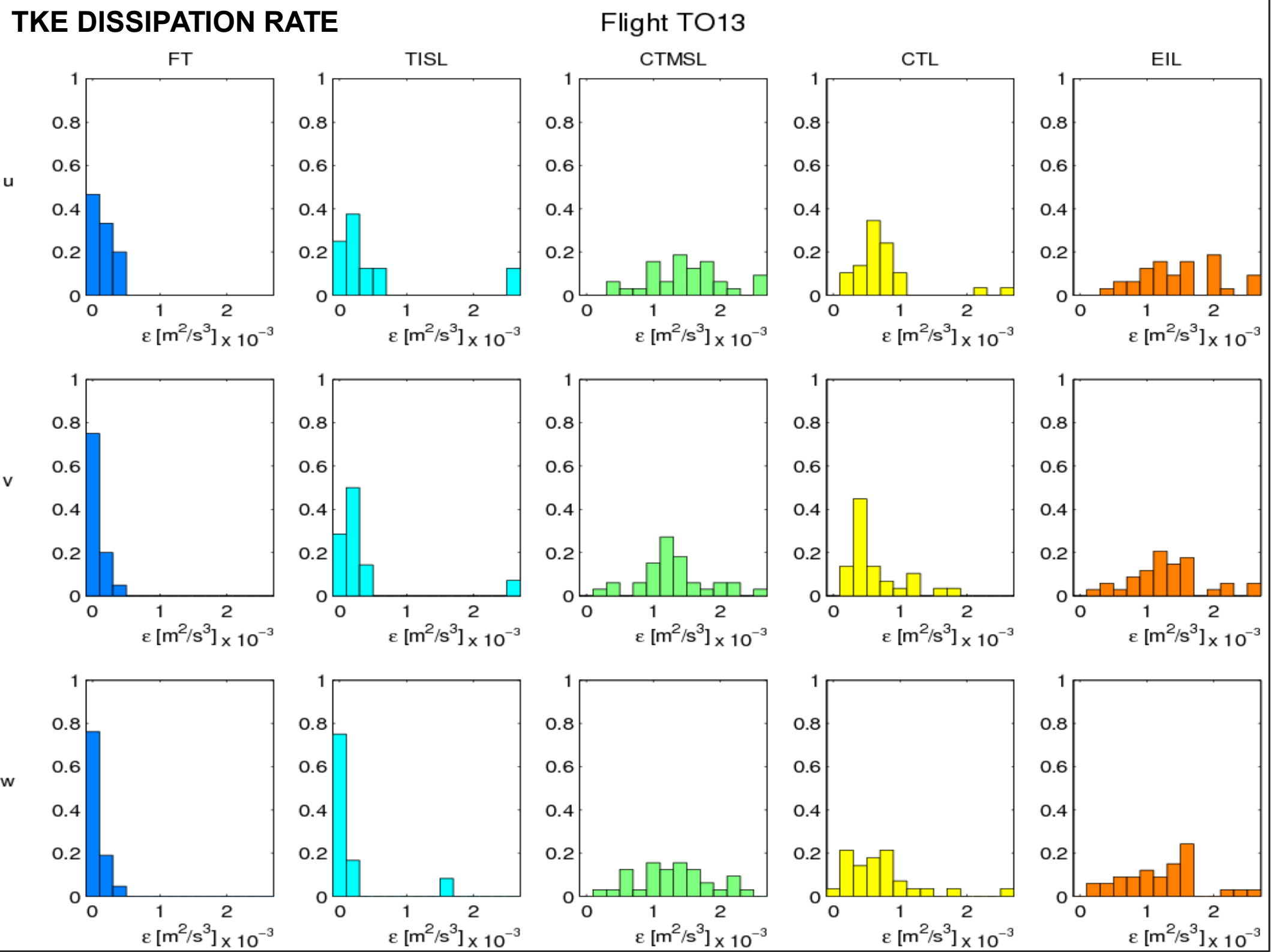

Corrsin scale $L_C = \sqrt{\varepsilon / S^3}$

Flight TO10

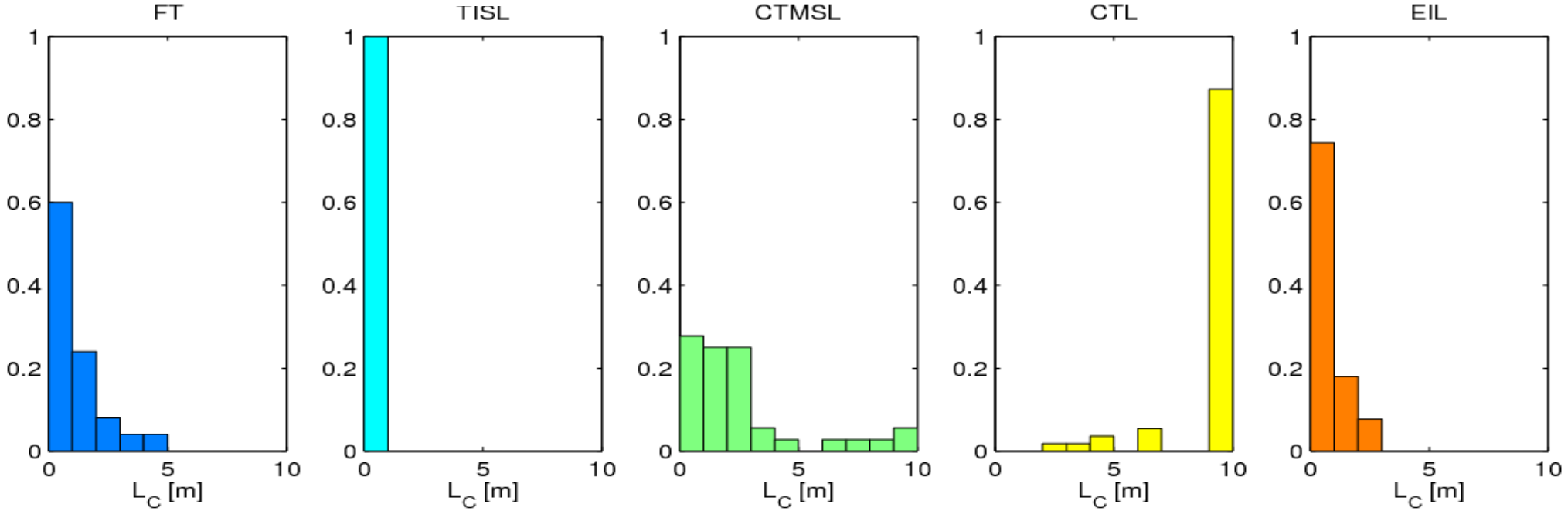

Ozmidov scale $L_O = \sqrt{\varepsilon / N^3}$

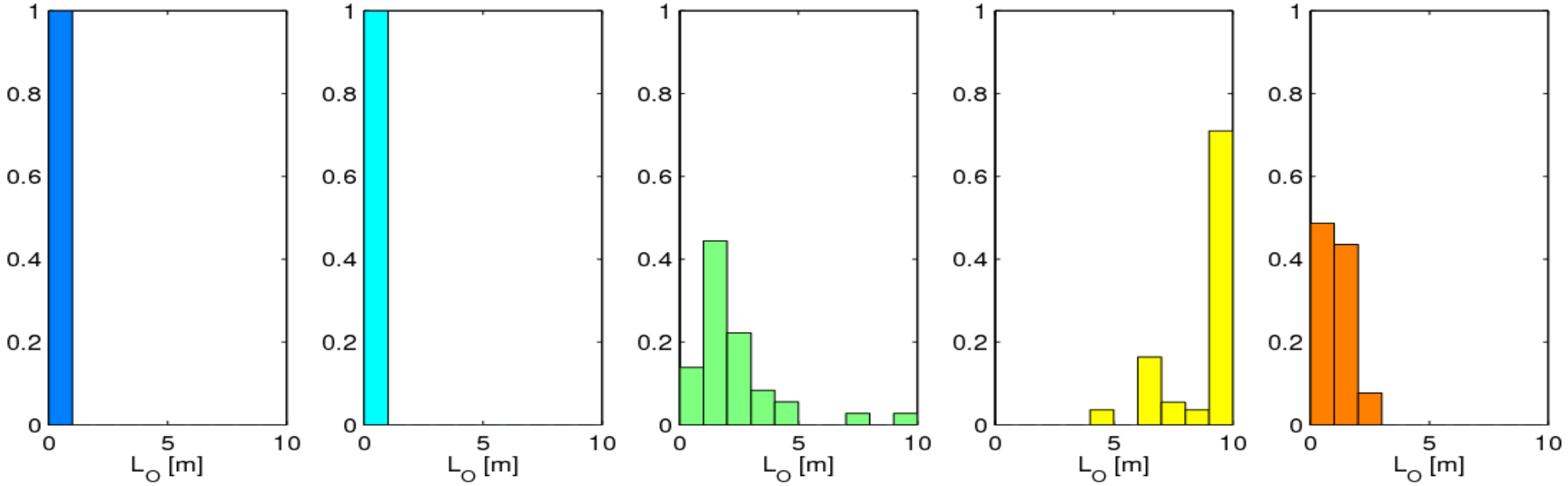

Corrsin scale $L_C = \sqrt{\varepsilon / S^3}$

Flight TO13

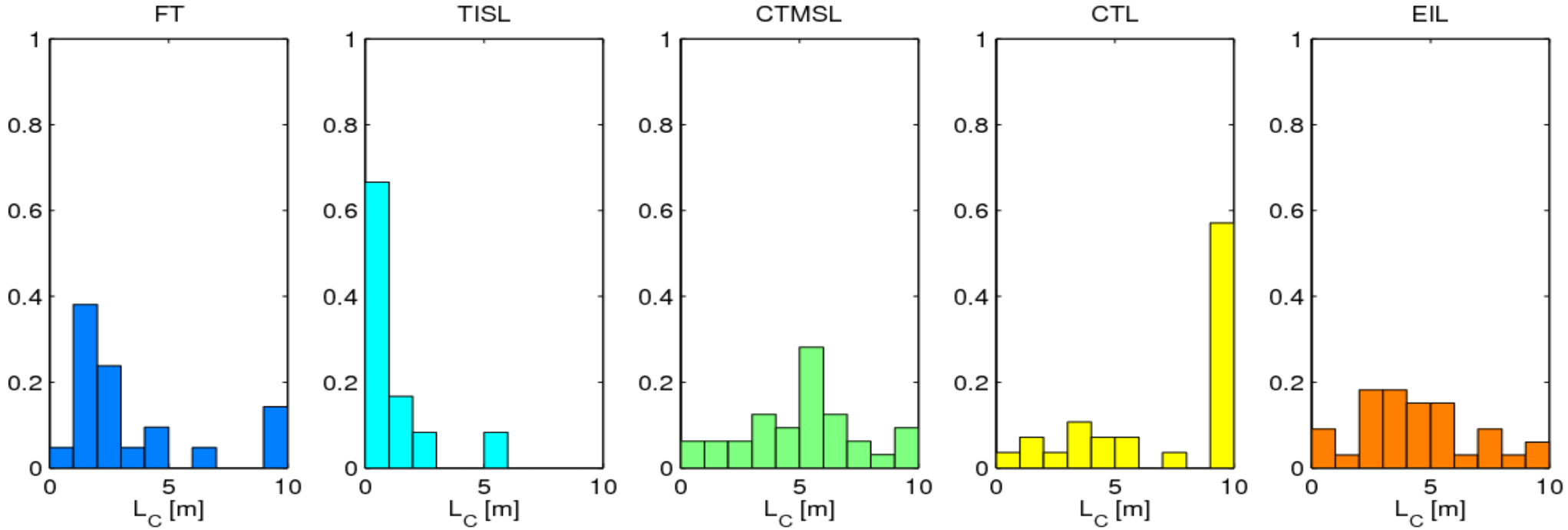

Ozmidov scale $L_O = \sqrt{\varepsilon / N^3}$

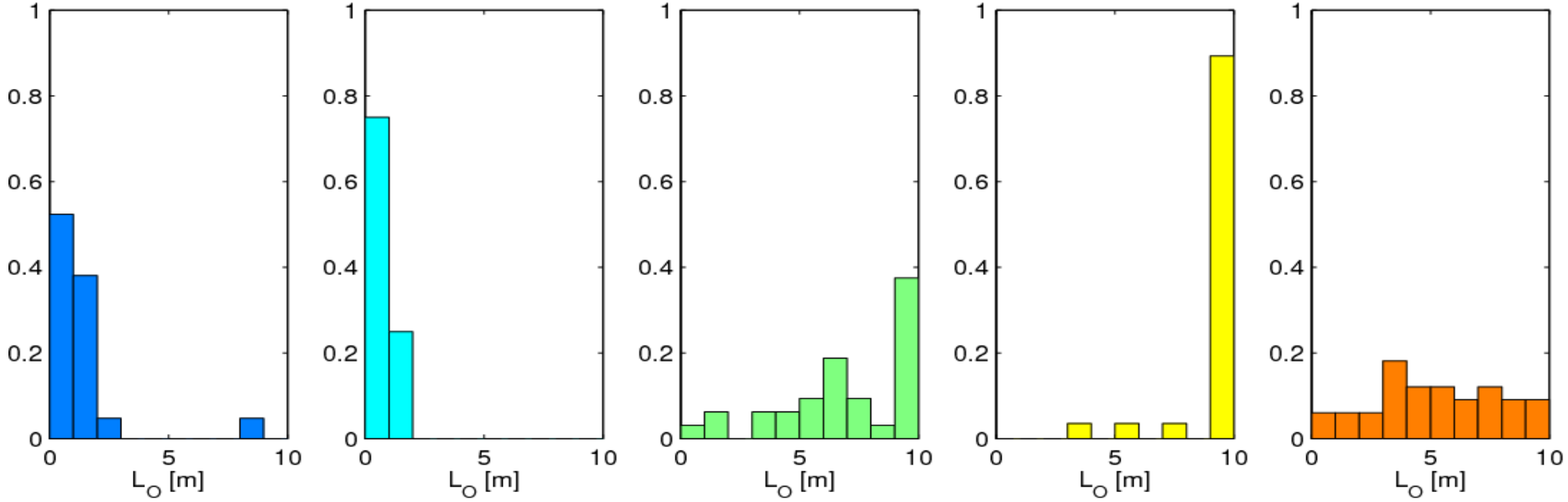

Summary turbulence

High resolution measurement from POST campaign allow **detailed study of turbulence and entrainment** at stratocumulus cloud top.

Analysis of dynamic stability shows **turbulence through the capping inversion** and cloud top, with **strong wind shear compensating static stability**.

EIL thickness **adapts** such that gradient **Richardson number** stays **near critical.**

Cloud Top Entrainment Instability influences effects of mixing.

Estimates of **TKE dissipation rate show turbulent inversion weakly turbulent, cloud top more turbulent**.

Stability in the inversion **influences isotropy and scales of turbulence.**